



REVIEW ARTICLE

Uranium, Thorium, Rare Earths and Other Metals in Cretaceous Age Basement Rocks: A Source for New Uranium District in Tertiary Age Sediments of the McCarthy Basin (A New Middle Cretaceous Age Impact Crater?), and an Associated New Metallogenic Locale Adjacent to the Death Valley, Eastern Seward Peninsula, Alaska

Campbell MD^{1*}, RI Rackley², RW Lee³, M David Campbell⁴, HM Wise⁵, JD King⁶, and SE Campbell⁷

¹Senior Principal (Emeritus), Chief Geologist / Chief Hydrogeologist, I2M Consulting, LLC, Houston, Texas, USA.

²Senior Geological Associate (Emeritus), I2M Consulting, LLC, Seattle, Washington, USA

³Senior Geochemical Associate, I2M Consulting, LLC, Austin, Texas, USA

⁴Senior Principal and Program Manager, I2M Consulting, LLC, Katy, Texas, USA.

⁵Remedial Services Senior Specialist, SWS Environmental Services (Now NRC), La Porte, Texas, USA.

⁶Senior Consultant – International Affairs, I2M Consulting, LLC, Seattle, Washington, USA

⁷Special Consultant, Alaska Programs, for I2M Consulting, LLC, Ex-Omega Energy Corp., Lancaster, Ohio, USA

Abstract

Mineral exploration conducted during the summers of the latter 1970s and early 1980s by personnel of United Resources International (URI) on behalf of the Omega Energy Corporation confirmed the existence of mineralized zones containing anomalous uranium, thorium, and rare earths, and other metals in the Kachauik area and in the Death Valley area of the Eastern Seward Peninsula of Alaska. According to the policy announced by the senior author (Campbell, 2017), this paper is based on data from the field work conducted by the senior author and associated URI personnel some 40 years ago and the work continues today. The geological mapping, sampling, and resulting analytical data, considered in the light of the detection limits, precision and accuracy of the analytical methods available at that time, remain relevant to mineral exploration today. Substantial work has been conducted on the metamict mineral referred to as allanite, and on the regional geology and geophysics over the past 40 years. This new information has also been incorporated in this paper.

Field reconnaissance and sampling, and petrographic, chemical, XRD, microprobe, cathodoluminescence and metallurgical analyses conducted in the late 1970s indicate that the mineralized zones occur within a composite alkaline intrusive complex related to, but separate from, the Darby pluton of the Darby Mountains area. The areas sampled contain uranium that has been leaching into the groundwater. The rocks sampled also contain thorium and rare-earth elements associated with allanite and common accessory minerals. The major zone of mineralization examined appears to be related to prominent phonolite dikes that occur along its margin in monzonitic country rock. Metasomatic introduction of uranium, thorium, and rare earths related to dike intrusion is postulated as the mechanism of metallogenesis. Areas with associated faulting and favorable host rocks, e.g., contact metamorphosed rock within fractured carbonate and graphitic rocks, as well as other favorable rock types, occur in the immediate area.

Of the total uranium contained in the whole-rock allanite-rich samples, approximately 88% is in one or more leachable mineral phases. Uranium present in one or more of the mineral phases is concentrated in the < 3.3% specific gravity fraction of the samples examined. Approximately 85 to 90% by weight of the total uranium present in the rock occurs in this fraction, which averages approximately 0.15% ${}^c\text{U}_3\text{O}_8$.

Uranium occupies lattice or inter-lattice positions within hornblende and feldspar and/or can also be present in separate uranium-bearing phases as minute inclusions within essential, varietal, and accessory minerals. The remainder of the uranium is present in the greater-than 3.3% specific gravity fraction, which also includes abundant allanite, the accessory minerals zircon, apatite, monazite, sphene, and other heavy minerals, such as siderite, barite, and magnetite. As a group, the heavy fraction contains approximately 10 to 15% by weight of the total uranium present in the whole rock.

Correspondence to: Michael D. Campbell, Chief Geologist / Chief Hydrogeologist, I2M Consulting, LLC, Houston, Texas, Tel: +01-713-248-1708, Email: mdc@i2mconsulting.com

Received: Aug 20, 2018; **Accepted:** Aug 24, 2018; **Published:** Nov 20, 2018
Revised: December 10, 2018

Based on the analytical work completed, chemical uranium appears to be in equilibrium with its radiogenic daughter products. And based on the mineralized samples examined to date, the rare-earth content consists predominately of the cerium (light) group. The distribution of the rare-earth elements is similar to uranium (i.e., the rare-earth elements occur in both specific gravity fractions. However, some segregation is apparent between the rare earths and uranium in the heavy fraction. The rare-earth elements preferentially occur within the allanite subfraction, while uranium is associated with other minerals of very low magnetic susceptibility. Strong geochemical anomalies exist within and around the Kachauik area, including bismuth, lead, niobium, molybdenum, copper, nickel, chromium, vanadium, lithium, fluorine, scandium, silver, cesium, tin, and arsenic, among other elements defined as threshold anomalies. In general, the data indicate that the region might be a new metallogenic province.

Interpretations of the geochemical and geophysical data presently available also reveal the possibility that the alkaline intrusive bodies might also include carbonatites, which would, if confirmed, expand the potential for the occurrence for other classes of mineralization as well. Based on the anomalous uranium content of the intrusive rocks, the plutons are also likely source rocks of uranium leaching into the groundwater system in a small, closed Tertiary basin, *McCarthy Marsh*, (created initially by an impact crater?), which is some 30 miles in diameter and is covered by tundra underlain by as much as 16,000 feet of fluvial and paludal sediments and lignite dating from early Tertiary to recent. The eastern part of the basin is underlain by a prominent dipole magnetic anomaly with a likely source in the shallow basement rocks below.

Classical bio-geochemical uranium roll-fronts likely occur in the McCarthy Basin, west and north-west of the outcrops of the Dry Canyon Creek pluton. To the northeast, a nearby smaller basin (i.e. a southern extension of Death Valley, a subsidiary impact crater?) contains previously reported uraninite in block-faulted Tertiary sediments along its southern boundary. Anomalous base metals also occur in much older faulted rocks to the north around the northern periphery of Death Valley east of the Windy Creek pluton. Death Valley fluvial sediments may also offer a suitable environment for the occurrence of uranium in the form of roll fronts.

Keywords: Seward Peninsula, Allanite, Uranium, Rare Earths, Thorium, Kachauik Pluton, Dry Canyon Creek Pluton, Burnt Creek Pluton, Darby Pluton, Windy Creek Pluton, Metasomatism, Metallogenic Area, Death Valley, Boulder Creek Basin, Geochemical Anomalies, McCarthy's Marsh, Magnetic Anomalies, Possible Meteor/Comet Impact Craters.

Introduction

Regional Evaluation

During early 1978, Omega Energy Corporation engaged URI to conduct a regional evaluation of the mineral potential on the eastern Seward Peninsula, Alaska. The URI team members and their functions are acknowledged at the end of this paper. The evaluation initially consisted of reviewing all available geological data on the Bendeleben Mountain area, the Granite Mountain area, and the Darby Range area. Emphasis was placed on alkaline intrusive-extrusive rock types that occur in the above areas. Based on the results of the evaluation, combined with U. S. Department of Energy NURE data and U. S. Geological Survey information available at the time, a Phase I field reconnaissance program was recommended by URI management for selected districts within the above regions.

Phase I Exploration Program

A Phase I field reconnaissance program was conducted during July and August, 1978, (see [Plate I](#) with link as [Plate IA](#), and [Figures 1, 2](#)).

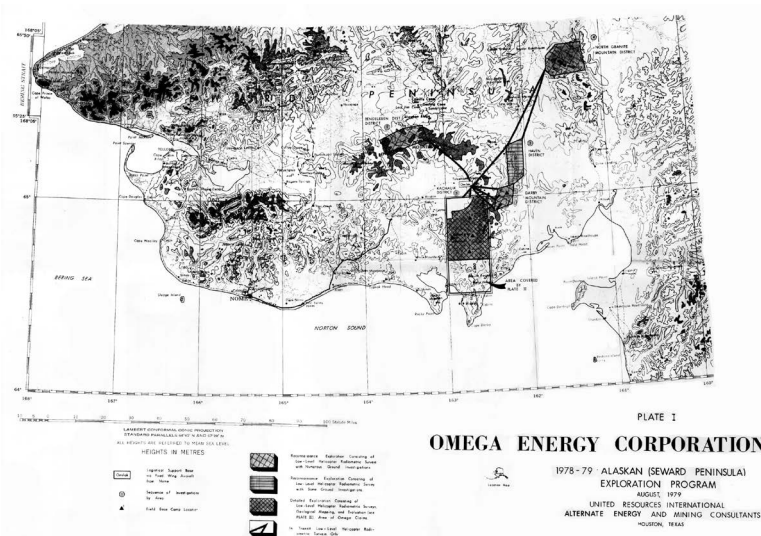


Plate I-Omega Activities during 1978 and 1979 (Click on Plate to Enlarge; For Plate IA ([here](#))).

Based on recently released NURE reports, URI conducted preliminary aerial and ground investigations in five districts during 1978:

District 1: Northern Darby Mountain areas were flown by low-level helicopter. Occasional anomalies were noted and investigated during short visits.

District 2: Bendeleben Mountain areas were flown in rugged topography. No radiometric anomalies. Complex folding and faulting were noted. Would be difficult to investigate

District 3: Haven area was flown to investigate areas north of reported uranium discovery by Houston Oil and Minerals Corp. (HOM). Heavy faulting observed.

District 4: North Granite Mountain area was investigated based on reported anomalies and widespread alteration. Some alteration and a few radiometric anomalies were noted.

District 5: Of the districts examined via helicopter and on the ground, the results of the reconnaissance program in the Kachauik area indicated significant uranium, thorium, and rare earth mineralization and suggested a strong potential for concentration of other elements of potential economic significance based in the presence of numerous dikes. The field work focused on this district for the next two years.

As a follow-up to previous reconnaissance conducted by the U. S. Geological Survey, URI field staff confirmed the presence of the allanite occurrences and determined that the occurrences may be regionally significant. Detailed reconnaissance identified locally abundant allanite and other mineralization within the district.



Figure 1: Omega Phase I Field Reconnaissance in Western Darby Range. Dr. Charles Weisenberg, Senior Geologist (URI), 1978.



Figure 2: Phase I Omega Energy Corporation-United Resources International Field Team.

Left to right: Dr. Charles Weisenberg, Senior Geologist (URI); Herb Nelson, Field Geologist (URI); Field Assistant #1 (Omega); Steve Campbell, Vice President-Operations (Omega); Field Assistant #2 (Omega); Pilot (Omega).
Field Base Camp Area occupied during Phase I and II Field Programs. Looking North toward the Bendeleben Mountains (top left), 1978.

Kachauik Area Investigations

The reconnaissance and subsequent investigations suggested that geologic conditions are favorable for potentially economic mineralization involving uranium, thorium, rare-earth, and other economic elements. Based on recommendations by URL, Omega subsequently funded detailed sampling and a claim-staking program in three areas within Omega’s exploration District 5 (see Figures 1 and 2). The areas are referred to herein as: northern, central, and southern areas of interest (Plate IA). Three noncontiguous areas of interest totaling approximately 9,300 acres were staked as federal mining claims in the late 1970s, which have since lapsed but claim corners were made of cement anchors to orange fiberglass rods with flags.

A total of 464 unpatented mining claims were staked and recorded by Omega in the Nome district office and with the U. S. Bureau of Land Management (BLM) in Fairbanks. The claims have since lapsed but the permanent claim boundary markers likely remain. The extensive claim staking was conducted during the Omega activities in 9,280 acres of contiguous claims in three areas of interest where mineralization was discovered on the surface or where anticipated a depth (see Table 1).

TABLE 1
OMEGA Areas of Interest
KACHAUIK DISTRICT
(SEE PLATES I AND II)

| <u>Area</u> | <u>Claim Name</u> | <u>Number</u> | <u>Acreage</u> |
|----------------------------|-----------------------------|-------------------|--------------------|
| Northern | Bethel** | 1-120 | 2,400 |
| | Bethzur** | 1-24 | 480 |
| | Total Northern Area: | 144 claims | 2,880 acres |
| Central | Behemoth* | 1-120 | 2,400 |
| | Solomon | 1-72 | 1,440 |
| | Canaan* | 1-111 | 2,220 |
| | Total Central Area: | 303 claims | 6,060 acres |
| Southern | Apostle | 1-17 | 340 |
| | Total Southern Area: | 17 claims | 340 acres |
| TOTAL OMEGA CLAIMS: | | 464 claims | 9,280 acres |

*See Figures 3, 4, and 8
**See Figure 5

In 1981, research on the region continued and additional field investigations were undertaken during the late fall of 1983 (during a week’s “weather window”) on the northern rim of the Death Valley area in the general Haven district (see Plate I and Plate IA). The work included geological sampling and geophysical surveys (ground magnetometer and radiometric surveys). URI investigations conducted north along the rim of Death Valley resulted in claim staking activities covering 2,300 acres (117 claims) in the mid-1980s. Later, blasting to remove overburden to expose rocks above a significant, very shallow dipole magnetic anomaly for additional sampling and assessment (see “Death Valley Investigations” later in this paper). All claims have since lapsed.

Geographical Considerations: Kachauik Area

The areas under consideration are located within the southeastern part of the Seward Peninsula, approximately 85 miles east of Nome (population 2,600) on the southwestern flank of the Darby Mountains (see Plate I, District 5). The southern part of the Darby Mountains is composed largely of the Darby pluton. It is bordered to the west by the Kachauik pluton, which in general forms the Kachauik Mountains, the Kwiktalik Mountains, the Golovin Peninsula, and Cape Darby to Norton Sound (see Plate IA).

The areas of interest are marked on the [Solomon C-2 and D-2 topographic sheets](#) (1:63,360 scale), which have been adopted as base maps for the Phase II investigations discussed later in this paper.



Figure 3: Aerial Oblique View from Helicopter near Hill 2047. Approximately 1 Mile South of Mt. Kachauik looking eastward. Glaciated Ground Covered by Grus and Rock Fragments.



Figure 4: Aerial Oblique View over Hill Looking West-South-West from above Mt. Kachauik (see [Plate II](#)).
Glaciated Ground Covered by Grus and Rock Fragments.

The southern area of interest is located approximately 12 miles north of Norton Bay and approximately 15 miles northeast of the village of Golovin, a settlement with a population of approximately 100 (circa year 1979). The central area is approximately 15 miles inland and the northern area (covering a small stock called the Dry Canyon pluton located approximately were 6 miles north of the Kachauik pluton) were approximately 26 miles from Norton Bay.

The highest elevation within the subject area is 2,109 feet, the same area covered by Omega's southern area of interest and the outcrops of allanite mineralization. The area is composed of rolling, barren and tundra-covered, glaciated hills and perennial, shallow streams. There are no roads present in the areas although construction is to begin on a Nome-Fairbanks highway in the future. Based on topography, the path of such a highway would probably pass within a few miles of Omega's northern claim group (see Plate I).

A direct highway link with Nome would be anticipated within 5 to 7 years, although as of 2018, there is no indication that such road construction has begun. In the meantime, logistical support from Nome for the URI-Omega operations has been accomplished by fixed-wing, single-engine aircraft using the Omilak airstrip, located approximately 10 miles northeast of Omega's northern claim group (see Plate I and Ia). Improved airport facilities now serve (2018) the small native village of Golovin, located approximately 15 miles southwest of Omega's southern area of interest. An air strip capable of receiving aircraft is also available at Moses Point, approximately 15 miles due east of the southern claim group and at Elim southeast of the southern area of interest.



Figure 5: Aerial Panorama View over Hill 1420.
Looking Southwest toward the Hill of the Southern Area of Interest.
Golovin in the Distance. Rathlatulik River in Foreground.

Weather Conditions and Field Work

The weather in the area under consideration is similar to that of much of the Seward Peninsula and is characterized by cool summers and very cold winters. During the summer field season (June to October?) long days, up to 22 hours duration, permit extensive field work and associated logistical support. The arrival of the spring thaw, however, varies from year to year as does the winter freeze. The beginning and closing of a field program are therefore dependent upon weather conditions. Minor interruptions of the field program because of inclement weather (fog and rain) are to be expected. Fog, rain, and windstorms are not infrequent during the summer field season.

Fieldwork can also be conducted in winter months during so-called “weather windows” when large high-pressure systems dominant the area for a week or two from time-to-time. However, winds are known to blow at 20 to 30 mph, which causes “white-outs” below 10 to 20 feet from the snow-covered surface. (See Death Valley Investigations: Figures DV-3 through DV-6 later in this paper).

The general area lies on the boundary between glacial terrains with zones of continuous and discontinuous permafrost. Table 2 includes some of the pertinent climatological data applicable to the area.

| | | | | | | |
|---|------|--------|-------|------|------|-----------|
| <u>Temperature</u> | | | | | | |
| Mean Winter Maximum Temperature (January): 8°F | | | | | | |
| Mean Winter Minimum Temperature (January): -8°F | | | | | | |
| | | | | | | |
| Mean Summer Maximum Temperature (July): 62°F | | | | | | |
| Mean Summer Minimum Temperature (July): 44°F | | | | | | |
| <u>Precipitation</u> | | | | | | |
| Mean Annual Precipitation: 16 inches | | | | | | |
| Monthly Distribution: | | | | | | |
| Pre-July | July | August | Sept. | Oct. | Nov. | Post-Nov. |
| <1" | 2.0" | 3.7" | 2.7" | 1.5" | 1.0" | <1" |
| 60% of all precipitation (rain) occurs during the summer field months | | | | | | |
| <u>Wind</u> | | | | | | |
| Average mean yearly velocity: 10-15 mph, with heavy windstorms associated with winter blizzards and light windstorms associated with summer thunderstorms | | | | | | |

Reference: NOAA Climate Records, Nome Office

Geological Setting

The geology of the Darby Mountains region, which includes the Kachauik and Dry Canyon plutons, has been described earlier by numerous geologists: Mendenhall [1] (1901); Smith and Eakin [2] (1911); West [3] (1953); Herreid [4] (1965); and Miller, et al. [5] (1972). The petrology has been discussed in some detail by Miller and Bunker [6] (1976), and Anderson [7] (1968).

The core of the Darby Mountains consists predominantly of a series of Cretaceous plutons that cover approximately 50 miles from Cape Darby in the south at the Norton Sound to Death Valley to the north-east and to the Bendeleben Mountains in the north. The plutons are bordered by Precambrian met sediments and Devonian (?) carbonates.

The Darby pluton is a relatively homogeneous quartz monzonite, but Miller and Bunker [6] (1976) found indications of lateral zoning and other similar igneous rock types. Modal analyses indicate a slight and gradual decrease in mafic minerals and plagioclase from south to north and a corresponding increase in K-feldspar and quartz.

The most characteristic features of the Darby pluton are its rather uniform coarse-grained porphyritic texture, homogeneous composition, and relative abundance of magnetite and allanite as accessory minerals. The latter mineral will be discussed in detail later in this paper (see: “Discussion of Results”). Conspicuous fluorite and rutile have also been reported and K-Ar ages of 81.4 ± 3 m.y. to 92.1 ± 2.8 m.y. have been assigned to the Darby pluton (Miller and Bunker [6] (1976)).

The Kachauik pluton, within which Omega’s central and southern areas of interest is located, occupies approximately 205 square miles in the southwestern part of the Darby Mountains. This pluton is reportedly a composite intrusion; the western half is composed of granodiorite and quartz monzonite (Plate II Unit Kkg) and the eastern half is composed of a monzonite-syenite (Plate II - Unit Kkms), which has been further subdivided into four subunits by Miller, et al. [5] (1972). K-Ar ages of 86.1 ± 3 m.y. and 97.5 ± 3 m.y. have been determined for the respective units. Numerous alkaline and basic dikes intrude the pluton.

The Dry Canyon Creek pluton, within which Omega’s northern area of interest is located, crops out over an area of approximately 4 square miles (see Plate II). It has been described by Miller, et al. [5] (1972) as a leucocratic to trachtyoid foyaitite. The literature indicates the stock has been intruded by blue-gray pulaskite dikes. It has been assigned a mid-Cretaceous age based on a K-Ar age of 105 ± 3 m.y., which indicates that this unit is possibly older than the Kachauik pluton.

Based on regional uranium investigations conducted by the U.S. Geological Survey (USGS), Miller and Bunker [6] indicated that the Darby plutons contain an above average content of uranium and thorium (11.2 ppm and 58.7 ppm, respectively), but that the Kachauik pluton ranges from average to above average uranium and thorium (5.7 ppm and 22.5 ppm, respectively). As early as 1948, a USGS reconnaissance for radioactive deposits revealed anomalous uranium and thorium in the Darby and Kachauik plutons [8]. The radioactivity was reported in minerals derived from felsic igneous rocks.

Miller and Bunker [6] indicate that not only do the three plutons show compositional differences, but also exhibit textural differences, which together show different magmatic sources for each of the three plutons, i.e., the Darby pluton, the Kachauik pluton and the Dry Canyon Creek pluton. The USGS established earlier that the region is in a uranium-thorium rich province and subsequently conducted a preliminary field reconnaissance in the area of the Kachauik pluton. The results of that evaluation were published by Miller, et al., [9] and indicated unusual amounts of allanite, which contained significant uranium, thorium and rare-earth elements. This information stimulated the URI interest in the areas herein under discussion.

Historically, the Darby Mountains have not been found to be especially rich in economic mineralization, although a number of prospects and geochemical anomalies have been reported that indicate a potential for several metals. The area has been under-explored until recently. The one mine that has produced is the Omilak mine, located approximately one mile northeast of the Omilak airstrip. Herreid [4] reported that this mine produced a few hundred tons of lead-silver ore prior to 1900 from a Precambrian marble (Plate II map unit pEm?). Additional minor lead and zinc occurrences have been reported a few miles south of the mine in similar rock Mulligan, [10] 1962.

Geochemical stream sediment sampling [Miller, et al., 1971; Miller and Grybeck, [11]1973 has yielded highly anomalous copper, nickel, cobalt, chromium, manganese, iron, boron, scandium, and vanadium from the eastern side of the Darby Mountains. Gossan zones with high bismuth and molybdenum have also been reported via previous USGS investigations. The anomalous elements are also reflected in the geochemical anomalies reported during the URI Phase II investigations (see “Geochemical Investigations”).

Geological Investigations

After confirmation was made of significant allanite mineralization, URI personnel conducted a preliminary field mapping and sampling program in order to examine the geological environment within which the allanite and associated uranium mineralization occurred, and with a view towards assessing allanite’s potential value as an ore of uranium, thorium and rare earths (see Figure 6 and 6a).



Figure 6: Weathered Outcrop Samples of Allanite Mineralization near Location C2-l. (See: “Geochemical Investigations”)



Figure 6a: Sample Recently Broken. Sample C-2
Black Euhedral Minerals are Allanite (Brown in Thin-Section). White Mineral is Feldspar.

The exploration program was also designed to investigate the allanite occurrences with a view towards developing a viable exploration guide to other types of uranium mineralization that might be present in the general area. Should allanite and associated minerals contain leachable uranium, the area might be a candidate source of uranium for the development of roll-front deposits in the adjacent Tertiary basin (i.e., McCarthy’s Marsh [12] (1988). This will be discussed later in detail.

Field mapping was accomplished during Phase II with helicopter support as required (via walkie-talkie communications) for rapid logistical support and coverage of the claim areas and vicinity. Two field teams consisting of two URI geologists each made both ground geologic and radiometric traverses and low-level helicopter geologic and radiometric traverses during Phase II field operations (see Figures 7 and 8). The principal objectives of the two-week field reconnaissance program were to: 1) locate, describe, and sample the numerous dikes in the areas of interest, 2) locate and describe the faults encountered, and 3) map and describe the geological contacts encountered.



Figure 7: Phase II - United Resources International Field Team.
Standing left to right: Steve Campbell, Vice President-Operations (Omega); Herb Nelson, Field Geologist (URI); Dr. Chuck Weisenberg, Senior Geologist (URI.); Dr. Kevin Biddle, Senior Geologist (URI); and Pilot
Kneeling left to right: Field Asst. #1 (Omega); Field Asst. #2 (Omega); Field Asst. #3 (Omega); Field Asst. #4 (Omega); and Dr. Charles Wielchowsky, Senior Geologist (URI).

More than 100 rock samples were collected and shipped to URI Houston offices for further analysis. Fifty thin-sections were subsequently prepared and described from selected rock samples. In addition, selected thin-sections were also investigated by scanning electron microscopy (SEM), x-ray imagery and cathodoluminescence techniques.



Figure 8: Phase II Base Located in Omega's Central Area of interest at Sundown.
(See Plates II and III, and Preliminary Mapping (Plate V ([more](#))))

Of the rock samples that were sectioned, seventeen samples were selected for geochemical analyses, i.e., whole rock total element scan, major element and minor element (XRF and "wet") analyses, sink-float and magnetic fraction analyses, and X-ray diffraction (XRD) for mineral identification. Additional analyses were made by delayed neutron activation (DNA) methods, and standard "wet" methods were employed to evaluate leachable uranium. Disequilibrium investigations were also undertaken.

Figure 9 illustrates the critical-path development of the various field and laboratory parameters considered during the Phase II field program.

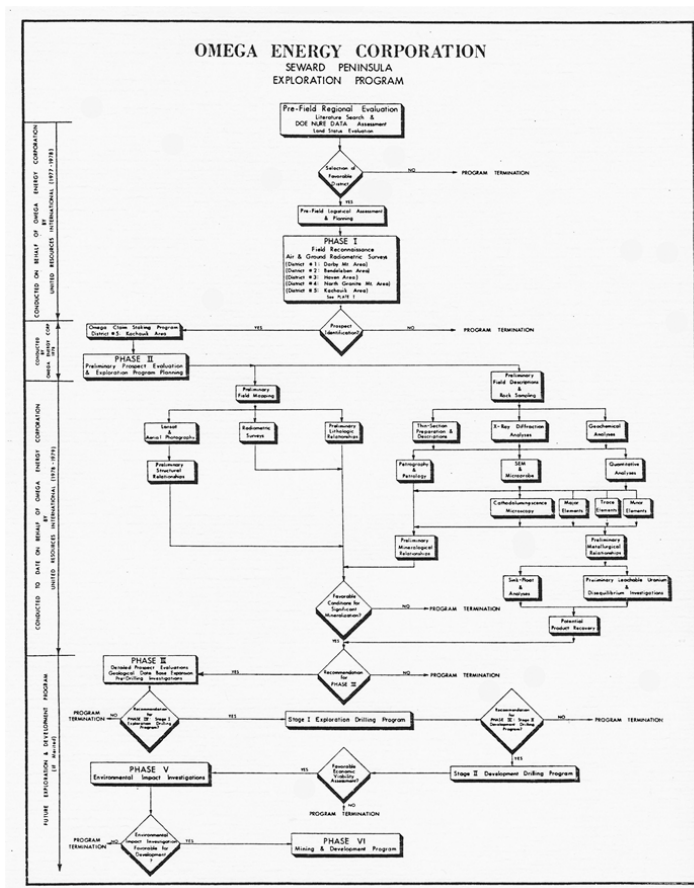


Figure 9: Critical Decision Path for Omega Exploration Program
(Click on Figure to Enlarge)

Preliminary Geological Mapping

Preliminary field mapping was conducted using the U. S. Geological Survey preliminary geologic map Miller, et al., [5]1972 as a base map. Plate II illustrates the modifications of the geological base map, where justified, and the sites visited, sample locations, and other significant data. A preliminary geological base map was prepared by Biddle and Wielchowsky with assistance from Weisenberg for follow-up field work (see Plate V and Acknowledgements).

Intrusive Rocks: The Kachauik pluton consists essentially of two rock units: monzonite and syenite (Plate II unit Kkms) and granodiorite and quartz monzonite (Plate II unit Kkg). These units are Cretaceous in age and are described in the legend of Plate II. The Precambrian (?) migmatitic zone (unit Mi) present in the area could be a large roof pendant overlying the Cretaceous monzonite and syenite units (Kkms). For field purposes, the Kkms unit occurring east of the migmatitic unit (Mi) is referred to as the Burnt Creek pluton. To the north, the Dry Canyon pluton consists of nepheline syenite, although other rock types have been reported, e.g., granites, monzonites and diorites. The Darby pluton to the east was not examined in detail, but is reported to be a quartz monzonite with a coarse-grained, hypidiomorphic granular texture without foliation (Jones and Forbes, [13] 1976).

The Kachauik, Burnt Creek, and Dry Canyon Creek plutons have been intruded by a swarm of alkalic dikes and it appears that significant uranium, thorium, rare earth and other types of mineralization might be directly or indirectly associated with these dikes (Drumheller, [14]1978; and Volborth, [15] 1962). The mineralization is associated directly with the monzonite unit of the Kachauik pluton (Kkms unit of Plate II).

Additional comments regarding that type of mineralization and its regional ramifications will be discussed later in this report (see "Discussion of Results"). Figure 10 illustrates the general field associations and sampling locations in the southern and central areas of interest. Field relations of the plutons and intruded country rock are indicated on Plate II. Some contacts are considered to be faulted and others intrusive. As indicated previously, the Kachauik pluton is a composite body of granodiorite and quartz monzonite to the west and porphyritic monzonite and syenite with well-developed flow-foliation to the east. Miller and Bunker [6] (1976) give a detailed petrologic description of this pluton.

The Burnt Creek intrusive body is probably a satellite pluton of the major Kachauik pluton and consists of poorly foliated monzonite and syenite. These bodies and rock types they encompass are characterized geochemically later in this paper. The magnetic anomalies shown in Figure 10 will also be discussed later via "Geophysical Investigations" in this paper.

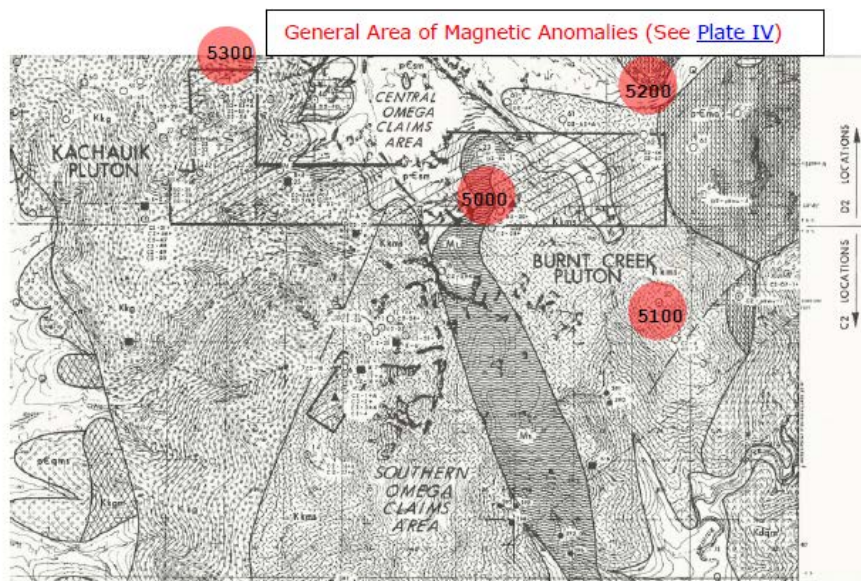


Figure 10: Location of Plutons and Other Geological Units, Southern and Central Areas of Interest and Sampling Sites, For Both URL and USGS, See [Plate II](#). (Click to Enlarge). See [Plate IV](#).

Figure 10a: Aerial Oblique View from Helicopter over Hill 1420 Southwest at Hill 1209. The Village of Golovin is indicated. (See [Plate II](#)) (Click to View).

The Dry Canyon pluton in the northern area of interest consists mainly of a well flow-foliated hornblende-biotite nepheline syenite with minor, more mafic phases. Other rock types were also identified during petrographic analyses: granite, monzonite and diorite. Jones and Forbes [13] (1976) presented a detailed description of these rocks.

Miller and Bunker [6] (1976) report that the granodiorite unit, when adjacent to the alkaline dike rocks, has been commonly metasomatized with incipient development of aegirine and riebeckite. As will be discussed later in this paper, (see “Discussion of Results”), metasomatic processes appear to have played an important role in the introduction of uranium, thorium, rare earth and other elements to the host monzonites. Miller and Bunker also collected samples in and around the central and southern areas of interest, as well as from around the general area. These data are discussed further in “Geochemical Investigations” and “Discussion of Results”.

Dike Rocks: The alkalic dikes that intrude the Kachauik pluton are indicated in [Plate II](#) and, in general, strike to the northeast (approximately N40E), although some exceptions are known. In one case, at least, a conjugate set is indicated at Location C2-19: MC: 18-D in [Plate II](#). In general, the dikes have steep to vertical dips and range up to 45 feet in width of disturbed surface. Their usual surface expression consists of a rubble pile in which individual fragment size seems to be directly proportional to grain size (i.e., the coarse-grained dikes yield large fragments and fine-grained dikes yield small fragments). The fine-grained dikes were generally found to the west and north in the Kachauik pluton.

One dike of moderate thickness was found in place at location D2-44, [Plate II](#) (Map Coordinates: 16-E). At this location chilled margins are not apparent. Advanced reaction and apparent alteration of the country-rock were not observed. However, phenocrysts of the country rock are, in part, being absorbed by the dike near its margin (see Figure 11). The dikes in the area range in color from blue-gray to tan to blue-green.



Figure 11: Outcrop View of Hornblende Biotite Granodiorite (Location D2-44: Sample D2-53). Intruded by Phonolite (Pulaskite) Dike (Sample D2-52); X marks Sampling Site and Sample Nos.

Locally, the density of dikes is quite high (e.g., four dikes within 450 feet). Their average length is unknown, but one has been traced on the surface for at least 2,700 feet. Some are offset by northwest-trending faults. Dike density does change significantly in the area, but this could be a function of large fragments of intrusive rock talus and large areas of tundra masking the dikes with talus and grus.

Miller [16] (1972a) determined that the alkalic dikes consist of pulaskite and pseudoleucite porphyry. Minerals reported include: Nepheline, one alkali feldspar, Melanite garnet, "pseudoleucite" phenocrysts, and accessory fluorite, among other minerals. Bornite, chalcopyrite, and allanite were observed in the field in some samples. Miller has been a prolific contributor to the geology of the Seward Peninsula through the 1970s, particularly for the Bendeleben and Solomon Quadrangles and their uranium potential and associated geological, geochemical, and geophysical features (such as in: Miller and Elliott, [6]1969; Miller, et al.,[9] 1972a and [11]1972b; Miller and Grybeck, [16] 1973; Miller and Bunker, [17] 1976; Miller, et al., [18] 1976a and [19]1976b; and Miller and Johnson, [20]1978. Earlier, Sainsbury also contributed and should be consulted when working in the subject areas such as: Sainsbury, et al., [21]1970a and [22]1970b; Sainsbury, et al., [23] 1972; and Sainsbury, et al.,[24] 1974).

Phase II preliminary petrographic analyses indicate that the plutons are intruded by a greater variety of dikes than previously reported by previous geologists. Lamprophyre (Location: D2-62: MC:17-L), aplite (Loc. C2-2: MC:22-G,) quartz latite (Loc. D2-9:MC:D-11), as well as pulaskite (Loc. D2-44:MC:16E), and a range of phonolite dikes, e.g, melanite (Loc. D2-48: MC:15-E; D2-44: MC:16E), amphibole (Loc. CZ-14: MC:22-F) and trachyte (Loc. D2-61: MC:16-K). Dikes of possible late-stage hydrothermal activity were also sampled, e.g., a siliceous hematitic dike (Loc. D2-34: MC: 13-C) and a silicite (rhyolite), with massive fine-grained pyrite (Loc. C2-16: MC: 19-H).

Metamorphic Rocks: Previous studies have divided the metamorphic rocks of the area into a number of units. Those described by Miller, et al. [5] (1972) have been temporarily retained as indicated in [Plate II](#). Of particular interest are three of the units e.g., a Precambrian schistose marble (p€sm), a separate Precambrian marble (p€m), and a Precambrian graphitic schist and metasiltstone (p€gs) (Winkler, [25]1967).

The contact between the intrusive Cretaceous alkaline rock unit (Kkg) and the Precambrian schistose marble (p€sm) received considerable attention during our field investigations as potential sites for mineralization. Where exposed, the contact appeared to be fault controlled. In one location (Loc. D2-52: MC: 13-D), anomalous radiometric readings were reported near the contact (see [Figure 12](#)), and slightly mineralized zones within the carbonate unit were noted at Location D2-46 (MC: 16-F). In the area of sample D2-PEL-2, other samples have shown anomalies in arsenic (D2-PEL-3) exhibiting 4,000 ppm arsenic and other minor metals.



Figure 12: Aerial Oblique View of Contact of Carbonate Unit (p€sm) with Intrusive (Kkg). Looking North in Vicinity of Hill 1380, Approximately 4 Miles North of Mt Kachauik.

It might be significant that the other carbonate unit (p€m) is probably associated with the silver mineralization of the now defunct Omilak mine. The old mine is approximately one mile northeast of the Omilak airstrip and northeast of the northern area of interest (see [Plate IA](#)).

Phase II field reports of the Precambrian schistose marble (p€sm) around the intrusive alkaline rocks indicate that the carbonate unit consists, in general, of thinly bedded limestones and argillaceous limestones. Marble and more siliceous beds are reportedly of minor distribution. The unit ranges in color from buff and orange (weathered?) to medium light gray. The unit appears to be non-fossiliferous; structurally, the unit is tightly folded and exhibits evidence of several phases of deformation.

The Precambrian graphitic schist and metasilstone unit (Plate II pĕgs) also is of significance as a potential host rock for uranium and other types of mineralization. The unit was inspected in the field in an area to the southwest of the Dry Canyon Creek pluton (MC: 9-H). Field reports indicate that the unit is a siliceous metasedimentary unit composed of siltstone, graywacke, slate, phyllite, mica schist, and thin argillaceous carbonate beds. No fossils have been recovered from this group of rocks. Most of the unit has been affected by greenschist-grade metamorphism, and the rocks exhibit multiple foliations. The remaining metamorphic rocks of interest (pĕmc) are predominantly of amphibolite grade and are assumed to be equivalent to the above siliceous metasedimentary unit (pĕgs). Most of the rocks of the unit show a well-developed schistosity.

Quaternary Sediments: Climate has been the major factor controlling the Quaternary geologic history of the area. The climate in this area can be classified as a frost climate; that is, annual average temperature is below freezing and the formation of permafrost is ongoing. As a result, periglacial erosional and downslope processes predominate in the area, producing a characteristic landscape. Highly exposed areas are virtually rocky deserts and have been subjected to intensive frost heaving and glacial encroachment over the past few thousand years at least. Lower areas are covered either by solifluction lobes of debris, frost polygons or tundra, dense mats of low bushes, grasses and moss (Figures 4, 5, 6, and 13).

A soil profile has formed in the area. The soil can be characterized as an orange-brown azonal soil containing a humus-rich surface layer, an underlying clay-rich layer, and a lower layer of grus-like material (see Plate II - Exploration Pits and Figure 13). Rock fragments are common throughout the soil profile. Development of this type of soil is common in arctic areas. The humus-rich layer has potential significance to the northern area of interest and to the adjacent Tertiary basin. The latter would receive recharge from occasional meltwater to the shallow groundwater around the periphery of the subject basin, and after hundreds of years discharge fluids to ponds (as internal drainage) in the center of the basin (see "Discussion of Results").

Geophysical Setting

Aeromagnetic Mapping

As a guide to exploration, all available magnetics data and mapping were sought from the USGS and other sources. Miller, et al, [5] 1972 Produced a series of aeromagnetic maps of quadrangles for the subject areas of interest. This coverage was flown in 1971 at a flight altitude of 1,000 feet. The scale of quadrangles is 1:63,360 and is referenced as Solomon quadrangles D-1, D-2, C-2, C-3, C-4, and B-2, B-3. These field maps have been digitally composited into Plate IV. Also see Decker & Karl (1977).

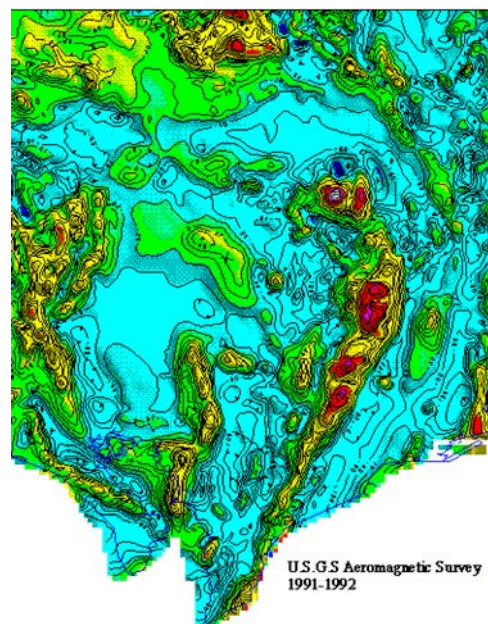


Plate IV: Compilation of Available Aeromagnetic Mapping.

(Map Shows Historical Aeromagnetic Coverage of Areas of Interest, and Identified Dipole)

The composite map of Plate IV shows the three areas of interest and the dipole anomaly near the top of the map, the latter of which shows the presence of an intrusive body covered by marsh sediments or a shallow highly magnetic mass. There are a number of other magnetic highs shown on the map. The core trend of the Darby Range runs north by northeast. Two major magnetic highs are indicated north and south of the eastern section of the central area of interest. A secondary magnetic high also occurs within the central section of the central area on interest. A prominent magnetic high also occurs northwest of the central area of interest. But both the northern and southern areas of interest are located in areas of generally low magnetic susceptibility. The mineralized zone of high radioactivity is clearly in an area of low magnetic susceptibility.

The relatively large, isolated dipole anomaly, located northwest of the northern area of interest, would appear to be below Tertiary basin sediments (the USGS estimated that this basin contained about 16,000 vertical feet of Tertiary sediments.). The configuration of the dipole is [Plus 5300] [minus or less than 4900 units], covering an area of about 3,000 acres, seems to be unrelated to the magnetic high and generalized lows to the east a few miles from the basin's surface expression. Whether this anomaly represents the rebounded central igneous/volcanic core resulting from an asteroid or comet impact or a segregation of magnetic minerals in rocks at or below the bottom of the crater remains uncertain. However, the geologic map of Foley and Barker) [26] (1986) shows:

- a. An impact creating McCarthy's Marsh with a meteor/comet entry from the southwest,
- b. A companion smaller impact creating Death Valley,
- c. Both impacts resulting in area volcanics and faulting within the Bendeleben and Darby Mountains beginning in the Cretaceous period (?) (Foley and Barker [27] (1980)), and
- d. Sedimentation and basin fill of craters during the Tertiary with continuing volcanism in some areas.

Any drilling (coring or cuttings) should be examined at or near the basin contact with the basement rock for indications of iridium, shocked quartz, or other petrographic or lithologic features for tell-tale signs of an impact, which based on the size of the crater (some 30 miles in diameter) should have readily apparent characteristics (e.g. see Wise and Campbell, [28], 2018, pp. 128-131) The areas discussed in this paper are also shown in the above Till-USGS map. Age dating of the carbon from this impact (if confirmed) should be interesting, e.g. Chicxulub impact crater ([more](#)).

Radiometric Mapping

During the Phase II field reconnaissance program, both geologic and radiometric data were recorded. [Plate III](#) summarizes the radiometric data collected. Aeroradiometric (slow, low-level helicopter surveys and ground radiometric surveys were conducted.



Figure 13: Ground View of Location of Exploration Pit #1(see [Plate III](#) and [IV](#)).
Hill 910: Loc. D2-2: MC: 6-I. Dry Canyon Pluton. Looking southward.

Aeroradiometric Surveys: Jones and Forbes [13] (1976) indicated two relatively large aeroradiometric anomalies, one over Kachauik Mountain and one over Hill 1420 (see Figure 10 and [Plate III](#)). During Phase I Omega operations, these reported anomalies were field checked and were generally confirmed (compare with [Plate IV](#)). This confirmation served to support other data that reinforced the potential for uranium and other mineralization in the central area.

During Phase II, the anomalous areas were examined via aerial traverses separated by approximately 1,000 feet. A Bell-Jet Ranger helicopter supported the Phase II reconnaissance program to facilitate a rapid preliminary assessment of the areas under consideration. The aeroradiometric surveys of the three areas of interest were conducted at an altitude of approximately five feet above the ground surface and at an air speed of approximately ten miles per hour. A Geometrics Model GR-101 scintillometer, positioned on the floor of the helicopter above the plastic front windscreen, was used to monitor gross gamma count during the reconnaissance surveys.

This positioning of the scintillometer proved to be effective in detecting relatively small variations in the ambient radiometrics. To check the responsiveness, we flew over and around the areas of known mineralization with high gamma counts. At any location where a significant increase in gamma count was noted, the helicopter was landed for a brief ground reconnaissance and collection of samples of interest at the location. Gross count was recorded and samples were taken, if merited. [Plate III](#) illustrates the general areas of aeroradiometric coverage.

Ground Radiometric Surveys: Ground radiometric surveys were conducted during all geological traverses. A Model 101 scintillometer was employed to record the local radiometric characteristics of both country rock and dike rocks. These data are shown on [Plate III](#). These radiometric surveys were conducted in the three areas of interest. [Plate III](#) presents the results of those surveys. It should be noted that the systematic surveys conducted in the central and southern areas of interest employed the Model 101 scintillometer, whereas the survey conducted in the northern area of interest employed a Model GR 310 spectrometer (Geometrics, Inc.). Uranium isotopes (Bi^{214}), thorium (Tl^{208}), and potassium⁴⁰ as well as total gamma flux were recorded for the principal purpose of evaluating the state and distribution of the degradation products of uranium constituents to determine whether leaching of uranium and daughter products has occurred.

The survey in the southern area indicates a highly radioactive zone which consists of abundant allanite mineralization. The radiometric survey also indicates the north-east trend of this zone (see [Plate III](#)). The north-south traverse shown in [Plate III](#) indicates two additional areas of possible mineralization, e.g., 1200-1400 north of Hill 2109 and near the northern termination of the traverse. The east-west traverse delineates a third anomalous area approximately 900 feet east of Hill 2109. The areas traversed do not exhibit conspicuous outcrops. Frost heaving and solifluction lobes of debris are common throughout the area. Therefore, although radiometric data from individual stations might be meaningful, radiometric trends indicated by a number of stations are considered to be of value in assessing the radiometric characteristics of in-place rocks, although some downhill transport of large blocks would be expected. Excavation will be required to evaluate many of the radiometric anomalies encountered now covered by glacial products, grus and talus.

A systematic northwest-southeast ground survey was also conducted in the large central area of interest. This survey was designed to evaluate the radiometric characteristics of the contact region between the migmatite unit (Mi) and the monzonite-syenite unit of the Burnt Creek pluton (Kkms). Although at the area's threshold level of significance, the interval between 900 and 1,400 feet from point of survey's origin is of interest. This could define either the boundary between the two units or another zone of covered mineralization of unknown extent. Again, excavation will be required to evaluate this further.

As indicated earlier, a special ground radiometric survey was conducted on northern area with Geometrics, Inc. Model 310 spectrometer. Based on data presented by Eakins [29] (1977), the thorium: uranium ratio (reported via fluorometric analysis) was generally found to be in excess of 1:1 for the Dry Canyon pluton. However, during the Phase II program, the radiometric surveys over the same pluton indicated an excess of uranium (Bi^{214}) over thorium (Tl^{208}) along many intervals of the two traverses (see [Plate III](#)). Uranium disequilibrium, furthermore, does not apparently exist (see "Geochemical Investigations: Equilibrium Analyses").

As will be discussed within the geochemical section of this paper, selected samples of the Dry Canyon pluton exhibit uranium (fluorometric) content of greater than 50 ppm and up to 130 ppm, far in excess of any values reported by Eakin [29] (1977). A total of four samples from this pluton have been analyzed, two of which are clearly anomalous in uranium. Three shallow exploration pits were excavated to a maximum depth of 39 inches during the Phase II program in the radiometrically anomalous areas within the Dry Creek pluton of the northern area. [Plate III](#) summarizes the results of the radiometric logging of the pits (see Figure 13 above).

Of special note is the field log of Pit #3, which indicated a bottom-hole radiometric (Bi^{214}) high of 24 ppm, which is equivalent to 1,000 cps on the Model 101 scintillometer. Thorium concentrations, in this pit, were in excess of uranium but showed similar conditions as indicated during the ground traverses in the two other pits. Potassium⁴⁰ content did not decrease with depth as might be expected with less weathered rock. The weathered zone is apparently not a thin veneer in the area, but thicker than anticipated.

A plot of U vs. Th data below shows that the USGS concentrations from samples around the Darby and Granite Mountain region are exceeded by most of the U-Th concentrations for the Kachauik, Burnt Creek and Dry Canyon Creek areas. This indicates that both uranium and thorium concentrations from rock samples of these plutons are characteristically higher than the rock samples from the Darby pluton but not for the "weathered" sediment samples containing similar uranium, but less thorium than the URI rock samples, excluding those of the mineralized zone. The latter zone would also be available for leaching into the groundwater system of the McCarthy Marsh (and basin).

TABLE 4
COMPARISON OF ROCK TYPES FROM
KACHAUIK, BURNT CREEK, DRY CANYON PLUTONS AND OTHER AREAS

| PLUTON AND MAP UNIT (SEE PLATE II) | COUNTRY ROCK | DIKE ROCK |
|--|--|--|
| I. Kachauik Pluton | | |
| <u>Kkms Unit:</u> | Allanite Monzonite Nepheline Syenite Augite Syenite Allanite Amph.Syen.(BC) Quartz Monzonite(BC) Granophyre(BC) | "Pseudoleucite" Phonolite Granite Aplite Phonolite Melanite Phonolite Lamprophyre(BC)* |
| <u>Kkg Unit:</u> | Quartz Monzonite Microgranite Hornblende Biot.Grano. Biot.Horn.Granodiorite | Phonolite Hematitic Rock** Pulsatite Phonolite Pseudoleucite Melanite Phon. |
| II. Dry Canyon Pluton | | |
| <u>Kdns Unit:</u> | Nepheline Syenite Granite Allanite Neph.Syenite Pyroxene Amph.Monzonite Mafic Nepheline Syenite Hornblende Diorite Syenite | Phonolite Biotite Monzonite/Syenite |
| III. Other Rocks | | |
| <u>Mt Unit:</u> <u>Kdgm(D)***</u> <u>pEmc</u> <u>GM(HC)****</u> | Granite Feldspar Gneiss | "Silicite" Rhyolite** Monzonite Aplite |

*(BC) Rock sample from Burnt Creek Satellite pluton, included here with Kachauik pluton rock types.
**Strong evidence for late stage hydrothermal activity in area.
*** (D) From Darby pluton.
**** (HC) From Hunter Creek area of North Granite Mt. region (see Plate I: District #4).

(Click on Table to Enlarge)

Kachauik Pluton: Most of Kachauik pluton samples examined to date are quartz bearing, although some are undersaturated. The mafic minerals of this pluton are fairly typical of circumpacific granitic rocks. This pluton has been divided into two units, i.e., Kkg (granodiorites and quartz monzonites) and Kkms (monzonites and syenites) (See Plate II). The quartz monzonites are coarser grained, contain less plagioclase, and show greater evidence of alteration (metasomatism?) than the granodiorites. The monzonites could be older than the granodiorites within this pluton.

The granodiorites contain a light green hornblende (titaniferous?), which is not reported in the other unit or other plutons of the area. One example has also been cited of the hornblende containing a colorless core of augite, which is a typical feature of the Sierra Nevada type tonalites, and which commonly contains accessory allanite. Allanite mineralization has only been reported to date within the Kkms unit, although minor accessory allanite was reported in one rock sample of microgranite of the Kkg unit. For example, Miller [6] reported that allanite is common and sporadically distributed within the granodiorite unit (Kkg) and the monzonite-syenite unit (Kkms); allanite is also present in many regions of the Seward Peninsula and Canada as a common accessory mineral.

Burnt Creek Satellite Pluton: This pluton appears to be a satellite intrusive to the Kachauik pluton. Plate II includes only the Kkms unit for this pluton, although other rock types have been reported (see Table 4). Accessory allanite appears to be common in this area as in other Kkms areas to the west. Nepheline, however, appears to be less abundant and plagioclase appears to be more abundant than in either Kkg, Kkms (west) or the Kdns (of the Dry Canyon Pluton) in the northern area.

Dry Canyon Creek Pluton: Nepheline is fairly abundant in the syenites of this pluton. Sodic amphibole and pyroxene are present, and the mineral cancrinite is also present. Radiation damage is very common in the biotite and hornblende as a result of the radiogenic zircon, apatite, and sphene inclusions. The pluton also contains an estimated average content of 10% mafic minerals, although the mafic content can vary considerably. Muscovite might be primary in a few of the samples examined.

Jones and Forbes [13] conducted a brief reconnaissance and sampling program on the Dry Canyon pluton. The principal results of their thin-section examinations are as follows:

- The predominant rock type is a hornblende-biotite nepheline syenite, but a hornblende-aegerine-augite alkali gabbro was also reported.
- The potassium feldspar is anorthoclase and occurs as subhedral grains, often showing a mottled scotch-plaid twinning, distinctively different from that found in microcline.
- Nepheline, which constitutes up to 35% of the rock, is in interstitial crystals, which have been largely altered to cancrinite. Often the anorthoclase and nepheline show evidence of exsolution structures including graphic and myrmekitic intergrowths, and what Bowen (1928) described as a fingerprint texture.

- d. The pyroxene is most common in the alkali gabbros where it is distinctively zoned, showing sodium enrichment towards the rim and a strong augite component towards the center of the crystal. Pyroxene constitutes up to 25% of some of the rocks sampled.
- e. Brownish hornblende is found in both the leucocratic and mesocratic varieties, sometimes as reaction rims around the pyroxene, and in other cases rimmed by biotite.
- f. The predominant texture is one that appears to be glomeroporphyritic, but might actually be a relict texture resulting from the exsolution of large subhedral leucite crystals, in a matrix of mafic minerals, predominantly biotite. The texture appears as circular aggregates of nepheline and anorthoclase, surrounded by bands of biotite and hornblende. Flow banding, or perhaps a minor shearing of the rock during the latest stages of crystallization, has caused some distortion and elongation of the pseudoleucite cross-sections. This period of deformation was not very severe, because little evidence of cataclastic deformation is evident along grain boundaries.
- g. The margins of some biotite crystals are black and appear similar to the pleochroic halos surrounding the inclusions in the biotite. This distortion of the pleochroism along grain margins shows that either adjacent minerals or previous minerals or fluids contained uranium in not insignificant amounts.
- h. A light colored garnet, perhaps andradite, is reported to occupy a substantial volume of the rock in some samples (up to 4%). The garnet occurs as anhedral grains in roughly circular swarms, indicating that a number of these small equivalent grains were part of a much larger garnet crystal.
- i. Melilite, characterized by high relief, low birefringence, a uniaxial negative sign, and light yellowish color, has been reported in a few samples to constitute up to 6% of the rock. This mineral occurs as small interstitial grains and occasionally as elongate subhedral crystals up to one mm in length. Carbonate is reported in all samples examined in minor or accessory amounts.

Jones and Forbes [13] also concluded that it was difficult to distinguish whether the carbonate is the result of remobilization of calcite or dolomite from the nearby metamorphic units (p€sm or p€m), or if it is primary. The carbonate grains are very small, usually 0.1 mm in size. They are anhedral but do not appear to be restricted to vein areas, nor do they appear to be replacing other minerals. The fact that the carbonate minerals are found in many samples as disseminated grains, along with the coexistence of melilite in these rocks strongly supports a primary origin. Carbonate-bearing vein rocks of primary origin have been reported in the Selawik Hills area [13].

Dikes: Table 4 indicates six fundamental types of dikes reported to date: 1) various types of phonolites, 2) aplites, 3) a monzonite/syenite, 4) a lamprophyre, 5) a hematite-dike and 6) a “silexite” rhyolite with massive fine-grained pyrite.

The phonolite dikes consist primarily of potash feldspar, probably orthoclase, with some microcline. The potassium feldspar occurs as laths with simple twinning and forms a trachytic flow structure. One feldspar phenocryst appears to be concentrically (or rhythmically) zoned. It is not twinned and lower in sodium than plagioclase inclusions. Such inclusions indicate early crystallization and late reaction with the magma. Nepheline is also common and constitutes up to 15% of the rock. Another feldspathoid identified is cancrinite, which forms a few interstitial grains.

Pseudoleucite is present in some samples and forms a “granophyric” intergrowth of K-spar and nepheline. Other non-mafic minerals include fluorite, purple to colorless, and a number of other minerals, unidentified at this date. Mafic minerals range from biotite and brown melanite garnet (euhedral) to numerous, very dark amphiboles or pyroxenes of various shades of green. The garnets usually show strong color zoning. The mafic minerals also include dark brown amphiboles that have black rims, as possible results of deuteric or metasomatic alteration. Aegerine appears to be altered in many cases.

Comparative Mineralogy: The following is a comparison of the mineralogy from (Table 3) for each pluton area (Burnt Creek has been included as Kkms for quartz only). See [Appendix I](#) and [Appendix II](#) for additional petrographic information.

Quartz:

| Southern Area | | | Central Area | | | Northern Area | | |
|---|--------------|------|---|--------------|------|---|--------------|------|
| Kkg Area | | | Kkms Area | | | Kdns Area | | |
| Total Samples | Country Rock | Dike | Total Samples | Country Rock | Dike | Total Samples | Country Rock | Dike |
| 10 | 5 | 1 | 18 | 4 | 2 | 10 | 3 | 1 |
| % Samples where Quartz Reported: 60% | | | % Samples where Quartz Reported: 33% | | | % Samples where Quartz Reported: 40% | | |

Orthoclase: Only the dike rocks of the Kkms unit of the Kachauik pluton have been reported to date to contain orthoclase. Additional work will not likely support this limited distribution.

Nepheline: Content is significantly less in the Kkg unit than the Kkms (Kachauik and Burnt Creek Plutons) and Kdns (Dry Canyon Creek Pluton).

Cancrinite: Is conspicuously common in phonolite dikes of the Kkms unit within the Kachauik pluton. Has not been reported in samples of Burnt Creek pluton. Of the eight dikes sampled in the Kkms unit (Kachauik pluton) four contain cancrinite. Of the four dikes sampled in the Kkg unit, only one contains cancrinite.

Allanite: The occurrence of this mineral will be discussed in greater detail later in this report. The petrographic characteristics and general distribution of allanite are described in [Appendix I](#) and [II](#). It should be noted here that the allanite mineralization appears to be post-zircon, post-plagioclase and post-hornblende.

Various rock types in which allanite has been recorded to date are summarized below:

1. *In Monzonite (2 occurrences) in Kkms unit (K) (see [Appendix I](#) and [II](#): Sample C2-1 Series, C2-17 Series). Also note that the green hornblende, dark augite, and at least two varieties of allanite, i.e., e.g. the brown variety altering to the yellow variety. The varieties can be based on the high concentrations of manganese and cerium, and speculating that the form might be much older than the light yellow cerium-rich variety of allanite.
2. In Monzonite (1 occurrence) in Kkms unit (BC) (see [Appendix II](#): Sample C2-28).
3. *In Amphibole Syenite (1 occurrence) in Kkms unit (BC) (see [Appendix II](#): Sample D2-30).
4. In Quartz monzonite (1 occurrence) in Kkms unit (BC) (see [Appendix II](#): Sample D2-39).
5. In Microgranite (1 occurrence) in Kkg unit (see [Appendix II](#): Sample D2-44).
6. *In Nepheline syenite (1 occurrence) in Kdns unit (DC) (see [Appendix II](#): Sample D2-12).
7. In Granite (1 occurrence) in Darby Pluton (see [Appendix II](#): Sample C2-DP-1).
8. In Monzonite aplite (1 occurrence) in North Granite Mt. area (see [Appendix II](#): Sample HC-2).

*Geochemical anomalies in uranium, etc. (see "Geochemical Investigations").

Epidote: Only reported in Burnt Creek pluton area in quartz monzonite and quartz diorite.

Hornblende and Biotite: These minerals are ubiquitous, color variations in hornblende from brown to green in thin section, altering to/from allanite?

Muscovite: Sporadic occurrences, no relationships established to date.

Aegerine: Only reported in country rocks and one dike rock of Kkms unit (Kachauik pluton) and in country rock only of Kdns unit (Dry Canyon Pluton). Not reported in Kkg unit or Kkms (or Burnt Creek Pluton).

Augite: Only reported from Kkms unit (K) in a syenite and from Kdns unit (DC) in a monzonite and a syenite.

Diopside: Only two occurrences reported: one in a dike (granite aplite) within the Kkms unit (K) and one from a lamprophyre within the Kkms unit of the Burnt Creek Pluton.

Melanite: Reported only in dike rocks: one phonolite within the Kkms unit (Kachauik pluton), one phonolite within the Kdns unit (DC), but three phonolites of the Kkg unit (Kachauik pluton).

Chlorite: Conspicuously absent in Kkms unit (K) but reported in lamprophyre in Kkms unit of the Burnt Creek Pluton. Four occurrences in Kkg unit (K) in: 1) quartz monzonite; 2) two granodiorites, and 3) one phonolite. Also reported in granite of Darby Pluton [27] (1980).

Clinzoisite: Two occurrences reported: one in pCmc unit and one in syenite of Kdns unit of Dry Canyon Pluton.

Olivine (?): A tentative identification in lamprophyre within Kkms unit of Burnt Creek Pluton.

Zircon: Locally abundant in allanite mineralized samples. Typical accessory in most other samples and plutons.

Apatite: Common as an accessory mineral in country rock of most samples, but present in only one dike rock (granite aplite) sampled near one of the allanite mineralized zones.

Sphene: Common in all samples as an accessory mineral. Unusually abundant in the allanite mineralized samples.

Monazite: Reported to date in only two samples: one in an allanite mineralized zone sample of monzonite and one in syenite of Kdns unit of Dry Canyon Pluton.

Fluorite: Reported only from dike rocks of Kkms unit (K. and BC) and one from within Kdns unit (DC). None reported in dikes within Kkg unit (K). It should be noted that fluorine was reported in unusually high concentrations in whole-rock samples that also contain abundant allanite (see Table 6).

Opaques: Reported only from dike rocks of Kkms (K arid, BC) and from only mineralized allanite monzonite samples. Also abundant in p̄esm carbonate unit near Kkg contact within Kachauik Pluton (Location 13-C)

Rutile: One reported occurrence in Kkms unit of mineralized allanite monzonite rock. Four occurrences reported in Kkg unit (K) in: 1) hematitic rock, 2) pulaskite phonolite, and 3) two in phonolites.

Pyrite: Two occurrences reported: one as dike within Mi unit (massive); another report of scattered pyrite mineralization within p̄esm carbonate unit near contact with Kkg unit (western area of central claim block: MC: 17-E).

Primary Calcite (?): Reported only from one sample to date: lamprophyre dike of Kkms unit of Burnt Creek Pluton.

Bornite (?): Reported tentatively in phonolite dike within Kkg unit (K).

Hematite: Reported from highly altered dike north of thermal spring area within Kkg unit of Kachauik pluton (MC: 14-C). Strong evidence for late stage hydrothermal activity in the area;

Barite: Based on mineral identifications conducted by personnel at the Colorado School of Mines Research Institute (CS: MRI) during sink-float analyses of allanite mineralization, XRD analyses indicated barite (see “Preliminary Geochemical Investigations” and discussed in [Appendix III](#)).

Magnetite: Identification made by CS: MRI as above: probably titan magnetite (see “Preliminary Geochemical Investigations” and [Appendix III](#), and Opaques discussed above). Should be noted that iron has been reported as major constituents in most samples obtained to date. Further, there are two magnetic anomalies in the central area (See Table 10), and as isolated, conspicuous dipole anomalies located northeast of the northern area of interest below McCarthy’s Marsh, and in the northern rim of the Death Valley area.

Siderite: Identification made by CS: MRI in one of three allanite samples examined (see ‘Preliminary Geochemical Investigations’ and [Appendix III](#)).

Uraninite: Identification made by XRD investigations conducted personnel at Rice University, Department of Geology (see [Appendix III](#)).

Leucite, Sodalite and Lepidolite: Identification made by XRD investigations conducted at Rice University, Department of Geology (see [Appendix III](#)).

A discussion of the implications and ramifications of the minerals reported (or indicated) to date is presented later in this paper (see “Discussions of Results”).

Geochemical Investigations

Introduction: Of the 100 rock samples taken in the field, approximately 50 were selected for thin-section preparation and preliminary petrographic analysis, as indicated previously. The selections were made on the basis of the rock sample’s apparent anomalous characteristics or for the purpose of investigating the fundamental petrographic nature of the rock types in the areas of interest under consideration.

Element Scan: Based on the results of the preliminary petrographic analysis, approximately 18 rock samples were selected from those previously selected for thin-section analysis and submitted to Commercial Testing and Engineering Laboratories (CT & E) in Denver, Colorado for chemical analysis. Initially, CT & E conducted a total element scan (via the spark source method) on each sample (see [Appendix III](#) for discussion of analytical methods, sample preparation and analytical error and precision considerations). Table 5 is a summary of the results of the elemental scan. The results are grouped according to the respective three areas of interest.

Although the results of the element scans are of limited value in establishing precise elemental abundance, the results do indicate relative abundance and are perhaps within $\pm 100\%$ to 200% of actual content. The utility of this method is in the comparison of the relative abundance reported for each element. Because of the strong bias involved in the field sampling procedures and in the selection of samples to be analyzed, statistical geochemical treatment of the results would be of limited value.

In order to identify possible anomalies within the samples scanned, a four-fold discrimination procedure was developed. First, four samples are considered mineralized (C2-1 Series and C2-17 Series); they contain at least one element of sufficient abundance to be of economic interest. These samples serve as a baseline for other analyses in determining a geochemical anomaly within the three areas under consideration. Second, if the indicated abundance approaches an order of magnitude higher than other results, (excluding the mineralized samples), the sample is considered strongly anomalous.

Third, Hawkes and Webb [30] (1962) present data on “normal” and anomalous geochemical content for various types of rocks. Again, if the sample is above “normal” it is considered as a “threshold anomaly.” If it is above by more than an order of magnitude, it is considered highly anomalous. Fourth, if, based on the experience of URI personnel, the reported values are considered high, they are defined herein as either a “threshold anomaly” or highly anomalous. It should be emphasized here that in the absence of a considerably greater number of samples, the available data cannot serve as a basis for a statistical determination of geochemical threshold values. However, a preliminary, systematic approach to defining a geochemical anomaly has been adopted and implemented during the URI Phase II investigations.

TABLE 5
WHOLE ROCK ANALYSES
(TOTAL MAJOR, MINOR & TRACE ELEMENT SCAN)
(ppm)

| SAMPLE LOC. | SAMPLE # | ROCK NAME | U* | Th* | Bi | Tl | Hg | As | Pb | Ir | Os | Re | W | Ta | Hf | Lu | Yb | Tm | Er | Ho | Dy | Tb | Gd | Eu | Sm | Nd* | |
|----------------------|----------|------------------------------|-----|-----|-----|------|----|----|----|----|----|----|----|----|----|----|----|----|----|----|----|----|----|----|----|-----|----|
| Southern Area | | | | | | | | | | | | | | | | | | | | | | | | | | | |
| C2-1 | C2-1** | Allanite Monzonite | MC | MC | 26 | 0.8 | NR | NR |
| C2-1 | C2-1A** | Allanite Monzonite | MC | MC | 15 | 20 | NR | NR |
| C2-1 | C2-1C** | Allanite Monzonite | MC | MC | 16 | 2 | NR | NR |
| C2-1 | C2-3 | Nepheleline Syenite | 24 | 150 | NR | 1 | NR | NR |
| C2-6 | C2-16 | Nepheleline Phonolite | 14 | 0.7 | 44 | 3 | NR | NR |
| C2-6 | C2-17** | Allanite Monzonite | MC | MC | 12 | 2 | NR | NR |
| C2-14 | C2-26 | Amphibole Phonolite | 30 | 18 | 2 | 5 | NR | NR |
| C2-14 | C2-27 | Augite Syenite | 30 | 81 | 0.4 | 5 | NR | NR |
| Central Area | | | | | | | | | | | | | | | | | | | | | | | | | | | |
| C2-15 | C2-28 | Allanite Monzonite | 52 | 180 | NR | 2 | NR | NR |
| C2-17 | D2-30 | Allanite Amphibole Syenite | 110 | 300 | 0.6 | 3 | NR | NR |
| D2-44 | D2-52 | Melanite Phonolite | 30 | 81 | 0.4 | 5 | NR | NR |
| D2-44 | D2-53 | Horn. Biotite Grandiorite | 3 | 17 | NR | 1 | NR | NR |
| D2-48 | D2-57 | Melanite Phonolite | 67 | 200 | 0.7 | 4 | NR | NR |
| D2-61 | D2-65 | Tremolite(?) Phonolite | 320 | 30 | 0.2 | 1 | NR | NR |
| Northern Area | | | | | | | | | | | | | | | | | | | | | | | | | | | |
| D2-2 | D2-8 | Nepheleline Syenite | 15 | 61 | 0.2 | ±0.5 | NR | NR |
| D2-2 | D2-9 | Nepheleline Phonolite | 11 | 140 | 2 | ±2 | NR | NR |
| D2-3 | D2-11A | Granite | 11 | 260 | NR | 1 | NR | NR |
| D2-3A | D2-12 | Allanite Nepheleline Syenite | 22 | 270 | 0.5 | 2 | NR | NR |

*Element reanalyzed (XRF, etc.). See Table 2 (vt.1). Not included in trace element content summary.
 **Considered mineralized.
 NR=Not reported.
 MC=Major component (±0.1%).
 — Considered anomalous.
 = Considered strongly anomalous.

TABLE 5 (cont.)
WHOLE ROCK ANALYSES
(TOTAL MAJOR, MINOR & TRACE ELEMENT SCAN)
(ppm)

| SAMPLE LOC. | SAMPLE # | ROCK NAME | Ge | Ga | Zn | Cu | Ni | Co | Fe* | Mn* | Cr | V | Ti* | Sc | Ca* | K* | Cl | S* | P* | Si* | Al* | Mg* | Na* | F* | O | H | |
|----------------------|----------|------------------------------|------|------|-----|----|------|------|-----|-----|-----|-----|-----|------|------|-----|----|----|----|-----|-----|-----|-----|----|----|----|----|
| Southern Area | | | | | | | | | | | | | | | | | | | | | | | | | | | |
| C2-1 | C2-1** | Allanite Monzonite | 8 | 250 | 50 | 23 | 3 | 0.6 | MC | MC | 7 | 140 | MC | 4 | MC | MC | MC | MC | MC | MC | MC | MC | MC | MC | MC | MC | NR |
| C2-1 | C2-1A** | Allanite Monzonite | ±0.2 | 6 | 56 | 3 | 0.9 | 1 | MC | MC | 17 | 64 | MC | 0.4 | MC | 4.3 | 59 | MC | MC | MC | MC | MC | MC | MC | MC | MC | NR |
| C2-1 | C2-1C** | Allanite Monzonite | 9 | 300 | 27 | 12 | 0.9 | 0.7 | MC | MC | 3 | 30 | MC | 53 | MC | MC | MC | MC | MC | MC | MC | MC | MC | MC | MC | NR | |
| C2-1 | C2-3 | Nepheleline Syenite | ±0.7 | 52 | 260 | 9 | 6 | 1 | MC | MC | 14 | 120 | MC | 9 | MC | MC | MC | MC | MC | MC | MC | MC | MC | MC | MC | NR | |
| C2-6 | C2-16 | Nepheleline Phonolite | ±0.4 | 32 | 63 | 3 | ±0.1 | NR | MC | MC | 0.5 | 58 | MC | ±0.1 | MC | MC | MC | MC | MC | MC | MC | MC | MC | MC | MC | NR | |
| C2-6 | C2-17** | Allanite Monzonite | 16 | 500 | 99 | 9 | 3 | 0.5 | MC | MC | 2 | 110 | MC | 9 | MC | MC | MC | MC | MC | MC | MC | MC | MC | MC | MC | NR | |
| C2-14 | C2-26 | Amphibole Phonolite | ±0.2 | 28 | 100 | 3 | 2 | ±0.3 | MC | MC | 0.5 | 11 | 990 | 1 | MC | MC | MC | MC | MC | MC | MC | MC | MC | MC | MC | NR | |
| C2-14 | C2-27 | Augite Syenite | ±0.9 | 50 | 120 | 64 | 35 | 4 | MC | MC | 54 | 360 | MC | 44 | MC | MC | MC | MC | MC | MC | MC | MC | MC | MC | MC | NR | |
| Central Area | | | | | | | | | | | | | | | | | | | | | | | | | | | |
| C2-15 | C2-28 | Allanite Monzonite | ±0.4 | 50 | 56 | 11 | 2 | ±0.1 | MC | MC | 240 | 22 | 36 | MC | 3 | MC | MC | MC | MC | MC | MC | MC | MC | MC | MC | MC | NR |
| C2-17 | D2-30 | Allanite Amphibole Syenite | 1 | 48 | 95 | 4 | 3 | 1 | MC | MC | 4 | 110 | MC | 0.4 | MC | 4.3 | 59 | MC | MC | MC | MC | MC | MC | MC | MC | MC | NR |
| D2-44 | D2-52 | Melanite Phonolite | ±0.9 | 28 | 120 | 26 | 8 | 6 | MC | MC | 2 | 320 | MC | 11 | MC | MC | MC | MC | MC | MC | MC | MC | MC | MC | MC | NR | |
| D2-44 | D2-53 | Hornblende Biotite Grano. | ±0.2 | 13 | 60 | 3 | 4 | ±0.3 | MC | MC | 310 | 10 | 7 | MC | ±0.2 | MC | MC | MC | MC | MC | MC | MC | MC | MC | MC | NR | |
| D2-48 | D2-57 | Melanite Phonolite | ±0.9 | 28 | 120 | 11 | 3 | 4 | MC | MC | 2 | 140 | MC | 5 | MC | MC | MC | MC | MC | MC | MC | MC | MC | MC | MC | NR | |
| D2-61 | D2-65 | Tremolite(?) Phonolite | ±0.4 | 13 | 48 | 5 | 38 | 2 | MC | MC | 310 | 230 | 68 | MC | 5 | MC | MC | MC | MC | MC | MC | MC | MC | MC | MC | NR | |
| Northern Area | | | | | | | | | | | | | | | | | | | | | | | | | | | |
| D2-2 | D2-8 | Nepheleline Syenite | NR | ±0.6 | 51 | 1 | 2 | ±0.3 | MC | MC | 1 | 7 | MC | 2 | MC | MC | MC | MC | MC | MC | MC | MC | MC | MC | MC | NR | |
| D2-2 | D2-9 | Nepheleline Phonolite | 1 | 48 | 210 | 11 | 3 | 2 | MC | MC | 4 | 110 | MC | 2 | MC | MC | MC | MC | MC | MC | MC | MC | MC | MC | MC | NR | |
| D2-3 | D2-11A | Granite | ±0.3 | 20 | 36 | 7 | 2 | ±0.1 | MC | MC | 69 | 4 | 10 | MC | 2 | MC | MC | MC | MC | MC | MC | MC | MC | MC | MC | NR | |
| D2-3A | D2-12 | Allanite Nepheleline Syenite | 0.3 | 9 | 18 | 2 | 1 | 3 | MC | MC | 64 | 71 | 5 | 330 | 0.9 | MC | MC | MC | MC | MC | MC | MC | MC | MC | MC | NR | |

*Element reanalyzed (XRF, etc.). **Considered mineralized. *Element reanalyzed (XRF, etc.). See Table 2 (vt.1). Not included in trace element content summary.
 MC=Major component (±0.1%). NR=Not reported. — Considered anomalous. = Considered strongly anomalous.

TABLE 5 (cont.)
WHOLE ROCK ANALYSES
(TOTAL MAJOR, MINOR & TRACE ELEMENT SCAN)
(ppm)

| SAMPLE LOC. | SAMPLE # | ROCK NAME | Pb* | Ce* | La* | Ba* | Ce | I | Te | Sb | Sn | In | Cd | Ag | Pd | Bh | Bu | Mo | Nb | Zr* | Y | Sr* | Rb | Br | Se | As | |
|----------------------|----------|----------------------------|-----|-----|-----|-----|----|-----|------|-----|-----|-----|-----|----|----|----|----|----|----|-----|----|-----|----|----|----|----|----|
| Southern Area | | | | | | | | | | | | | | | | | | | | | | | | | | | |
| C2-1 | C2-1** | Allanite Monzonite | 990 | MC | MC | 360 | 28 | 2 | NR | 1 | 7 | STD | 2 | NR | NR | NR | NR | NR | NR | NR | NR |
| C2-1 | C2-1A** | Allanite Monzonite | 990 | MC | MC | 260 | 12 | 0.4 | 1 | 3 | 6 | STD | 64 | NR | NR | NR | NR | NR | NR | NR | NR |
| C2-1 | C2-1C** | Allanite Monzonite | MC | MC | MC | 11 | 5 | 0.7 | 2 | 8 | STD | 29 | NR | NR | NR | NR | NR | NR | NR | NR | NR | NR | NR | NR | NR | NR | NR |
| C2-1 | C2-3 | Nepheleline Syenite | 36 | 230 | 360 | MC | 10 | 7 | NR | NR | 6 | STD | 0.9 | NR | NR | NR | NR | NR | NR | NR | |
| C2-6 | C2-16 | Nepheleline Phonolite | 22 | 230 | 330 | MC | 14 | 2 | NR | NR | 0.6 | STD | 0.7 | NR | NR | NR | NR | NR | NR | NR | |
| C2-6 | C2-17** | Allanite Monzonite | MC | MC | MC | 720 | 5 | 7 | ±0.2 | 1 | 11 | STD | 9 | NR | NR | NR | NR | NR | NR | NR | |
| C2-14 | C2-26 | Amphibole Phonolite | 25 | 280 | 490 | 900 | 3 | 7 | ±0.4 | NR | 0.7 | STD | 0.3 | NR | NR | NR | NR | NR | NR | NR | |
| C2-14 | C2-27 | Augite Syenite | 40 | 280 | 490 | MC | 12 | 4 | NR | NR | 7 | STD | 0.6 | NR | NR | NR | NR | NR | NR | NR | |
| Central Area | | | | | | | | | | | | | | | | | | | | | | | | | | | |
| C2-15 | C2-28 | Allanite Monzonite | 10 | 280 | 490 | MC | 7 | 2 | NR | NR | 2 | STD | 1 | ±2 | NR | NR | NR | NR | NR | NR | NR | NR | NR | NR | NR | NR | |
| C2-17 | D2-30 | Allanite Amphibole Syenite | 75 | 320 | 420 | MC | 4 | 7 | NR | 6 | 12 | STD | 2 | NR | NR | NR | NR | NR | NR | NR | |
| D2-44 | D2-52 | Melanite Phonolite | 44 | 320 | 320 | MC | 4 | NR | 1 | NR | 1 | NR | STD | 1 | NR | NR | NR | NR | NR | NR | NR | NR | NR | NR | NR | NR | |
| D2-44 | D2-53 | Horn. Biotite Grandiorite | 5 | 24 | 44 | MC | 6 | 2 | NR | 0.3 | 2 | STD | 0.1 | NR | NR | NR | NR | NR | NR | NR | |
| D2-48 | D2-57 | Melanite Phonolite | 99 | 490 | 880 | MC | 28 | 2 | NR | 0.7 | NR | STD | 0.6 | NR | NR | NR | NR | NR | NR | NR | |
| D2-61 | D2-65 | Tremolite(?) Phonolite | 19 | 130 | 74 | MC | 5 | 2 | NR | 1 | NR | | | | | | | | | | | | | | | | |

TABLE 5 (cont.)
WHOLE ROCK ANALYSES
(TOTAL MAJOR, MINOR & TRACE ELEMENT SCAN)
(ppm)

| SAMPLE LOC. | SAMPLE # | ROCK NAME | C | B | Be | Li | H | Pb | TOTAL TRACE ELEMENT CONTENT (ppm) | ELEMENTS OF POTENTIAL SIGNIFICANCE*** |
|----------------------|----------|----------------------------|----|----|-----|-----|----|-----|-----------------------------------|--|
| Southern Area | | | | | | | | | | |
| C2-1 | C2-1A** | Allanite Monzonite | NR | 18 | 84 | NR | NR | 110 | 2,739 | (#)THRESHOLD ANOMALY |
| C2-1 | C2-1A** | Allanite Monzonite | NR | 18 | 32 | 12 | NR | 150 | 2,276 | -----Considered Mineralized----- |
| C2-1 | C2-1C** | Allanite Monzonite | NR | 9 | 15 | 6 | NR | 74 | 2,110 | -----"----- |
| C2-1 | C2-1 | Nepheline Syenite | NR | 4 | 3 | 22 | NR | 71 | 1,215 | (7)U, Th, Eu, Ce, La, Nb, Zr (1)Rb* |
| C2-6 | C2-16 | Nepheline Phonolite | NR | 9 | 7 | 90 | NR | 44 | 746 | (6)U, Th, Ce, La, Nb, Cl (0)----- |
| C2-6 | C2-17** | Allanite Monzonite | NR | 63 | 63 | 53 | NR | 120 | 3,612 | -----Considered Mineralized----- |
| C2-14 | C2-26 | Amphibole Phonolite | NR | 4 | 0.7 | 7 | NR | 250 | 922 | (7)U, Th, Ce, La, Zr, Zn, Cl (3)Bi*, Pb*, Nb* |
| C2-14 | C2-27 | Augite Syenite | NR | 18 | 3 | 180 | NR | 87 | 1,732 | (13)U, Th, Cd, Er, Sm, Ce, La, Y, Ga, Zn, Co, B (6)Mo*, Cu, Ni, Cr, V*, Se*, Li* |
| Central Area | | | | | | | | | | |
| C2-15 | C2-28 | Allanite Monzonite | NR | 8 | 7 | 53 | NR | 87 | 694 | (9)U, Th, Ce, La, Ag, Zr, Sr, Ga, S (1)Ag* |
| C2-17 | D2-30 | Allanite Amphibole Syenite | NR | 8 | 1 | 20 | NR | 130 | 850 | (18)U, Th, Er, Ho, Dy, Tb, Cd, Eu, Sm, Ce, La, Zr, Sr, Br, Ga, Zn, V, Se (3)Cs*, Sn, Rb* |
| D2-44 | D2-52 | Melanite Phonolite | NR | 4 | 3 | 530 | NR | 35 | 1,808 | (16)U, Th, Ho, Dy, Gd, Er, Sm, Ce, La, Zr, Y, Sr, Rb, Zn, Co, Se (3)Cu, V*, Li* |
| D2-44 | D2-53 | Horn. Biotite Granodiorite | NR | 9 | 2 | NR | NR | 17 | 442 | (2)U, Th (0)----- |
| D2-48 | D2-57 | Melanite Phonolite | NR | 2 | 1 | 27 | NR | 87 | 734 | (13)U, Th, Gd, Er, Sm, Ce, La, Ce, Zr, Y, Zn, Co, V (2)Nb*, Rb* |
| D2-61 | D2-65 | Tremolite(?) Phonolite | NR | 2 | 0.7 | 13 | NR | 7 | 619 | (2)U, Th (4)As*, Ni, Cr, S* |
| Northern Area | | | | | | | | | | |
| D2-2 | D2-3 | Nepheline Syenite | NR | 4 | 0.7 | 34 | NR | 44 | 895 | (3)U, Th, Cl (1)Rb* |
| D2-2 | D2-9 | Nepheline Phonolite | NR | 31 | 5 | 300 | NR | 130 | 1,422 | (13)U, Th, Gd, Er, Sm, Ce, La, Sr, Rb, Ga, Zn, V, B (6)Bi*, Mo*, Nb*, Li* |
| D2-3 | D2-11A | Granite | NR | 1 | 0.2 | NR | NR | 62 | 559 | (3)U, Th, Rb (0)----- |
| D2-3A | D2-12 | Allanite Nepheline Syenite | NR | 3 | 3 | 9 | NR | 51 | 898 | (5)U, Th, I, Rb, Cr (1)Ag* |

*Anomalous with respect to worldwide average content. **Considered mineralized. NR-Not reported. ----- Considered anomalous. ----- Considered strongly anomalous. ***Except as indicated by *, all other anomalies defined by relationship between indicated sample values contained herein.

Although based on a limited number of analyses, some samples appear to exhibit geochemical anomalies. In particular, some of the “pathfinder” elements that are commonly associated with certain types of economic mineralization are present in concentrations that appear to be significant, e.g., uranium, thorium, some rare earths, in addition to bismuth, lead, niobium, molybdenum, vanadium, scandium, lithium, silver, cesium, arsenic, sulfur, rubidium and possibly nickel, chromium, tin and copper (see Table 5, “Elements of Potential Significance”).

By inspection of (Table 5), five samples (C2-27 (Loc. C2-14:MC:22-F; D2-30 (Loc. D2-17:MC18-J); D2-52 (Loc. D2-33:MC:16-E); D2-57 (Loc. D2-48:MC:15-E); and D2-9 (Loco D2-2:MC:6-I) appear to be of special interest.

The former two are from country rock: the latter three are dike rocks. All contain anomalous uranium and other significant elements, indicating that both country rock (as indicated by C2-27 and D2-30, as well as the four mineralized samples (C2-1, C2-1A, C2-1C and C2-17: Loc. 21-G) and dike rocks are enriched in certain elements, although the two rock types are of different ages. This suggests that either mineralizing fluids were introduced during the intrusion of the dikes and thereby enriched the country rock, or that the magma, from which the country rocks crystallized, contained similar quantities of the anomalous elements, such as uranium, thorium, and rare earths, as well as the other anomalous elements indicated.

Sample D2-30 and C2-27 analyses are of particular interest in that they are from locations within the central area that are on the general northeast trend to the strike of the dike and associated mineralized zones of the southern claim group (see Plate II).

Similar types of mineralization are indicated by samples: D2-52, D2-57 and D2-9 dike samples within the central and northern areas of interest. Both igneous segregations and dike (or structurally controlled) occurrences of uranium and associated elements are considered possible.

A third general type of mineralization (and future exploration target) was also under investigated. A skarn-type of mineralization might be present at or near the contacts of the intrusives and the psm carbonate units in the central area of interest. A preliminary evaluation of some of the carbonate units sampled show abundant opaques of possible pyrite and other metal sulfides.

As indicated earlier, two magnetic anomalies occur in the central area, one near the contact with the pluton with the carbonate unit (see Table 10). Furthermore, it appears that the country rock intrusives as well as the dikes may have contained abundant mineralizing fluids which, upon encountering carbonate rocks having sufficient permeability, would have precipitated significant quantities of metals or other skarns of mineralization.

A thermal spring reported near the contact with of the Kachauk pluton with the carbonate unit that when combined with conspicuous fluorite, barite, siderite and other characteristic minerals, support this possibility. The genesis of uranium, thorium and rare earth-rich allanite (and associated minerals, e.g., monazite, sphene, etc., and the role they might have played in this third type of mineralization, will be discussed later in this paper (see “Discussion of Results”).

Major Elements: Some major elements are present as major components (MC), or are present in amounts equal to or greater than one thousand ppm, were reanalyzed via XRF or other appropriate methods in terms of weight percent as major element oxides (see Table 6).

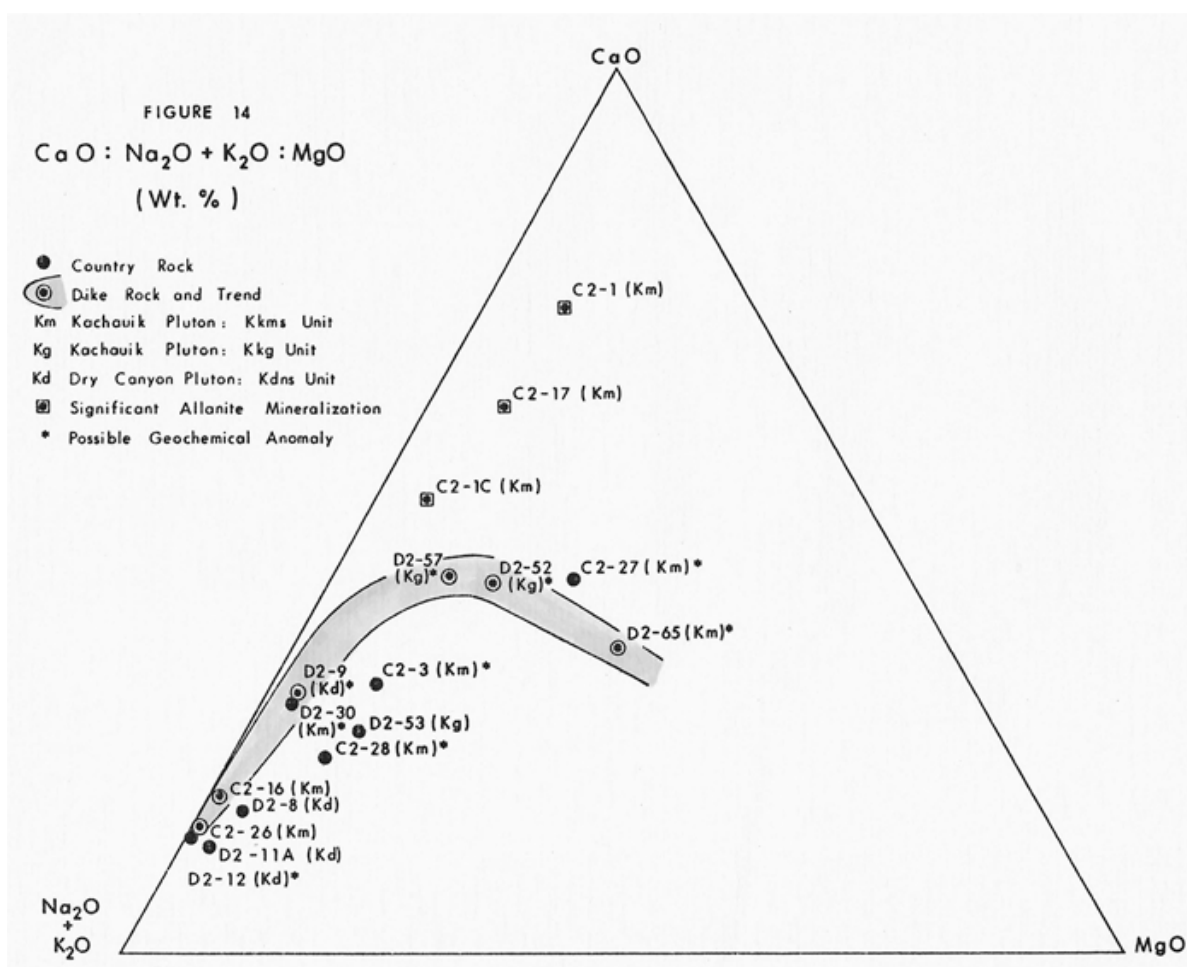
To characterize the rock types sampled, and to evaluate where the mineralized zones fit into the geophysical and geochemical anomalies in the area. a Na₂O + K₂O / CaO: MgO plot was prepared (Figure 14). Some clustering is noted with respect to samples from the Dry Canyon Creek Pluton. If such a plot is meaningful with regard to the relative extent of differentiation, then the Dry Canyon Creek pluton sample analyses are indicative of a pluton that is highly differentiated, relative to the Kachauk and related to the Burnt Creek plutons.

TABLE 6
WHOLE ROCK ANALYSES
MAJOR ELEMENTS*

| SAMPLE LOCATION** | SAMPLE # | ROCK NAME | (Wt. %) | | | | | | | | | | | TOTAL MAJOR ELEMENTS (%) | | | | |
|----------------------|----------|---------------------------------|------------------|--------------------------------|------------------|--------------------------------|-------|------|------------------|-------------------|-----------------|-------------------------------|------|--------------------------|------|------|--------------------------------|--------|
| | | | SiO ₂ | Al ₂ O ₃ | TiO ₂ | Fe ₂ O ₃ | CaO | MgO | K ₂ O | Na ₂ O | SO ₃ | P ₂ O ₅ | SrO | | F | BaO | Mn ₃ O ₄ | |
| Southern Area | | | | | | | | | | | | | | | | | | |
| C2-1 | C2-1 | Allanite Monzonite | 40.49 | 16.01 | 1.82 | 8.24 | 17.41 | 1.94 | 1.45 | 2.76 | 0.05 | 0.41 | 0.02 | 0.76 | 1.01 | 0.11 | | 92.48 |
| C2-1 | C2-1C | Allanite Monzonite | 49.51 | 17.98 | 0.94 | 4.80 | 8.79 | 0.82 | 5.69 | 1.74 | 0.02 | 0.19 | 0.04 | 0.34 | 0.83 | 0.05 | | 91.74 |
| C2-1 | C2-3 | Nepheline Syenite | 53.68 | 20.16 | 0.58 | 6.36 | 5.21 | 1.71 | 6.58 | 3.47 | 0.00 | 0.43 | 0.11 | 0.19 | 0.20 | 0.13 | | 98.81 |
| C2-6 | C2-16 | Nepheline Phonolite | 55.11 | 23.09 | 0.22 | 3.83 | 3.06 | 0.19 | 7.55 | 6.23 | 0.12 | 0.07 | 0.28 | 0.30 | 0.27 | 0.13 | | 100.45 |
| C2-6 | C2-17 | Allanite Monzonite | 44.48 | 16.75 | 1.63 | 7.76 | 11.99 | 1.50 | 3.79 | 2.17 | 0.00 | 0.06 | 0.02 | 0.47 | 1.23 | 0.09 | | 97.94 |
| C2-14 | C2-26 | Amphibole Phonolite | 56.44 | 22.78 | 0.13 | 3.59 | 2.52 | 0.05 | 6.81 | 7.89 | 0.00 | 0.09 | 0.20 | 0.62 | 0.06 | 0.14 | | 101.32 |
| C2-14 | C2-27 | Augite Syenite | 49.09 | 17.96 | 0.85 | 8.03 | 9.05 | 5.11 | 4.99 | 2.22 | 0.00 | 0.52 | 0.09 | 0.31 | 0.21 | 0.14 | | 98.57 |
| Central Area | | | | | | | | | | | | | | | | | | |
| C2-15 | C2-28 | Allanite Monzonite | 58.43 | 18.39 | 0.50 | 5.18 | 3.41 | 1.42 | 6.62 | 3.67 | 0.22 | 0.40 | 0.07 | 0.35 | 0.16 | 0.04 | | 98.91 |
| C2-17 | D2-30 | Allanite Amphibole Syenite | 58.93 | 19.55 | 0.50 | 4.70 | 4.37 | 0.44 | 7.15 | 3.36 | 0.00 | 0.17 | 0.12 | 0.12 | 0.21 | 0.10 | | 99.72 |
| D2-44 | D2-52 | Melanite Phonolite | 45.88 | 19.28 | 0.96 | 9.66 | 7.71 | 3.01 | 7.28 | 0.31 | 0.00 | 0.62 | 0.05 | 0.04 | 0.46 | 0.17 | | 95.43 |
| D2-44 | D2-53 | Hornblende Biotite Granodiorite | 63.87 | 18.37 | 0.30 | 3.15 | 3.66 | 1.54 | 4.62 | 4.45 | 0.00 | 0.15 | 0.07 | 0.01 | 0.12 | 0.08 | | 100.36 |
| D2-48 | D2-57 | Melanite Phonolite | 46.57 | 20.98 | 0.90 | 8.87 | 7.23 | 1.91 | 7.59 | 0.17 | 0.00 | 0.36 | 0.21 | 0.08 | 0.47 | 0.18 | | 95.52 |
| D2-61 | D2-65 | Tremolite(?) Phonolite | 55.07 | 16.27 | 0.68 | 4.49 | 6.91 | 6.53 | 3.27 | 3.21 | 2.27 | 0.36 | 0.07 | 0.14 | 0.11 | 0.09 | | 99.47 |
| Northern Area | | | | | | | | | | | | | | | | | | |
| D2-2 | D2-8 | Nepheline Syenite | 54.65 | 24.75 | 0.23 | 3.29 | 2.53 | 0.67 | 8.04 | 3.92 | 0.00 | 0.15 | 0.11 | 0.63 | 0.34 | 0.08 | | 99.91 |
| D2-2 | D2-9 | Nepheline Phonolite | 47.14 | 22.38 | 0.47 | 6.40 | 5.70 | 0.67 | 7.22 | 5.98 | 0.03 | 0.19 | 0.32 | 0.77 | 0.62 | 0.20 | | 98.09 |
| D2-3 | D2-11A | Granite | 70.33 | 16.10 | 0.27 | 2.21 | 1.54 | 0.34 | 5.93 | 4.72 | 0.00 | 0.10 | 0.03 | 0.89 | 0.10 | 0.02 | | 102.58 |
| D2-3A | D2-12 | Allanite Nepheline Syenite | 56.83 | 25.92 | 0.15 | 1.57 | 2.28 | 0.04 | 7.76 | 6.61 | 0.00 | 0.04 | 0.08 | 0.21 | 0.06 | 0.04 | | 101.59 |

*See Appendix III: Commercial Testing and Engineering Co., Instrument Analysis Division, Denver, Colorado.
**See Plates II and III.

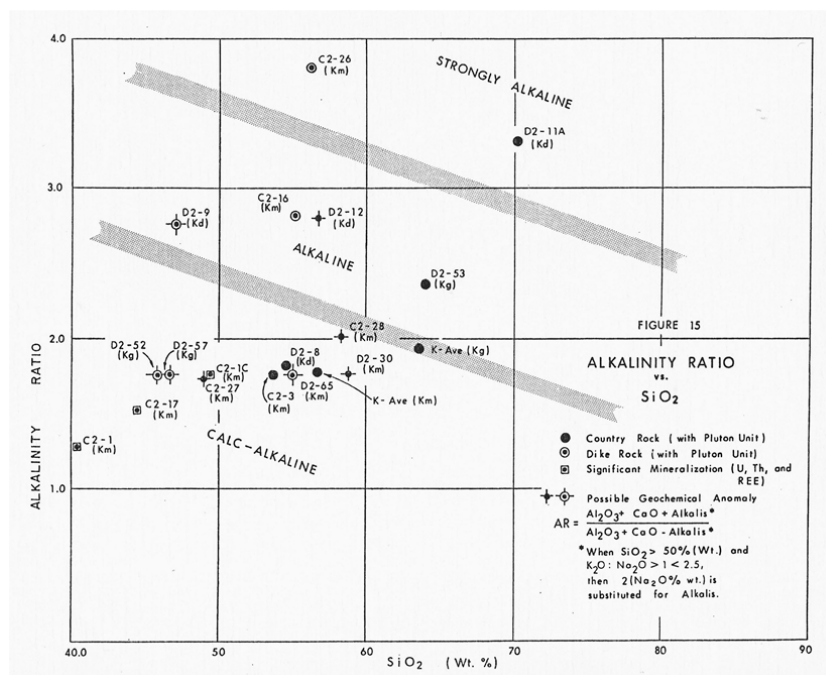
(Click on Table to Enlarge)



The mineralized allanite monzonite samples (C2-1, C2-1C, and C2-17) also show a trend in the plot, the significance of which, if any, is uncertain, but increasing CaO might indicate that carbonate fluids have been and still are in the subsurface geothermal groundwater system in the area as mineralizing fluids. There is one report of residual heat at the so-called Kachauik Hot Springs [31] (2005, p.55), also known as Battleship Mountain Hot Springs, are located 20 miles north of Golovin.

The spring is located on a small bedrock terrace on the eastern back of the east fork of Cliff Creek. The spring has a distinctive sulfur odor with a temperature of approximately 17°C. The host rock is granodiorite of the Kachauik pluton near its contact with Precambrian schistose marble [11].

The dike rock plots show a trend that supports the view that sample D2-65 is the least differentiated (and highly altered?) whereas sample C2-26 is highly differentiated (also highly altered?). Another plot illustrating the relation between the alkalinity ratio and the SiO₂ content of the whole-rock analyses available is presented in Figure 15.

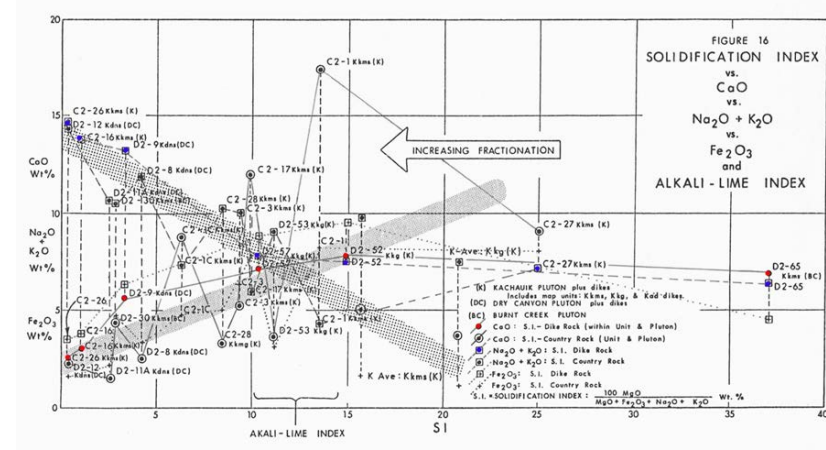


This plot indicates the calc-alkaline nature of the mineralized samples. Some segregation in the alkaline and strongly alkaline fields is also apparent. Note that mineralized samples (C2-1C, C2-17, and C2-1) show a trend toward depletion of SiO₂ in the Calc-Alkaline field. The chemical data from Miller & Bunker (1976) are also plotted as “K-Ave” for the two plots. A plot of the solidification index versus Na₂O + K₂O is presented in Figure 16.

This plot also includes an overlay of Saturation Index (SI) vs. CaO (wt%) and total iron (wt. %Fe₂O₃). It is interesting to note that the Dry Canyon Creek pluton samples appear to be the most fractionated (or differentiated), whereas the Kachauik pluton samples (Kkms unit - samples D2-65 and C2-27) are relatively unfractionated (undifferentiated) and plot in the basaltic range. The mineralized samples (C2-1, C2-1C, and C2-17) occupy a median position in the plot, although there is strong variability in reported geochemistry analyses at sample site C-1, and within the monzonite sampled (see Table 10).

The future utility of such plots might be in discriminating the extent to which late-stage alteration has modified the rocks’ initial composition. In general, the silica content of the samples analyzed ranges from strongly alkaline to calc-alkaline, the latter exhibited in samples C2-1 and C2-17 of the mineralized zones (Figure 15).

Based on the aluminum content, most samples are peraluminous, with the exception of C2-1 and C2-17, which are metaluminous (see Figure 10 for location and (Table 7) for ranges in wt. % of the major and minor oxides).

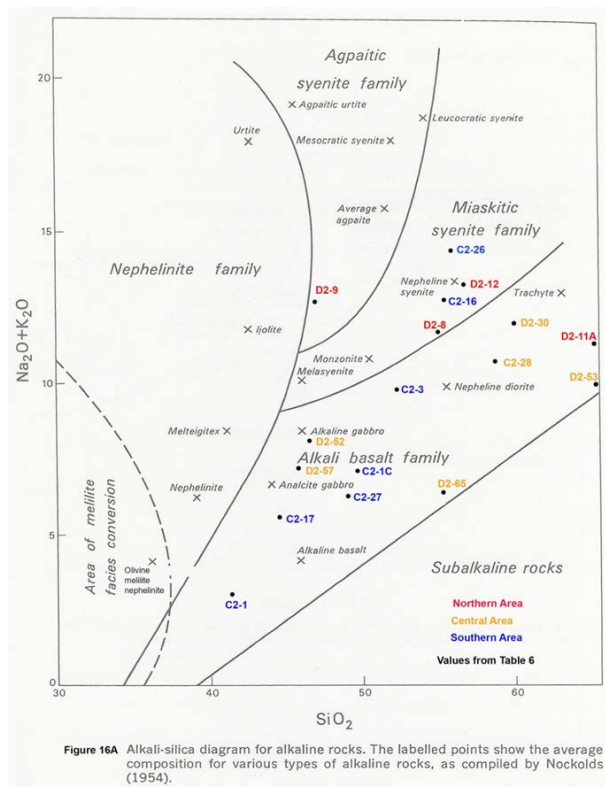


(Click on Figure to Expand for Clarity)

An alkali-silica plot in Figure 16A below indicates that samples from the southern area (blue) containing the mineralized zones range from the alkali basalt field to the miaskitic syenite field as the sodium and potassium oxides rise. Samples from the central area (orange) cluster with increasing silica and sodium + potassium.

The northern samples (red) plot upper fields ranging from high level alkali basalt to agpaite syenite field (near the nephelinite field). Currie [32](1973) indicated that the alkali versus silica plot of Figure 16A was recognized as an effective discriminator between alkaline and subalkaline rocks.

Currie emphasizes that chemically, strong differentiation is usually evident in the alkaline basalts, with SiO₂ rising from about 45 % in primitive samples to 60 to 62% in some trachytes, and Na₂O + K₂O varying from 5% to 11 to 13% in the same range. Mineralogically, some nepheline-rich alkaline basalts (basanites) show transitions to nephelinite. Alkaline basalt lavas are known to show strong temporal and geographic connection with agpaite complexes of plutonic character.



Young [33] (1989) concluded that the silica-saturation ratio is useful to categorize crystalline rocks according to their composition and silica saturation. Nockolds [34] provided the standard years ago on the average rock compositions. The ratio also provides petrologic inferences about the origin of granitic rocks, i.e., whether magmatic or metamorphic-metasomatic processes were involved. Supported by agreement with other independent methods (by using Al₂O₃ + Na₂O + K₂O in the rocks) regarding their origin, the petrologic inferences are valid and agree with geologic field data.

When comparing (Figure 16A) with (Figure 16), the mineralized samples (i.e., C2-1, C2-17, C2-27, and C2-1C) occupy the intermediate position in the fractionation trend, but overall fractionation ranges from a low with D2-65 to relatively high fractionation in sample C2-26 passing from field of alkali basalt to the miaskitic syenite field. (Table 7) presents a summary of the highest and lowest abundances of the whole rock major oxides of the samples analyzed.

TABLE 7
MINIMUM-MAXIMUM WHOLE ROCK
MAJOR AND SELECTED MINOR OXIDES

| OXIDE | LOW | | | HIGH | | |
|---|-----------------------------|------|-----------------------|----------|------|-----------------------|
| | SAMPLE # | WT.% | ROCK TYPE | SAMPLE # | WT.% | ROCK TYPE |
| Al ₂ O ₃ | C2-1 | 16.1 | Mineralized Monzonite | D2-12 | 25.9 | Neph.Sye. |
| | C2-17 | 16.8 | Mineralized Monzonite | D2-8 | 24.8 | Neph.Sye. |
| | D2-11A | 16.1 | Granite | C2-16 | 23.1 | Neph.Phono. |
| | D2-65 | 16.3 | Phonolite | C2-26 | 22.8 | Amph.Phono. |
| TiO ₂ | C2-26 | 0.13 | Amph.Phono. | C2-1 | 0.94 | Mineralized Monzonite |
| | D2-12 | 0.15 | Neph.Sye. | C2-17 | 1.82 | Mineralized Monzonite |
| | D2-12 | 1.6 | Neph.Sye. | D2-52 | 9.7 | Mel.Phono. |
| Fe ₂ O ₃ (TOTAL IRON) | D2-11A | 2.2 | Granite | D2-57 | 8.9 | Mel.Phono. |
| | C2-1 | | Mineralized Zone | C2-1 | 8.2 | Mineralized Zone |
| CaO | D2-11A | 1.5 | Granite | C2-1 | 17.4 | Mineralized Zone |
| | C2-26 | 2.5 | Amph.Phono. | C2-17 | 12.0 | Mineralized Zone |
| MgO | D2-12 | 0.04 | Neph.Sye. | D2-65 | 6.5 | Phonolite |
| | C2-26 | 0.05 | Amph.Phono. | C2-27 | 5.1 | Aug.Sye. |
| K ₂ O | C2-1 | 1.5 | Mineralized Zone | D2-8 | 8.0 | Neph.Sye. |
| | | | | D2-12 | 7.8 | Neph.Sye. |
| | | | | D2-57 | 7.6 | Mel.Phono. |
| Na ₂ O | D2-52 | 0.31 | Mel.Phono. | C2-26 | 7.9 | Amph.Phono. |
| | D2-57 | 0.17 | Mel.Phono. | D2-12 | 6.6 | Neph.Sye. |
| SO ₃ | Numerous At Detection Limit | | | D2-65 | 2.3 | Phonolite |
| | | | | D2-52 | 0.62 | Mel.Phono. |
| F ₂ O ₅ | D2-12 | 0.04 | Neph.Sye. | C2-27 | 0.52 | Aug.Sye. |
| | C2-17 | 0.06 | Mineralized Zone* | | | |
| | C2-16 | 0.06 | Neph.Phono.* | | | |
| SrO | C2-1 | 0.03 | Mineralized Zone | D2-9 | 0.32 | Neph.Phono. |
| | C2-17 | 0.02 | Mineralized Zone* | C2-16 | 0.28 | Neph.Phono.* |
| | D2-11A | 0.03 | Granite | | | |

* Country Rock - Dike Rock Sampling Pairs (See Sample Locations: Plate II)

TABLE 7 (CONTD.)
MINIMUM-MAXIMUM WHOLE ROCK
MAJOR AND SELECTED MINOR OXIDES

| OXIDE | LOW | | | HIGH | | |
|-----------------------------------|-----------------------------|-------|------------------|----------|-------|------------------|
| | SAMPLE # | WT. % | ROCK TYPE | SAMPLE # | WT. % | ROCK TYPE |
| Fe | D2-53 | 0.01 | Hn.Bt.Grano. | D2-11A | 0.89 | Granite |
| | D2-52 | 0.04 | Mel.Phono. | C2-1 | 0.76 | Mineralized Zone |
| | | | | D2-9 | 0.77 | Neph.Phon. |
| | | | | D2-8 | 0.63 | Neph.Sye. |
| | | | | C2-26 | 0.62 | Amph.Phon. |
| BaO | D2-12 | 0.06 | Neph.Sye. | C2-17 | 1.23 | Mineralized Zone |
| | C2-26 | 0.06 | Amph. Phon. | C2-1 | 1.01 | Mineralized Zone |
| Mn ₂ O ₄ | D2-11A | 0.02 | Granite | D2-9 | 0.20 | Neph.Phon. |
| | D2-12 | 0.04 | Neph.Sye. | D2-57 | 0.18 | Mel.Phon. |
| | C2-1C | 0.05 | Mineralized Zone | D2-52 | 0.17 | Mel.Phon. |
| ZrO ₂ | D2-8 | 0.005 | Neph.Sye. | C2-1C | 3.45 | Mineralized Zone |
| | D2-65 | 0.005 | Phonolite | C2-17 | 0.70 | Mineralized Zone |
| | D2-53 | 0.005 | Hn.Bt.Grano. | C2-1 | 0.16 | Mineralized Zone |
| | | | | D2-30 | 0.11 | Amph.Sye. |
| U ₃ O ₈ | Numerous at Detection Limit | | | C2-17 | 0.21 | Mineralized Zone |
| | | | | C2-1 | 0.21 | Mineralized Zone |
| | | | | C2-1C | 0.15 | Mineralized Zone |
| ThO ₂ | C2-3 | 0.001 | Neph.Sye. | C2-17 | 1.26 | Mineralized Zone |
| | | | | C2-1 | 1.22 | Mineralized Zone |
| | | | | C2-1C | 0.92 | Mineralized Zone |
| | | | | C2-17 | 1.59 | Mineralized Zone |
| Ce ₂ O ₃ ** | D2-11A | 0.02 | Granite | C2-1 | 1.29 | Mineralized Zone |
| | D2-65 | 0.02 | Phonolite | C2-1C | 0.95 | Mineralized Zone |
| | D2-8 | 0.03 | Neph.Sye. | D2-9 | 0.09 | Neph.Phon. |
| | D2-53 | 0.03 | Hn.Bt.Grano.* | D2-57 | 0.09 | Mel.Phon. |
| | C2-28 | 0.03 | Monzonite | D2-30 | 0.08 | Amph.Sye. |
| | C2-27 | 0.04 | Aug.Sye. | D2-52 | 0.07 | Mel.Phon.* |

* Country Rock - Dike Rock Sampling Pairs (See Sample Locations: Plate II)
**For Other Rare-Earth Oxides, See Table 8.

(Click on Table to Enlarge)

An unusual number of elements are represented in the dikes in the mineralized zone in the southern area of interest, although there are indications that other dikes that have not yet been identified are likely to also carry similar mineralization. The elements include: aluminum, titanium, calcium, magnesium, potassium, sodium, fluorine, barium, manganese, zirconium, and of course, uranium, thorium, and the rare earths. Iron is also likely present is high concentration in and around the two magnetic anomalies in the central area of interest (see Table 10 and [Plate IV](#)).

Minor Elements: Elements that are not usually included in major element analyses were reported as minor element oxides. These include: zirconium, uranium, thorium and four of the lanthanide group (neodymium, praseodymium, cerium, and lanthanum). Table 8 presents the minor elements in weight percent.

TABLE 8
WHOLE ROCK ANALYSES
MINOR ELEMENTS*

| SAMPLE LOCATION** | SAMPLE # | ROCK NAME | (Wt. %) | | | | | | | TOTAL MAJOR PLUS MINOR ELEMENTS (C) | TOTAL MAJOR PLUS MINOR PLUS TRACE (C) |
|-------------------|----------|--|------------------|-------------------------------|------------------|--------------------------------|--------------------------------|--------------------------------|--------------------------------|-------------------------------------|---------------------------------------|
| | | | ZrO ₂ | U ₃ O ₈ | ThO ₂ | Nd ₂ O ₃ | Pr ₂ O ₃ | Ce ₂ O ₃ | La ₂ O ₃ | | |
| Southern Area | | | | | | | | | | | |
| C2-1 | C2-1 | Allanite Monzonite | 0.164 | 0.210 | 1.22 | 0.415 | 0.290 | 1.19 | 0.665 | 96.73 | 97.00 |
| C2-1 | C2-1C | Allanite Monzonite | 3.45 | 0.149 | 0.922 | 0.325 | 0.221 | 0.950 | 0.500 | 98.26 | 98.47 |
| C2-1 | C2-3 | Nepheline Syenite | 0.020 | 0.003 | 0.001 | 0.009 | 0.001 | 0.043 | 0.013 | 98.90 | 99.02 |
| C2-5 | C2-16 | Nepheline Phonolite | 0.039 | 0.005 | 0.012 | 0.005 | 0.001 | 0.033 | 0.021 | 100.58 | 100.66 |
| C2-5 | C2-17 | Allanite Monzonite | 0.703 | 0.234 | 1.26 | 0.534 | 0.358 | 1.59 | 0.831 | 103.43 | 103.79 |
| C2-14 | C2-26 | Amphibole Phonolite | 0.035 | 0.005 | 0.025 | 0.005 | 0.001 | 0.044 | 0.027 | 101.46 | 101.55 |
| C2-14 | C2-27 | Aegirine Syenite | 0.010 | 0.005 | 0.012 | 0.011 | 0.001 | 0.037 | 0.009 | 98.65 | 98.82 |
| Central Area | | | | | | | | | | | |
| C2-15 | C2-48 | Allanite Monzonite | 0.067 | 0.005 | 0.030 | 0.005 | 0.001 | 0.034 | 0.011 | 99.06 | 99.15 |
| C2-17 | D2-30 | Allanite Amphibole Syenite | 0.111 | 0.007 | 0.056 | 0.036 | 0.001 | 0.076 | 0.036 | 100.04 | 100.13 |
| D2-44 | D2-52 | Melanite Phonolite | 0.032 | 0.005 | 0.015 | 0.005 | 0.001 | 0.073 | 0.019 | 95.58 | 95.76 |
| D2-44 | D2-53 | Norrbottenite Nephelinite Granodiorite | 0.005 | 0.005 | 0.019 | 0.005 | 0.001 | 0.027 | 0.039 | 100.45 | 100.49 |
| D2-48 | D2-57 | Melanite Phonolite | 0.054 | 0.009 | 0.018 | 0.011 | 0.001 | 0.086 | 0.022 | 95.72 | 95.79 |
| D2-61 | D2-63 | Tremolite (?) Phonolite | 0.005 | 0.005 | 0.012 | 0.007 | 0.001 | 0.023 | 0.003 | 99.52 | 99.58 |
| Northern Area | | | | | | | | | | | |
| D2-2 | D2-8 | Nepheline Syenite | 0.005 | 0.005 | 0.016 | 0.005 | 0.001 | 0.027 | 0.008 | 99.45 | 99.54 |
| D2-2 | D2-9 | Nepheline Phonolite | 0.042 | 0.007 | 0.020 | 0.006 | 0.001 | 0.088 | 0.025 | 98.28 | 98.42 |
| D2-3 | D2-11A | Granite | 0.011 | 0.005 | 0.015 | 0.005 | 0.001 | 0.022 | 0.009 | 101.64 | 101.70 |
| D2-3A | D2-12 | Allanite Nepheline Syenite | 0.014 | 0.006 | 0.046 | 0.015 | 0.006 | 0.048 | 0.028 | 101.75 | 101.83 |

*See Appendix III: Commercial Testing and Engineering Co., Instrument Analysis Division, Denver, Colorado.
**See Plates II and III.

(Click on Table to Enlarge)

Among the mineralized samples, the relation between the abundance of uranium and the rare earth minerals is proportional as is the relation between the four rare earths indicated. It appears that for the mineralized samples (i.e., C2-1, C2-1C, and C-17), if given the abundance of uranium, then the concentrations of thorium and four rare earths can be estimated with reasonable accuracy for the available samples. There does not appear to be a relation between the abundance of zirconium and uranium, although zirconium is present in significant amounts in some of the mineralized samples. As will be discussed later, the relative abundance of uranium, thorium and rare earth elements is generally related to the relative abundance of the mineral allanite, which is present in significant amounts in the mineralized samples and to a lesser extent in other samples (see Table 4, 5, and 7).

Rare Earth Elements: The REE concentrations in the mineralized zone of the southern area are substantial. Figures REE-1 through REE-3 characterizes the REE in the three principal areas of sampling. Samples obtained earlier by the U.S.G.S. are shown in the figures as histograms. Those samples also came from Hill 2109, the location of the mineralized zones.

Figure REE-1 illustrates not only the REE characteristics relative to the chondrite standard of the mineralized samples and the non-mineralized samples in the southern area of interest, but also the noticeable difference between the two URI analyses and those of the U.S.G.S., in terbium and thulium values. The U.S.G.S. is known to have sufficient laboratory checks that the values should be valid, the difference being likely related to a difference in samples.

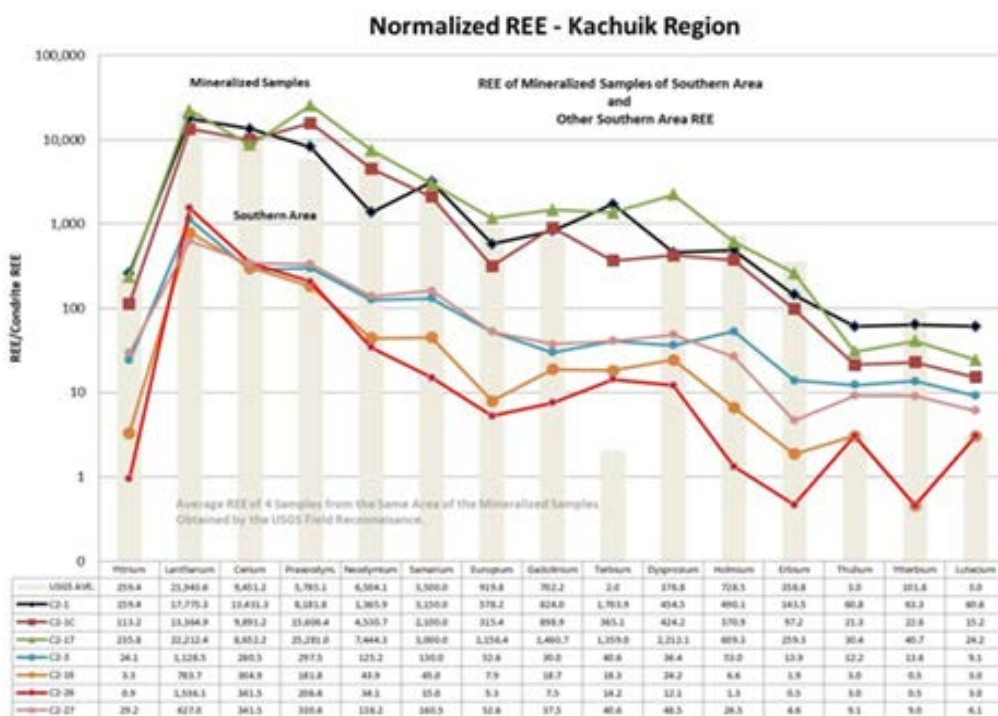


Figure REE-1

(Click on Figure to Enlarge)

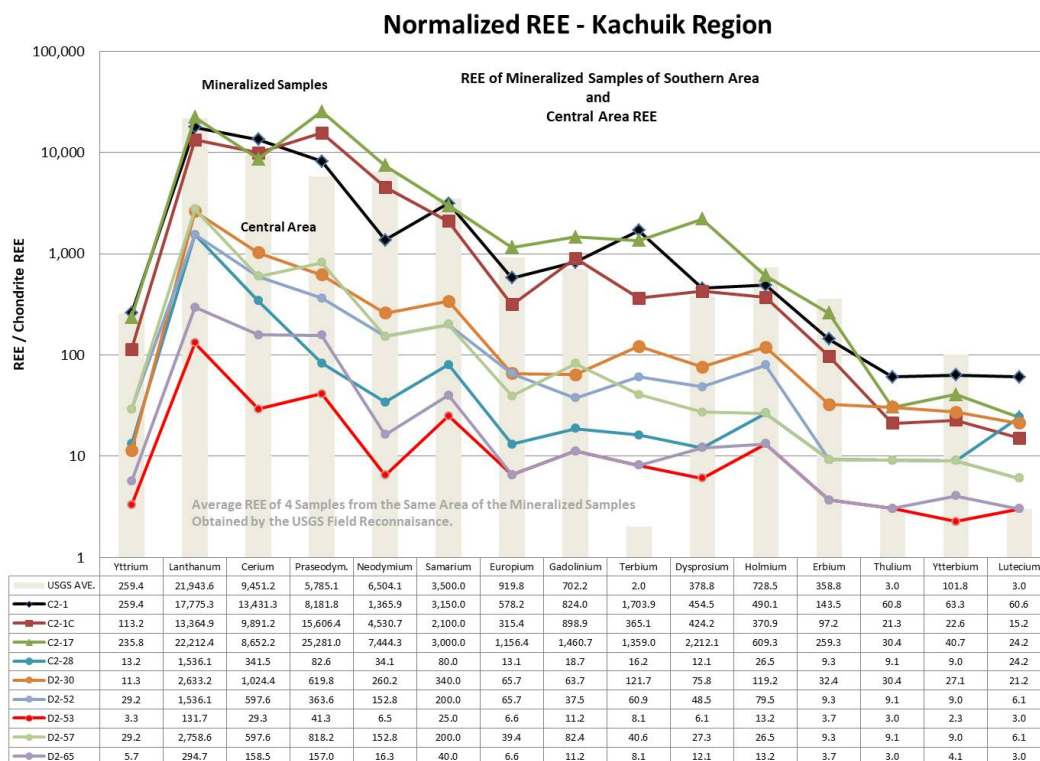


Figure REE-2

(Click on Figure to Enlarge)

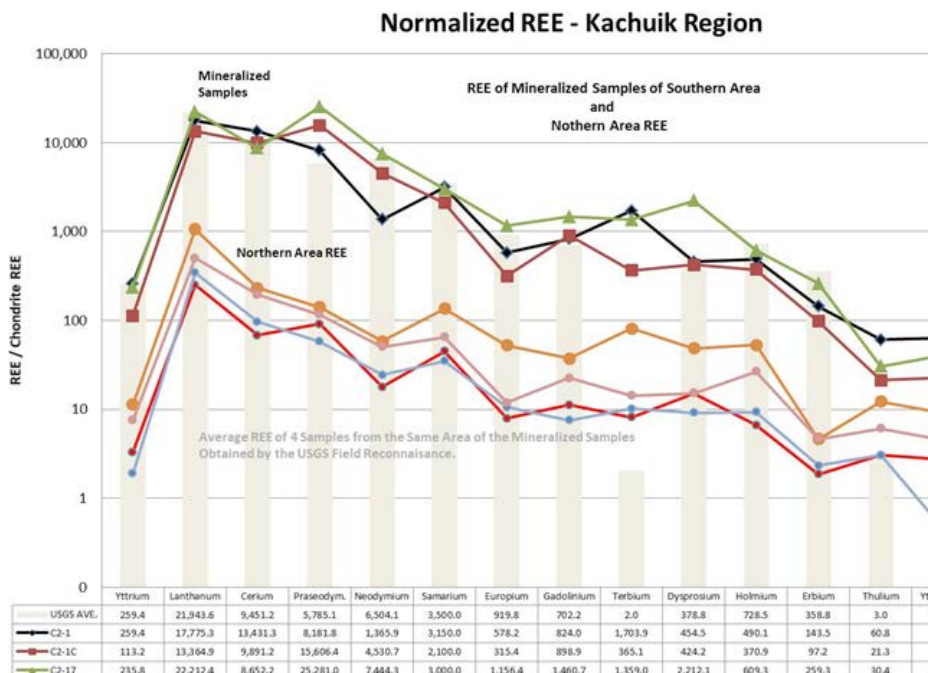


Figure REE-3

(Click on Figure to Enlarge)

The difference between the REE patterns in the above figures relate to the concentrations of REE. They appear to be a similar overall pattern, perhaps representing a fingerprint for the REE in the area, notwithstanding the U.S.G.S. values (histograms).

Uranium: Thorium: The relationship between uranium and thorium is not directly proportional for all samples, as would be expected. Uranium and thorium are present in various minerals with relative resistance to weathering. Weathering of the allanite at the surface is apparent (more). Based on element scans, delayed-neutron analyses (DNA) and fluorometric analyses, samples D2-30, see p. 30 (Appendix II) and D2-11A, see p. 29 (Appendix II) appear to be deficient in uranium. This might be from diagenetic leaching of the uranium, a topic which will also be discussed later in this paper (see “Metallurgical Analyses: Leachability Analyses”).

Sample D2-65, on the other hand, appears to be especially enriched in uranium relative to thorium. Sample D2-12 also appears to be slightly enriched in uranium. A fairly complete series of samples were taken during the NURE program around the northern area (and to the south), and confirmed that the pluton exhibits an unusually high uranium content. The significance regarding the adjacent basin (i.e, the McCarthy’s Marsh) will also be discussed in some detail later in this paper.

SEM, X-Ray, XRF Image Investigations: A preliminary investigation involving the scanning electron microprobe and X-ray and the newer XRF analytical techniques have been conducted on samples from the mineralized zones located within the southern area of interest, e.g., Samples C2-1 and C2-17 series. For detailed lithologic and mineralogical descriptions of the C2-1 series, see Appendix II, pp. 2-7.

- SEM: C2-1 Series: Appendix I: (Figures 17 to 35)
- XRF: C2-1 Series: Appendix I: pp.9-14
- XRF: Sample C2-17, Appendix I: pp. 15-18
- XRF: Sample D2-Mi-1, Appendix I: pp. 18-20

The initial objective of this investigation was to characterize the partially metamict mineral having the general physio-chemical affinities of allanite. This mineral appears to be a mineraloid on the basis that it does not always produce a diagnostic XRD pattern, even upon heat treatment (see work reflected by the Colorado School of Mines Research Institute memo, [Appendix III](#)).

Allanite occurs in a number of mineral varieties, depending upon the available elements similar in ionic size to calcium, usually either yttrium, cerium, lanthanum, but also manganese, iron, and magnesium. The chemical formulae of the known varieties of allanite-like minerals are provided below. Some have earned different mineraloid names:

Allanite Subgroup of the Epidote Group

| “Mineral” Name | URI Sample REE Data: | Formulae: |
|-----------------------|-----------------------------|--|
| Allanite-(Ce) | ~ 13,000 ppm | {CaCe} {Al ₂ Fe ²⁺ } (Si ₂ O ₇)(SiO ₄)O(OH) |
| Allanite-(La) | ~700 ppm | {CaLa} {Al ₂ Fe ²⁺ } (Si ₂ O ₇)(SiO ₄)O(OH) |
| Allanite-(Y) | ~500 ppm | {CaY} (Al ₂ Fe ²⁺)[Si ₂ O ₇][SiO ₄]O(OH) |
| Allanite-(Nd) | ~400 ppm | {CaNd} {Al ₂ Fe ²⁺ } (Si ₂ O ₇)(SiO ₄)O(OH) |

Other Varieties:

Formulae:

| | |
|----------------------|---|
| Androsite-(Ce) | {Mn ₂ +REE} {Al ₂ Mn ²⁺ } (SiO ₄)(Si ₂ O ₇)O(OH) |
| Dissakisite-(Ce) | {CaCe} {Al ₂ Mg} (Si ₂ O ₇)(SiO ₄)O(OH), aka [35] 2003 |
| Dissakisite-(La) | {CaLa} {Al ₂ Mg} (Si ₂ O ₇)(SiO ₄)O(OH), aka [35] 2003 |
| Ferriakasakaite-(La) | {CaLa} {Fe ³⁺ +AlMn ²⁺ } (Si ₂ O ₇)(SiO ₄)O(OH) |
| Ferriallanite-(Ce) | {CaCe} {Fe ³⁺ +AlFe ²⁺ } (Si ₂ O ₇)(SiO ₄)O(OH) |
| Ferriallanite-(La) | {CaLa} {Fe ³⁺ +AlFe ²⁺ } (Si ₂ O ₇)(SiO ₄)O(OH) |
| Ferriandrosite-(Ce) | {Mn ²⁺ +REE} {Fe ³⁺ +AlMn ²⁺ } (SiO ₄)(Si ₂ O ₇)O(OH) |
| Ferriandrosite-(La) | {MnLa} {Fe ³⁺ +AlMn ²⁺ } (Si ₂ O ₇)(SiO ₄)O(OH) |

Complex Varieties:

| | |
|------------------------|--|
| Manganiakasakaite-(La) | {CaLa} {Mn ³⁺ +AlMn ²⁺ } (Si ₂ O ₇)(SiO ₄)O(OH) |
| Manganiandrosite-(Ce) | {Mn ²⁺ +Ce} {Mn ³⁺ +AlMn ²⁺ } (Si ₂ O ₇)(SiO ₄)O(OH) |
| Manganiandrosite-(La) | {Mn ²⁺ +La} {Mn ³⁺ +AlMn ²⁺ } (Si ₂ O ₇)(SiO ₄)O(OH) |
| Uedaite-(Ce) | {Mn ²⁺ +Ce} {Al ₂ Fe ²⁺ } (Si ₂ O ₇)(SiO ₄)O(OH) |
| Vanadoallanite-(La) | {CaLa} {V ³⁺ +AlFe ²⁺ } (Si ₂ O ₇)(SiO ₄)O(OH) |
| Vanadoandrosite-(Ce) | {Mn ²⁺ +Ce} {V ³⁺ +AlMn ²⁺ } (Si ₂ O ₇)(SiO ₄)O(OH) |

Complex Associations:

UM1989-32-SiO:AlCaFeHREE: (Ca_{0.5}+0.5) (Ce,La,Nd) Fe³⁺+Al₂(Si₂O₇)(SiO₄)O(OH)

Unnamed (Ce- and Mn-analogue of Ferriakasakaite (La)) {Ca,(Ce,La,Nd),Mn²⁺}₂(Mn³⁺,Fe³⁺,Al)Al(Mn²⁺,Mg)(Si₂O₇)(SiO₄)O(OH)

Unnamed (Mg-analogue of Ferriallanite: (Ce)) {CaCe} {(Fe³⁺,Al)Al(Mg,Fe²⁺)}(Si₂O₇)(SiO₄)O(OH)

Unnamed (Mn-analogue of Ferriallanite-(Ce)) {CaCe} {Fe³⁺+AlMn²⁺}(Si₂O₇)(SiO₄)O(OH).

Based on the URI samples of the area, the relative concentrations of cerium, lanthanum, and yttrium, can be characterized as a Ce-rich allanite, annotated as **allanite-(Ce)**. However, based on the manganese, magnesium, aluminum, and iron concentrations present in many samples, other varieties are likely present, e.g. androsite, ferriallanite, etc.

Alekseev and Marin [36] (2015) point out that the speciation, paragenesis, main **typomorphic features**, and tendencies of accessory mineral evolution steadily repeat in rare-metal granites over the entire Far East from Primorye (Vladivostok) to Chukchi Peninsula (just west of the Bering Straits and western Seward Peninsula), reflecting the genetic and compositional uniformity of the Late Cretaceous rare-metal magmatism. The main regional features of accessory mineralization in lithium-fluorine granites are expressed in: (i) presence/lack of presence of tungsten, sodium, niobium, and bismuth minerals; (ii) tungsten and scandium admixtures in accessory minerals; (iii) prevalence of niobium over tantalum; and (iv) obvious contribution of yttrium, REE, arsenic, thorium, and uranium cumulates with late-stage dike injections.

Alekseev and associates have further explored the role allanite in the metallogenesis of the plutons in the areas ([37] (2013) and [38] (2016)). Eby, et al., [39] (1993) worked on the radiation damage found in vesuvianite, another variety of cumulate mineral (or mineraloid) similar to allanite. The proximity of the subject areas of interest to a carbonate (just northwest of the central area of interest) raises the issue as to whether allanite was formed from a skarn-associated mineralizing fluid or from another deep source of fluids, as discussed by Smith, et al., [40] (2002) and Forster [41] (1998).

The uniform accessory mineralization in lithium-fluorine granites of the eastern coast of Russia near the Seward Peninsula is evidence for the existence of a rare-metal granitic province or belt of lithium-fluorine granites, which appear to extend into eastern Seward Peninsula as represented by the fluorine-rich rocks present, from the Kauchick area northward to Death Valley area and beyond as discussed in this paper.

In 1980, Himmelberg and Miller [42] 1980, reported that upon further evaluation the mineraloid previously reported as allanite in the southern area was identified as vesuvianite. Based on the complex mineraloid, metamict character of the material, it can accommodate a variety of elements and crystalline forms and it is not unanticipated that name competition would come into play, **allanite** or **vesuvianite**.

A mineralogical discussion on the identity of the subject mineral (mineraloid) is for another time. In this paper, the term allanite will be retained with the understanding that the principal objectives discussed in this paper are to characterize its mineralogical associations and its likely mode of formation as a possible source and/or ore of uranium, thorium, and REE, as in other deposits in the world. For example, as possible guidance for this study, Smith, et al., [40] (2002) reported that allanite-(Ce) occurs as a metasomatic phase in diopside-hedenbergite-anorthite-hastingsite endoskarn from the Beinn an Dubhaich granite aureole, in Skye (the UK).

Their fluid-inclusion studies indicate formation of pyroxene at temperatures in the range 600 to 700°C from Na-K-Fe-Ca bearing brines (45 to 60 wt. % NaCl eq.) assuming pressures of 280 to 640 bars. Allanite and amphibole formed from similar brines at 500-600°C (mean ~ 550°C). Fluorite formed during cooling and dilution of these brines. Vesuvianite formed at much lower temperatures (230 to 250°C) from low- to moderate-salinity fluids (~ 0 to 15wt % NaCl eq.). High fluorine contents in both allanite-amphibole and vesuvianite indicate that the fluids were fluorine-bearing at all stages in the paragenesis.

Petrographic Evaluations

Recent thin sections of the mineralized samples from the southern area of interest show allanite in three varieties in the C2-1 sample: 1) brown allanite (heavily shocked?), 2) light brown to light orange alteration, and 3) orange-yellow surrounding or distal crystalline form of allanite. Additional thin-section and XRF analyses are presented in **Appendix II**.

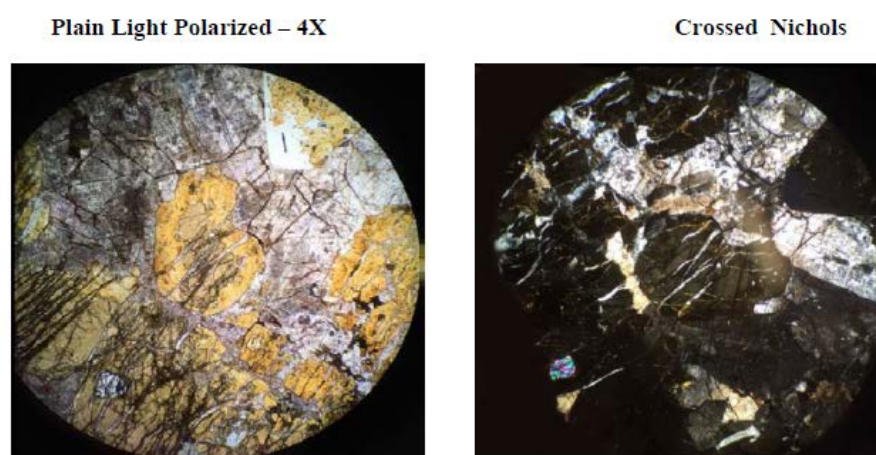


Figure C2-1 Series

Plain Polarized Light – 3X

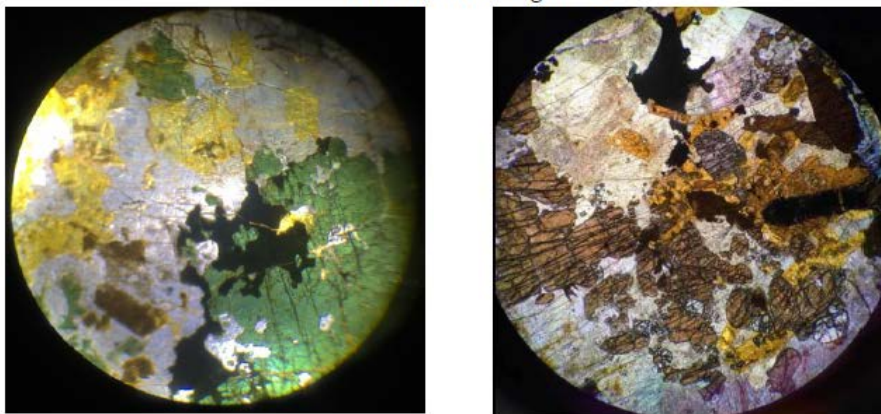


Figure C2-17 - Series (Click to Enlarge One View)

In the C-17 series, hornblende (green) appears as a dominant mineral in association with augite (black). Brown allanite is slightly embayed by yellow allanite? as late-stage injection(?). Note stringer in augite in center of left view in thin fracture. Individual zircons scattered around field of left view. For additional descriptions, see Appendix II, p. 12, for C2-17 series, and p. 2 for C2-1 series of descriptions.

Other thin sections (in Appendix II) exhibit abundant augite but no apparent hornblende (or example, right field of view above). Brown allanite appears to be heavily “shocked” whereas the light orange variety exhibits fewer to no fractures. Large and medium-sized zircons and numerous small crystals of monazite are also present. The feldspar shows light fractures compared to that in the adjacent brown allanite. XRF confirms calcium and titanium within allanite in the above Figure C2-1 thin sections (below Figure C2-1A). The titanium mineral sphene is ubiquitous in the samples, but the titanium-rich rims of the allanite are likely not sphene but another mineral. For additional XRF views, See Appendix I, p. 9 for C2-1 and C2-17 series.

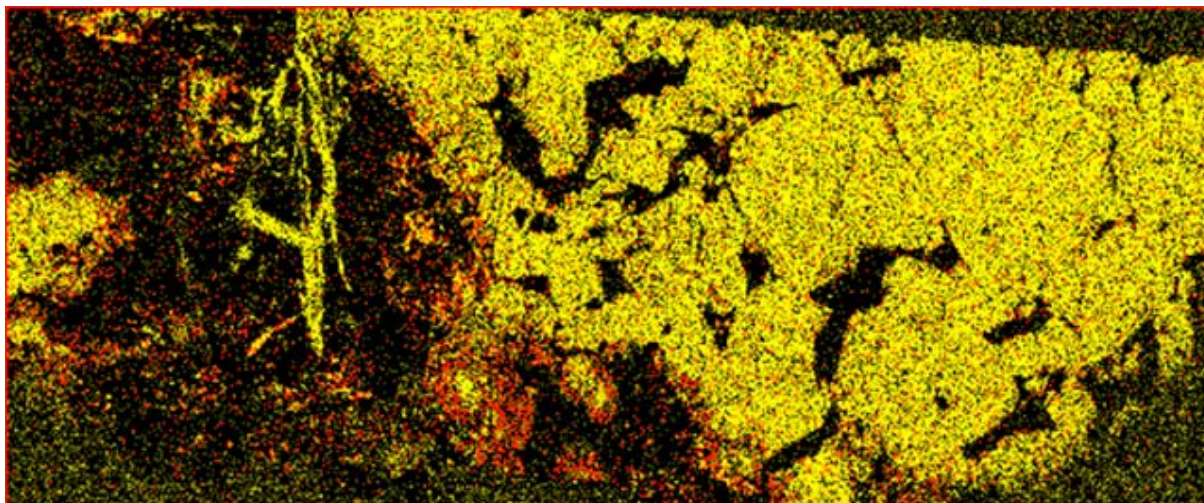
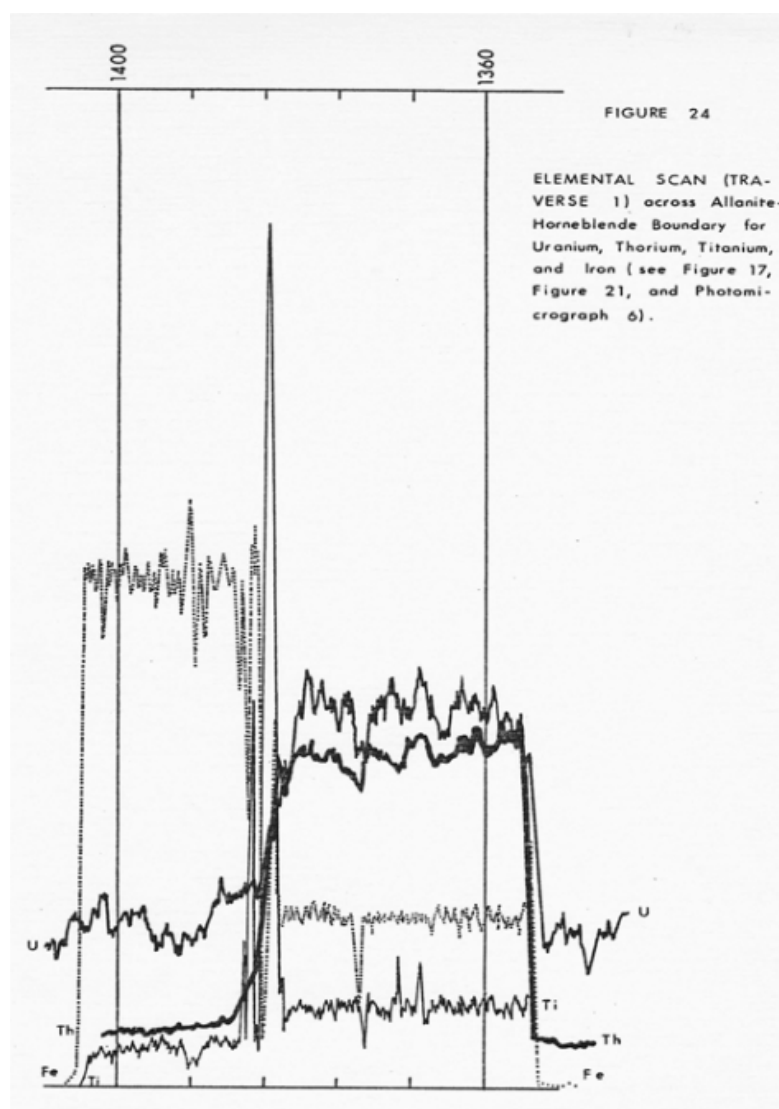


Figure C2-1A - XRF of Allanite for Calcium (Bright Yellow) with Titanium (Red) of Rims of Allanite. Feldspar (Black).



To simplify the layout of this paper and to minimize the inter-referencing between Scanning-Electron Microprobe (SEM) photomicrographs, related thin-section mapping, and X-Ray (XRF) photomicrographs made in the late 1970s with data tables, figures, and the discussions within this paper, additional petrographic descriptions have been relegated to [Appendix I](#). The continuity of the figure numbering system has been maintained. For example, Figures 17 and 18 are from sampling site Site #1 within a thin-section of Sample C2-1C (see Photomicrograph #6 in [Appendix II](#)).

Figure 18 shows Location 1 and illustrates the contact between allanite-(Ce) and K-feldspar. Figures 19 and 20 show the relative distribution of thorium and uranium. It should be noted that thorium and uranium are shown to be uniformly distributed within the allanite-(Ce), but uranium, because of its lower concentration relative to thorium ($U/Th = 0.17$ as indicated by the whole rock analyses; see Table 8 above), is also uniformly distributed throughout the Kfeldspar crystalline structure.

Figure 21 shows SEM view (275X) and traverses 1 across allanite and hornblende at Location 2 within Site #1 of Sample C2-1C in [Appendix I](#) and illustrates the path of Traverse #1 across Location 2 of Sample C2-1C (see Photomicrograph #6, in [Appendix II](#)). Figure 22, (in [Appendix I](#)) illustrates the widespread thorium concentration within allanite, whereas the uranium distribution appears to be distributed in both allanite and hornblende and only faintly indicates preference for allanite (see Figure 23). Similarities of uranium distribution in feldspar and hornblende are also evident.

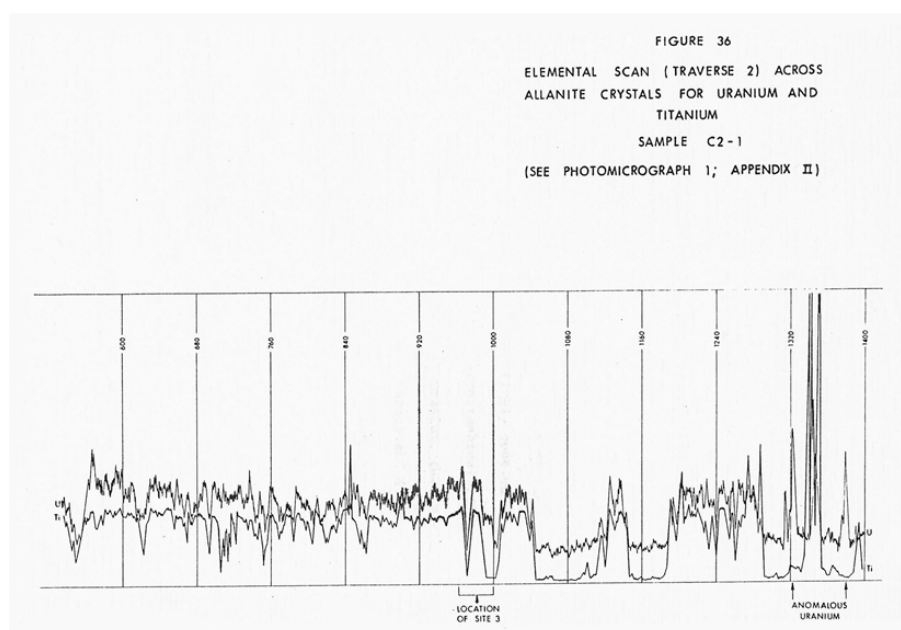
Figure 24 is the element scan for the traverse (uranium, thorium, iron and titanium) and illustrates the relative concentration of those elements. As expected, iron content is relatively high within the field of hornblende (on the left) and relatively low within allanite. Interestingly, titanium shows a peak at the contact between hornblende and allanite, which might represent a titanium-rich transition or alteration product of either hornblende or allanite, which is also evident in the earlier XRF showing titanium around the edge of allanite “crystals”.

Figure 25 illustrates Site #2 of Sample C2-1C (see Photomicrograph #6 in [Appendix I](#)). This shows a large euhedral zircon is present on the left of the field and is surrounded by allanite. Figures 26, 27 and 28 show the distribution of zirconium, thorium, and uranium, respectively. Thorium is clearly concentrated in the allanite and uranium is uniformly present within the allanite as well as within the zircon, although the faint outline of the zircon can be observed in Figure 28.

The distribution of uranium in both allanite and zircon, discounting the effects of low concentration and the X-ray response pattern, raises the question of uranium preference. Chemical analyses do not indicate a direct proportional relationship between zirconium and uranium, although it is clear that at least some of the uranium occupies sites within zircon and other accessory minerals present. Primary metallurgical investigations involving uranium leachability will be discussed later in this report (see “Preliminary Metallurgical Investigations”).

Figure 29 shows the location of Site #3 within Sample C2-1, at the margin of a large allanite crystal (see Photomicrograph #1). The path of Traverse 2 is also shown in (Figure 29). And in Photomicrograph #1 in [Appendix II](#). Figure 30 is an expanded view. The distributions of iron, zirconium, titanium, thorium, and uranium, respectively, are shown in Figures 31, 32, 33, 34 and 35. The X-ray images indicate that allanite contains relatively abundant iron, titanium, thorium, and uranium. An isolated zircon is indicated in Figure 32 (as shown in the SEM view in Figure 30).

Figure 36 below is the uranium and titanium traverse across a thin-section of Sample C2-1. This indicates that titanium and uranium content are comparable in abundance within allanite. However, a significant uranium anomaly, located near the right margin, is present that is not associated with titanium content (of either allanite or sphene).



Other thin-section descriptions of particular note are:

- 1) Mi unit: [Appendix II](#): Index and p. 21: Sample # C2-29; XRF, p. 18;
- 2) the “pulaskite” dikes series: [Appendix II](#), pp. 43, 46, and 48;
- 3) the Dry canyon Creek sample series: [Appendix II](#), pp. 27-39;
- 4) the Burnt Creek pluton samples: [Appendix II](#), pp. 51-53, and
- 5) the North granite Mountain area: Sample # HC-2, [Appendix II](#), p. 54.

It is clear that additional SEM and X-ray investigations are warranted to further evaluate uranium anomalies that are apparently not located within allanite or within the crystalline structures of the accessory minerals. The possibility exists that a uranium mineral might be present as inclusions, as has been indicated by catholuminescence and XRD investigations (see Figure 37 and [Appendix III](#), respectively). This will be discussed later on in this paper (see “Preliminary Metallurgical Investigations”).

Cathodoluminescence Investigations: XRD investigations on the allanite-like mineral indicated a poorly crystalline, slightly metamict, semi-mineraloid structure (see [Appendix III](#)). To further evaluate the composition and internal structure of allanite, the mineral was subjected to cathodoluminescence investigations at Rice University, Department of Geology, under the supervision of Dr. Charles Weisenberg (URI) and Ms. Kathy Balshaw, B.S. (Figure 37) is of Sample C2-17, one of the mineralized samples containing abundant “allanite” containing anomalous amounts of uranium, thorium and rare-earth elements.

The light blue area shown in Figure 37 is feldspar; the white-yellowish minerals are zircons, the largest of which is zoned. The black area containing small, spherical, multi-colored inclusions is allanite. We concluded that the allanite is partially metamict internally, but retains an outer crystalline structure with elemental and petrographical characteristics illustrated in the various thin-sections containing allanite.

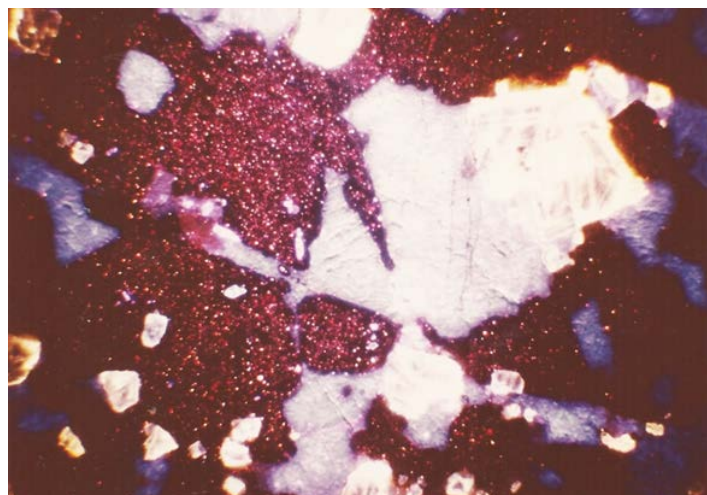


Figure 37: Cathodoluminescence Photograph of Sample C2-17. 85X.
Light Blue Areas: Feldspar; White-Yellow Areas: Zircon (Zoned in Part);
Black Areas with Spherical Multicolor Inclusions: Allanite-(Ce?)

To account for the anomalous uranium, thorium and rare-earth elements, the inclusions appear to be separate and distinct uranium, thorium, and rare-earth minerals, e.g., identified as uraninite, uranothoranite, thorite, cerite?, as well as a variety of related minerals held within the metamict mineral, allanite or its varieties. There are also black areas that might contain the uranium minerals [14, 43]. The mineral associations indicate that the allanite was formed late as indicated in Figure 37 where allanite intrudes the feldspar. The rims of the feldspar also appear to be “corroded”, perhaps from radiation damage, where they are in contact with allanite. The zoned character and proximity of the large zircon in the above figure also indicates that it formed at a late stage within allanite. Further cathodoluminescence investigations are clearly warranted to determine if the inclusions are present in similar quantity and density in all mineralized samples containing allanite-(Ce? La? Mn ?Mg?F?) or other varieties of epidote. An iron variety is also a candidate based on its very high iron content in the samples examined.

Preliminary Metallurgical Investigations

Mineralized samples with allanite appearing as a black, shiny crystals in freshly broken rock are typical for allanite-(Ce), shown in Figure 6a, were evaluated with respect to their specific gravity and magnetic susceptibility of the constituent minerals liberated after crushing and heavy-liquid separation of the fine particles. This is to characterize the mineralized samples to determine whether the elements of interest can be concentrated as separate fractions.

Sink-Float Analyses: Preliminary sink-float analyses were conducted on selected mineralized samples to determine the relative distribution of specific gravity and magnetic susceptibility for lanthanum, uranium, thorium, titanium, and zirconium within the rock samples for such minerals as allanite (Al), zircon (Zr), sphene (Sp), monzonite (Mon), hornblende (Hb), and magnetic iron fines (Mag Fe).

Three samples (C2-1B, C2-1C and C2-17) were crushed and separated via heavy liquid into a greater than 3.3 specific gravity fraction and a less than 3.3 specific gravity fraction. The greater than 3.3 samples were further subjected to a Frantz Isodynamic Magnetic Separator, which produced a five-fraction concentrate. Each fraction was subsequently weighed and analyzed for: cU_3O_8 , ThO_2 , La_2O_3 , ZrO_2 and TiO_2 . Each fraction was also described mineralogically, by both optical microscopy and XRD methods.

Table 9 contains the separation and mineral identification data. Of special note is the identification of siderite and barite that have been identified among the normally expected accessory minerals.

TABLE 9
SEPARATION AND MINERAL IDENTIFICATION DATA***

| Fraction | Sample C2-1B | | Sample C2-1C | | Sample C2-17 | |
|---|-----------------------------------|-------------|-------------------------------|-------------|---|-------------|
| | Weight g | Weight % | Weight g | Weight % | Weight g | Weight % |
| Head | 210.7 | 100 | 174.32 | 100 | 286.17 | 100 |
| <3.3 sp gr | 209.0 | 99.2 | 167.0 | 95.8 | 284.9 | 99.5 |
| >3.3 sp gr | 1.7 | 0.8 | 7.32 | 4.2 | 1.27 | 0.5 |
| Frantz Fraction from >3.3 sp gr | | | | | | |
| 1 | **hornblende, minor allanite | | magnetite, iron filings | | allanite, hornblende | |
| 2 | allanite = hornblende | | hornblende, minor allanite | | allanite, sphene | |
| 3 | zircon = allanite | | allanite, minor zircon | | allanite = hornblende | |
| 4 | **zircon, tr. sphene, monazite | | **zircon, allanite | | **sphene, zircon siderite, tr. allanite | |
| 5 | **zircon, tr. barite monazite | | combined with fraction 4 | | zircon, sphene | |
| 6 | nil | | combined with fraction 4 | | nil | |
| 7 | nil | | zircon | | nil | |

* magnetic susceptibility decreases from fraction 1 to fraction 7.

** identified by XRD

*** conducted by Colorado School of Mines Research Institute (see Appendix III).

Also of note is the low percentage of heavy minerals (>3.3 specific gravity), a factor that is of significance when the uranium, thorium, and rare-earth distributions are considered.

Table 10 contains the fraction weights and chemical analyses for each fraction. Figures 38 and 39 are plots of the chemical analyses of Sample C2-1B against the respective five fractions (of decreasing magnetic susceptibility) and of the weighted distribution among the fractions for each element (as oxides).

TABLE 10
FRACTION WEIGHTS AND CHEMICAL
ANALYSES FOR > 3.3 SPECIFIC
GRAVITY FRACTIONS*
(WT.%)

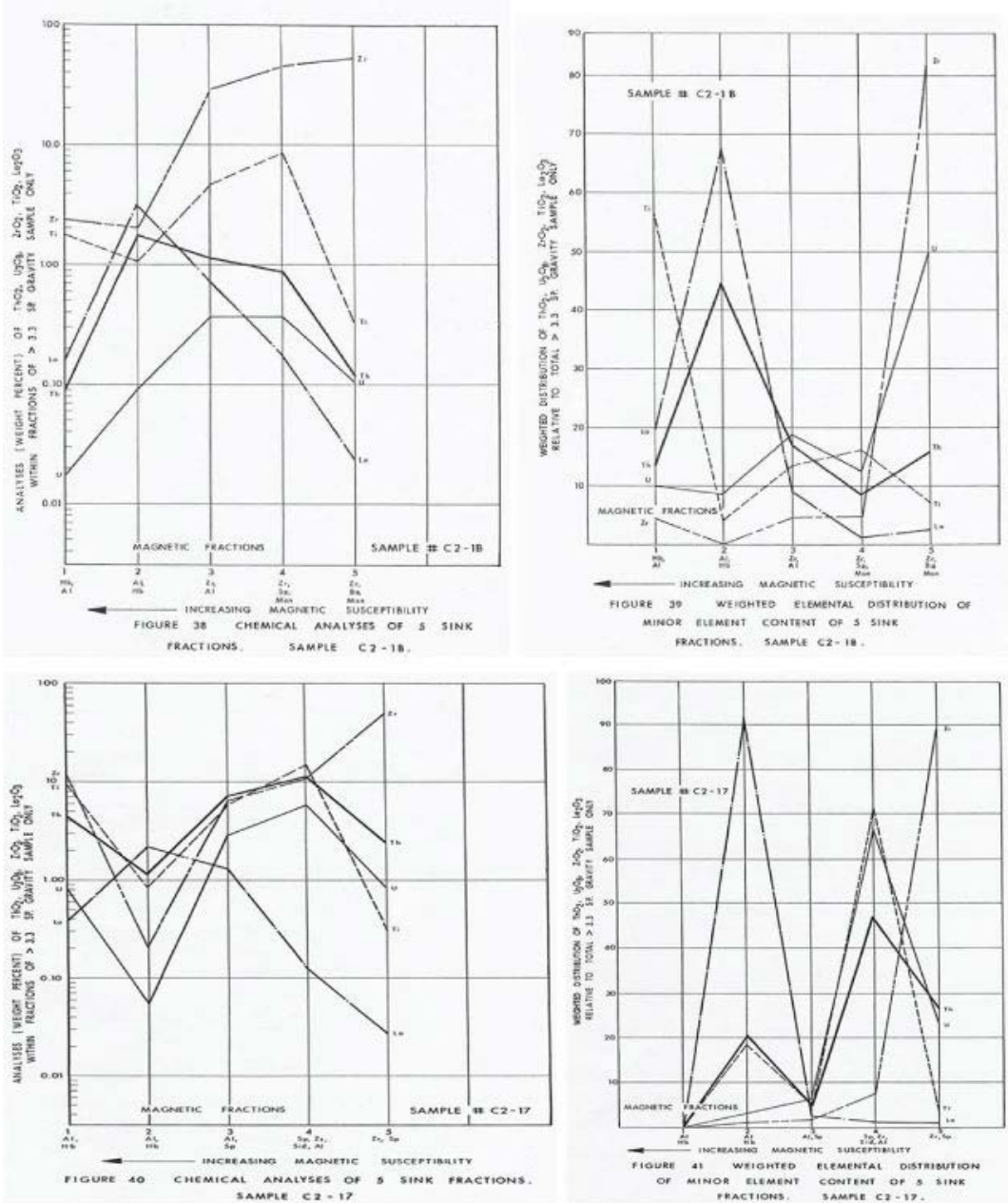
| Element | C2-1B-1 | C2-1B-2 | C2-1B-3 | C2-1B-4 | C2-1B-5 |
|--|---------|---------|---------|---------|---------|
| U ₃ O ₈ | 0.017 | 0.091 | 0.364 | 0.365 | 0.106 |
| ThO ₂ | 0.084 | 1.76 | 1.15 | 0.888 | 0.121 |
| La ₂ O ₃ | 0.146 | 3.25 | 0.717 | 0.184 | 0.025 |
| ZrO ₂ | 2.40 | 2.06 | 29.66 | 44.94 | 54.36 |
| TiO ₂ | 1.80 | 1.07 | 4.86 | 8.83 | 0.30 |
| Total | | | | | |
| Fractioning wt: | 0.7943g | 0.1230g | 0.0716g | 0.0462g | 0.6325g |
| Total CT&E Weight: 1.6676g sum of fraction | | | | | |
| Element | C2-1C-1 | C2-1C-2 | C2-1C-3 | C2-1C-6 | C2-1C-7 |
| U ₃ O ₈ | 0.18 | 0.005 | 0.304 | 0.226 | 0.112 |
| ThO ₂ | 0.10 | 1.10 | 1.40 | 0.736 | 0.108 |
| La ₂ O ₃ | 0.253 | 3.98 | 0.907 | 0.256 | 0.037 |
| ZrO ₂ | 2.50 | 0.77 | 30.12 | 46.56 | 52.62 |
| TiO ₂ | 3.20 | 0.72 | 1.49 | 0.80 | 0.30 |
| Total | | | | | |
| Fractioning wt: | 0.0095g | 0.3749g | 0.2724g | 0.4472g | 6.2557g |
| Total CT&E Weight: 7.3597g sum of fraction | | | | | |
| Element | C2-17-1 | C2-17-2 | C2-17-3 | C2-17-4 | C2-17-5 |
| U ₃ O ₈ | 0.84 | 0.055 | 2.97 | 5.99 | 0.855 |
| ThO ₂ | 4.50 | 1.13 | 7.16 | 11.76 | 2.61 |
| La ₂ O ₃ | 0.38 | 2.38 | 1.63 | 0.151 | 0.027 |
| ZrO ₂ | 12.00 | 0.22 | 6.50 | 11.34 | 52.74 |
| TiO ₂ | 9.60 | 0.87 | 5.97 | 15.30 | 0.30 |
| Total | | | | | |
| Fractioning wt: | 0.0020g | 0.687g | 0.0272g | 0.1487g | 0.3703g |
| Total CT&E Weight: 1.2353g sum of fraction | | | | | |

*See Appendix III

(Click on Table to Enlarge)

Figure 39 indicates thorium (45% of total thorium) and lanthanum (68% of the total lanthanum) appear to segregate in Fraction 2, which contains an allanite-hornblende concentrate. Uranium (50% of the total uranium present in all fractions) appears to segregate in the heaviest fraction, along with zircon, monazite and, of special note, barite. Zircon is the major mineral in Fractions 3, 4 and 5 but does not show a direct relation with uranium concentrations, except for Fraction 5.

Some other heavy mineral containing appreciable quantities of uranium is indicated, perhaps associated with barite or in the form of very fine-grained uraninite, uranothoranite, or other radiogenic minerals, as inclusions, in allanite, which have been only partly liberated from the allanite as the result of sample preparation and crushing. Titanium (56% of the total titanium) is apparently present in Fraction 1 within hornblende or other titanium mineral. The element also shows an increase in Fraction 4 wherein sphene has been concentrated.



Figures 40 and 41 (above) of sample C2-17 are similar plots. These also show segregation of lanthanum (and to a lesser extent thorium and titanium) in the allanite-rich Fraction 2. However, uranium, thorium, and titanium have been segregated in Fraction 4, in which sphene, zircon, siderite(?) and allanite occur with decreasing frequency. Because the sphene fraction of Sample C2-1B did not show a linear relation with uranium concentration and because uranium abundance is not related the zircon concentration, it is tentatively concluded that the uranium is associated either with siderite, heavier phases of allanite, or with another radiogenic mineral or minerals such as very fine-grained uraninite, uranothoranite. Uranium, thorium, the rare earths, zirconium, and titanium have not been concentrated to any significant extent in the heavy mineral fraction (>3.3 specific gravity fraction). Table 11 indicates that uranium is either associated with one or more of the lighter essential (or varietal) minerals or it is present within separate uranium mineral phases in the form of very fine-grained uraninite, uranothoranite. See Updates ([here](#)).

TABLE 11
CHEMICAL ANALYSES OF <3.3 SPECIFIC GRAVITY FRACTIONS*

| Oxide | Sample # | | | | | |
|--------------------------------|----------|--------|-------|--------|-------|--------|
| | C2-1B | | C2-1C | | C2-17 | |
| | % | PPM | % | PPM | % | PPM |
| U ₃ O ₈ | 0.146 | 1,460 | 0.155 | 1,550 | 0.181 | 1,810 |
| ThO ₂ | 0.665 | 6,650 | 0.857 | 8,570 | 0.869 | 8,690 |
| Nd ₂ O ₃ | 0.545 | 5,450 | 0.574 | 5,740 | 0.610 | 6,100 |
| Pr ₂ O ₃ | 0.226 | 2,226 | 0.258 | 2,580 | 0.341 | 3,410 |
| Ce ₂ O ₃ | 0.795 | 7,950 | 0.950 | 9,500 | 1.120 | 11,200 |
| La ₂ O ₃ | 0.436 | 4,360 | 0.473 | 4,730 | 0.620 | 6,200 |
| TiO ₂ | 1.240 | 12,240 | 1.290 | 12,900 | 1.650 | 16,500 |
| ZrO ₂ | 0.163 | 1,630 | 0.949 | 9,490 | 0.958 | 9,580 |

*See CT&E Analyses (Appendix III)

Young [33] (1989) discussed the role of specific gravity of rock samples because the most fundamental properties of a rock are its specific gravity. However, it does not play a role in any rock classifications, largely because it would not be a meaningful indicator on a standard QAPF double ternary diagram. On the other hand, specific gravity becomes very meaningful when it is used with the felsic-mafic concept (F) Young and other has developed.

Crystalline rocks show a gradual increase in specific gravity from felsic to mafic types as measured by the F concept. Probably the most exhaustive work on the correlation of specific gravity and rock composition has been done by Kopf [44] (1966, 1967), Saxov and Abrahamsen [45] (1964) and Platou [46](1968) have also grappled with the specific gravity-rock composition problem. It is particularly useful to this study for the purpose of placing the gravity fractions in some context with separation issues.

Leachability Analyses: Six whole rock samples, ranging from highly mineralized samples (C2-1, C2-1C, and C2-17) to samples of low but significant uranium content (D2-12, D2-30, and D2-57), were analyzed by delayed neutron activation (DNA) and by standard fluorometric (20% acid) methods to characterize leachability of the uranium present. The relative contribution of the uranium contained in accessory minerals present to the uranium content of the whole rock sample also can be investigated on a preliminary basis. Table 12 is a summary of the leachability analyses:

TABLE 12
URANIUM LEACHABILITY
(WHOLE ROCK - WT%)
AND PPM

| Sample # | Rock Type | Total U ₃ O ₈ | | Leachable U ₃ O ₈ | | % Leach- ability |
|----------|-----------------------------|-------------------------------------|-------|---|-------|---------------------|
| | | DNA* | | Fluorometric HNO ₃ | | |
| | | CT&E | B-C** | CT&E | B-C** | |
| C2-1 | Allanite Monzonite (CR) | 0.25% | 0.21% | 0.22% | | 88.0 |
| C2-1C | Allanite Monzonite (CR) | 0.19% | 0.15% | 0.17% | | 89.5 |
| C2-17 | Allanite Monzonite (CR) | 0.25% | 0.21% | 0.22% | | 88.0 |
| D2-12 | Allanite Neph. Syenite (CR) | 150ppm | 60ppm | 125ppm | | 83.3 |
| D2-30 | Allanite Amp. Syenite (CR) | 120ppm | 70ppm | 98ppm | | 81.6 |
| D2-57 | Melanite Phonolite (D) | 60ppm | 90ppm | 38ppm | | 63.3 |

CR = Country Rock (Plutonic Rock)

D = Dike

*DNA = Delayed Neutron Activation Analyses (Bonder-Clegg)

** = Bonder-Clegg 20% HNO₃ Fluorometric Analyses Used to Calculate % Leachability (See Appendix III)

Based on the mineralized samples analyzed to date, the uranium: thorium ratios are presented in Table 13. In general, U/Th values obtained during the two-year field investigation by URI personnel are clearly higher than previous values reported from the same region earlier by the U.S.G.S. (see Appendix III). In addition, the spectrometer surveys in the northern area of interest (Dry Canyon pluton) indicate radiometric uranium exceeds thorium along many segments of the traverses (see Plate III).

TABLE 13
URANIUM/THORIUM RATIOS (SELECTED SAMPLES)

| Omega Areas of Interest | U ₃ O ₈ % | ThO ₂ % | U/Th | Omega U/Th | Eakins (1977) U/Th |
|-------------------------|---------------------------------|--------------------|------|------------------|--------------------|
| <u>Southern Area</u> | PPM | PPM | | | |
| C2-1 | 0.245 (2,450) | 1.22 (12,200) | 0.20 | Interest | Darby |
| C2-1C | 0.170 (1,700) | 0.92 (9,200) | 0.18 | Areas | Reconn. |
| C2-17 | 0.265 (2,650) | 1.26 (12,600) | 0.21 | $\bar{x}=0.24$ | Dry |
| <u>Northern Area</u> | | | | $s=0.07$ | Canyon |
| D2-12* | 150 ppm | 460 ppm | 0.33 | #Samples: | #Samples: |
| <u>Central Area</u> | | | | 6 | 108 |
| D2-30 | 120 ppm | 560 ppm | 0.21 | | 18 |
| D2-57 | 60 ppm | 180 ppm | 0.33 | | |

*Dry Canyon Pluton

However, the element scan in Table 5 indicates that other samples might be anomalous in uranium and thorium content. Although the analytical error of the analyses presented could be excessive for some purposes, they still can be used to infer that some samples might have been enriched (e.g., C2-16, C2-26, D2-65), whereas others might have been leached (e.g., D2-11A).

Equilibrium Analyses: Uranium equilibrium was investigated according to standard U₃O₈ (DNA) vs. Bi²¹⁴ analyses. (Table 14) presents the pertinent data for the three mineralized samples, i.e., C2-1, C2-1C and C2-17.

TABLE 14
URANIUM EQUILIBRIUM
(WHOLE ROCK - WT.%)

| Sample # | Rock Type | Total%U ₃ O ₈ * DNA | Bi ²¹⁴ * %U ₃ O ₈ Eq. | U ₃ O ₈ (DNA) U ₃ O ₈ (Bi ²¹⁴) |
|----------|--------------------|--|---|---|
| C2-1 | Allanite Monzonite | 0.248 | 0.245 | 1.012 |
| C2-1C | Allanite Monzonite | 0.176 | 0.170 | 1.035 |
| C2-17 | Allanite Monzonite | 0.264 | 0.265 | 0.996 |

Average: 1.01

*See Appendix III

Discussion of Results

Introduction: The results of the investigations conducted to date on samples from the mineralized zone of the southern area and on samples from the central and northern areas indicate that an allanite-like mineral contains most of the uranium, thorium, and numerous rare-earth elements in sufficient quantities to be of potential economic interest.

And, although these investigations are preliminary in nature and would benefit from the NURE data, maps, and reports that became available after the field work and report were completed by URI personnel, other metals are reported in the form of geochemical anomalies that indicate the presence of a metallogenic province in the general vicinity of the areas studied in this investigation. Work conducted by URI northeast of the Omega areas, reinforced this view (see Death Valley Area discussed later in this paper).

Regional Geology and Geochemistry: The alkali intrusive rocks in the vicinity of the three areas of focus during this investigation exhibit geological features that are typical of many other alkaline intrusives in the world. Although based on limited data, there are indications that the rocks examined during Phase II are part of an alkalic complex containing carbonatites. However, Heinrich [47] (1966) cautions that nearly all carbonatites are within, or are satellites to, intrusive bodies of alkalic igneous rocks, but that all alkalic igneous rocks do not have associated carbonatites (Doroshkevich, [48](2010). In the area under consideration, a number of geochemical and mineralogical features indicate that the nepheline syenites are of miassic composition and therefore possibly are associated with carbonatites, either at depth or in outcrop or below the weathering zones of talus somewhere in the immediate area.

Heinrich [47](1966, p.19) cautions that most carbonatites are associated with miassic rocks having the following affinities:

- Main Elements:** $\frac{Na_2O + K_2O}{Al_2O_3}$, where (wt%) < 1 (See Table 5)
- Significant Elements:** Calcium, Magnesium, and Fluorine are "significant elements" (See Table 5), also in the Death Valley area discussed later in this paper.
- Main Maics:** Biotite, diopside, augite and hornblende are the main mafics. However, aegirine has been reported, which

indicates an agpaitic composition which is not favorable for the occurrence of carbonatites (See [Appendix II](#)). Young [33] (1989) factored the mafics into a useable classification that could be useful for discriminating rock type and anticipated minerals.

- d. **Main Feldspathoids:** Nepheline and cancrinite (not sodalite) are the main feldspathoids. It should be noted that cancrinite has been reported in one nepheline syenite (in the northern area), but the mineral commonly occurs in dike rocks of the area, which indicates a miascitic composition and possible carbonatite associations [49].
- e. **Accessory Elements:** Relative abundance of accessory elements presents a mixed (agpaitic and miascitic) affiliation. For example, rocks with agpaitic affinities contain high concentrations of titanium, zirconium, niobium, rare earths (lanthanides), strontium, thorium and phosphorus. However, miascitic affinities also include accessory elements such as titanium, phosphorus, barium, strontium and niobium. The presence of rare earths and thorium in the immediate area indicates an agpaitic composition, but the presence of barium and strontium indicates a miascitic affinity. It should be noted too that niobium is apparently present only in very low concentrations in the area as indicated by the analyses available to date (see Table 5). However, West [8](1953) reported a niobate mineral from placers in the general vicinity of the subject area. All of the other elements are present in significant amounts. No mention of the affinity of uranium for either of the two classifications is made by Heinrich [47](1966).
- f. **Accessory Minerals:** Spene, rutile, zircon, apatite, suspected ilmenite and titanium-magnetite have been reported in the area and indicate a miascitic composition. Pyrochlore would also be present but has not been identified to date. However, the sink-float analyses (see "Preliminary Metallurgical Investigations: Sink-Float Analyses) on the less than 3.3 specific gravity fraction indicate both zirconium and titanium are present in substantial quantities. The mineral zircon is present in many samples and all of the zirconium should have been collected in the greater than 3.3 specific gravity fraction as zircon, unless zirconium was also present in the form of a lightweight, complex silicate of zirconium. Incomplete sample preparation, digestion, or improper heavy-liquid make-up could have complicated interpretations.

Conclusion: Some of the rock samples indicate a general miascitic composition with some indications of an agpaitic affinity. They also show many metasomatic alteration features, which could be related to fenitization. Miascitic complexes, whether or not they have carbonatites as discrete phases, commonly are enriched in CO₂, which manifests as cancrinite or calcite or both, appearing as late magmatic or deuteritic species. Both have been reported in the areas of interest. Agpaitic rocks contain very little CO₂, and accessory calcite is absent, which does not appear to be the case in the subject areas [47].

The relationship of the carbonate units (p_fsm) to the alkali intrusives has not been fully evaluated. Petrographic and geochemical analyses of the carbonate samples should be conducted. Although field reports indicate that the carbonate units are sedimentary in origin, some of the units might be a part of a carbonatite complex that has intruded sedimentary carbonate units that has not been recognized in the field to date. But based on the limited number of samples of the carbonate unit, at least some of the carbonate was found to be mineralized, containing scattered blebs of pyrite, and other unidentified opaques.

The literature on carbonatites is replete with controversies regarding their origin, which commonly border or are present within alkali intrusive areas (Sorensen, [50](1974). Decker and Karl [51](1977) Indicate that aeromagnetic lows surround hill 2109 of Omega's southern area, which might be related to a carbonatite or other igneous intrusion at depth (Modreski, et al.,[49] (1995) 1995. Aeromagnetic highs have been mapped just to the east and south of the southern area of interest (Alaska Geological Survey, (1985).

The ramifications of a carbonatite being present in the area are substantial. Many carbonatites are known to be miascitic and metalliferous, e.g., Magnet Cove (Arkansas), Mountain Pass (California), Alna (Sweden), Haliburton-Bancroft (Canada). It should also be noted that the Ilimaussaq Complex (Greenland) is agpaitic and carries, in part, significant rare earth and thorium elements in particular minerals that have not been identified in the Omega areas to date [67]. More recent work on carbonatites involve Berger, et al., [52](2009) (2009) and Gwalani, et al.,[53] (2010) (2010). Additional investigations on the carbonate units northwest of the central area of interest have merit.

The Ilimaussaq deposit contains considerable tonnages of low-grade rare earth and thorium ores. The agpaitic alkaline intrusives of the Kola Peninsula (USSR), however, are prolific in economic rare-earth and related mineralization [54].

Allanite Mineralization: The mineral allanite is common as an accessory mineral in the intrusives of the Seward Peninsula and elsewhere in Alaska and other states (see White, [55](1946); Moxhew and West (1952)cited in White and Tolbert [56] (1954); Wedow and Tolbert [57](1954); West and Matzke, [58](1953). Allanite has also been reported in pan concentrates in the Golovin Bay area southwest of the Omega areas of interest from placers in a granitic terrain [8].

The radioactivity of these concentrations was attributed to spene, allanite, zircon, monzonite, uranothorite and an unidentified uranium-titanium niobate, but mineralized zones were not located until recently when the U. S. Geological Survey reported the abundant allanite occurrences as part of the NURE program Miller, et al.,[9]1976.

Allanite also commonly occurs in siliceous phanerites and pegmatites Smith, et al., [59] 1957 and Volborth, [15] 1962. Furthermore, the uranium content was found to be highest in granitic rocks. In allanite concentrates, uranium ranged from 0.35% to 2.33% eU_3O_8 . Allanite was found to be of exceptionally uniform composition. Although seldom considered a uranium ore mineral, allanite also has been reported as an accessory mineral in many of the major uranium occurrences in igneous rocks, e.g., Trites and Tooker, [60] 1953; Whitfield, et al., [61]1959; Ford, [62]1955; Olson, et al., [63]1954; Lang, et al., [64]1960; Neverburg, [65]1955; and Rose, [66] 1979).

The occurrence of allanite as a major uranium (as well as a thorium and rare-earth) ore mineral has special significance to the present investigations. For example, the Mary Kathleen uranium-rare earth deposit in northwestern Queensland, Australia, was Australia's only major hardrock, uranium-rare-earth producer until recently Brooks [67] (1972). This of course will change when other recently discovered uranium deposits go into production ([68], 1979, see p. 10). The deposit consists essentially of allanite mineralization Miles, [69] 1955, Wilde [70] (2013).

In the Australian deposit, for the most part, uraninite is disseminated throughout the allanite as irregular ovoidal grains of 0.1 to 0.01 mm in diameter, which are similar to the type of uranium occurrence in the mineralized zones of the southern area of interest (see Figure 37). Uraninite also occurs within apatite. Ore mineralization was controlled by a specific fracture system and formed an irregular honeycomb of connected shoots of mineralization, which vary in thickness from a few feet to 250 feet Hughes and Muro [71] (1967). In outcrop, allanite ore occurs over lateral distance of up to 900 feet. The senior author was impressed during a visit to the mine area in late 1960s by the varied color of the altered rocks in the area, which no doubt attracted geologists for a closer look at the alteration and subsequently discovered ore-grade material during drilling programs (Derrick, [72] 1977).

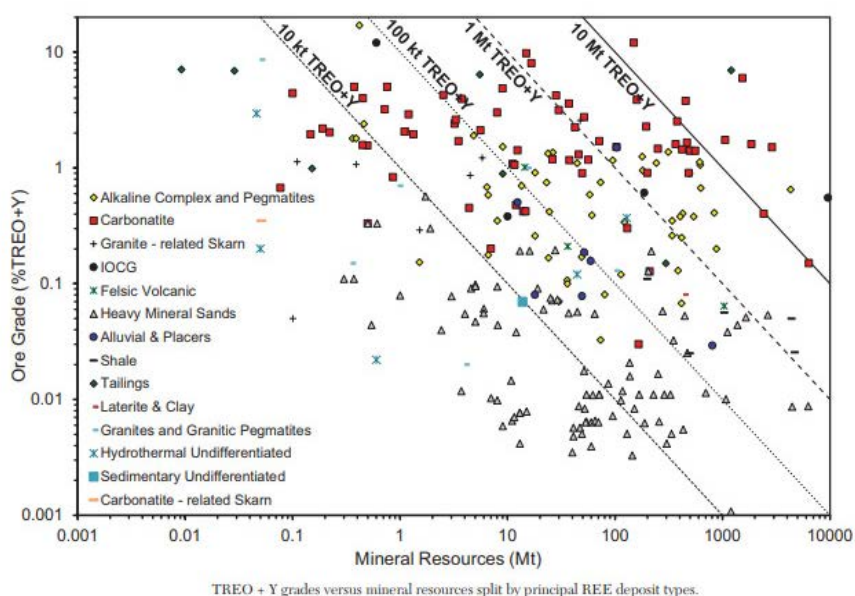
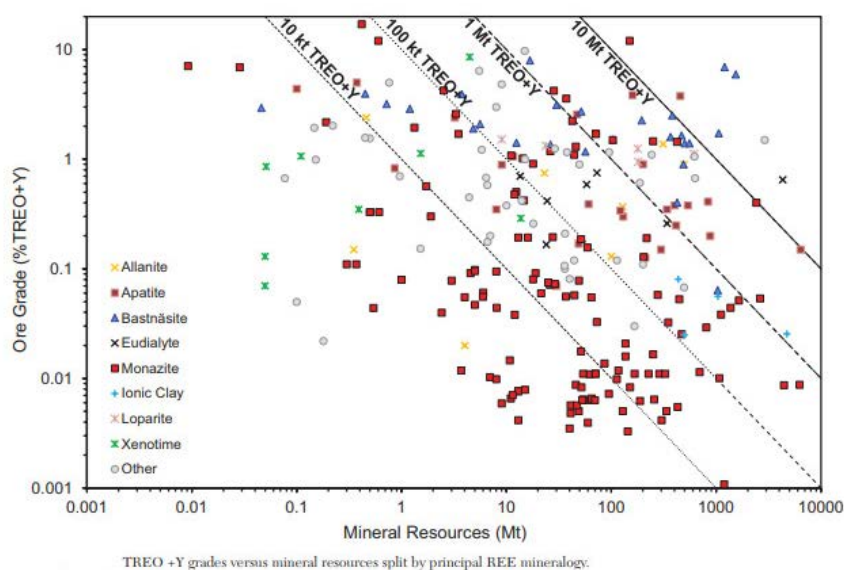


Figure AI-1A: (Above) and Figure AI-1B: (Below) (From Weng, et al., (2015).



(Click on Figures to Enlarge)

Allanite is a substantial part of many REE deposits in the world. The above plots indicate that allanite is part of the mineralogical and geological associations of alkaline, pegmatites and carbonatites of many REE deposits in the world (see Figures AI-1A and 1B; Weng, et al., 2015). Remarkable similarities in mineralogy, general geology and geochemistry appear to exist between the mineralized rock occurrences (that could be perceived) and the ore of the Mary Kathleen deposit. Both have similar concentrations of the lighter rare-earth elements as inclusions within massive allanite mineralization. Thorium is present in both occurrences, but thorium is higher than in the allanite of the Mary Kathleen deposit. Both occurrences are possibly metasomatic in origin, and both can be examples of disseminated skarn-type replacement of carbonate and calc-silicate rocks.

TABLE 15
COMPARISON OF URANIUM, THORIUM AND RARE-EARTH ELEMENT ANALYSES
FOR
MINERALIZED ZONE AND MARY KATHLEEN ORE

| | Omega Mineralized Zone* (C2-17 Sample Series) | Mary Kathleen Ore** (Surface Bulk Sample) |
|---|--|--|
| U ₃ O ₈ | 0.75% ⁺ (7,500 ppm) | 0.50% ⁺⁺ (5,000 ppm) |
| ThO ₂ | 4.20% (42,000 ppm) | 0.20% (2,000 ppm) |
| Cerium (Light REE) Sub-Group ⁺⁺⁺ | 11.74% (117,400 ppm) | 19.71% (197,100 ppm) |
| Yttrium (Heavy REE) Sub-Group ⁺⁺⁺⁺ | 0.45% (4,500 ppm) | 1.86% (18,600 ppm) |

*Recalculated as a 100% Allanite Concentrate
 **Analyses of a typical brown allanite concentrate (Miles, 1955)
 +Analyses in terms of leachable ^cU₃O₈
 ++Presumed to be leachable ^cU₃O₈
 +++Lanthanum through Europium
 ++++Gadolinium through Yttrium

A preliminary comparison of bulk sample analyses for the mineralized zone and the outcropping Mary Kathleen ore is shown in (Table 15). It should be noted that although only a limited number of samples have been analyzed to date on the subject mineralized zones, the recalculated values indicated in (Table 15) show a remarkable similarity, with the exception of thorium, to the Mary Kathleen surface ore. The data appear to further demonstrate that combined with the other geological similarities, the uranium and rare earth analyses of allanite mineralization are similar to the Mary Kathleen ore Derrick [72] (1977).

The Mary Kathleen deposit is one of the major rare-earth deposits in igneous rocks known in the world, probably being exceeded in magnitude of reserves only by the apatite-bearing deposits of the alkali intrusives of the Kola Peninsula (UBSR), the Chinese (Mongolian) deposits (BGR-MRAM, 2015), and the bastnaesite-barite-siderite-calcite-carbonatite ore body of the Mountain Pass District of California Olson, et al., [63] 1954; Evans, [43]1966, all of which also contains allanite.

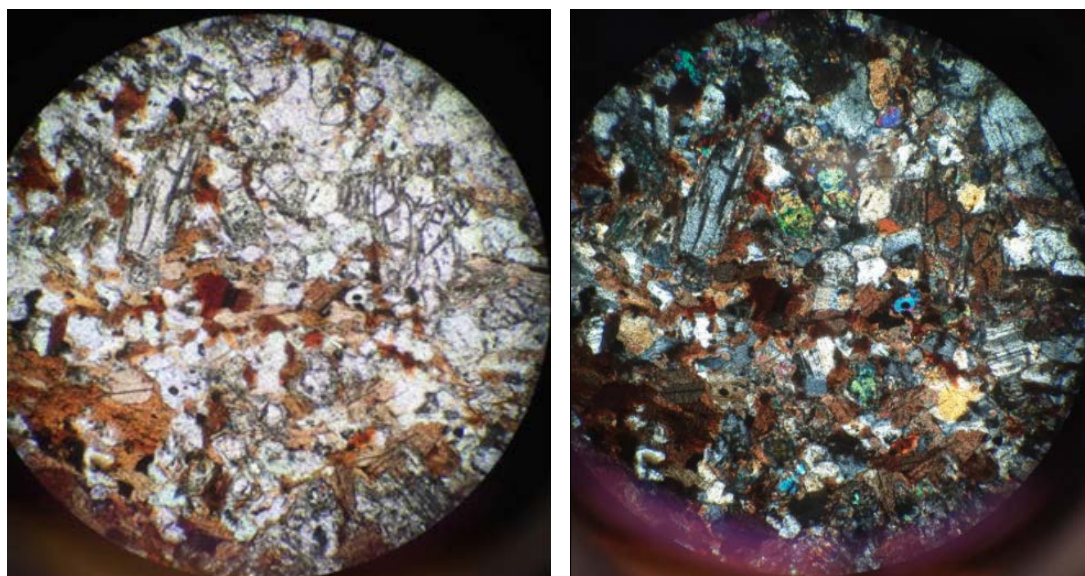
The Kola Peninsula occurrence has a strong geological affinity with the alkali intrusives that occur in and around the Omega claim areas Sorensen, [74] 1970a and [54] b, and [50]1974 and with other alkalic complexes. The run-of-mine ore of the Mary Kathleen deposit reportedly contains rare-earth oxides slightly under 2 percent REO after Rose, [66] 1979, although the run-of-mine content of the Mountain Pass deposit averages 5 to 10 percent (Evans, [43] 1966). Based on the analyses of the mineralized occurrences, the presently available data indicate a run-of-mine REO content of approximately 6 percent. Additional sampling and drilling will be necessary to appropriately characterize the REO content and magnitude of the occurrence. The allanite mineralized zones occur in a medium to coarse-grained syenite-monzonite of the Kkms Unit (see Plate II) and appear to be associated with the alkaline dikes (melanite phonolites: see Appendix II and Plate II); however, these zones are apparently not in contact with the dikes. Allanite occurs as large (up to 5 mm) brownish-black crystals constituting up to 60 percent of the rock (see Photomicrograph #1; Appendix II).

Field Conditions: Extensive frost-heaving has reduced the outcrop areas to rubble, and allanite-rich rock can be found as float over the crest of hill 2109 in an indistinct zone 20 to 45 feet in width. The prominent phonolite dike (see Figure 10) at the margin of the mineralized zone can be traced for approximately 2,500 feet to the northeast and southwest of hill 2109. Large boulders of allanite float can be found along the margin of this phonolite dike. The actual width and length of the mineralized zone could not be estimated during the field investigations. The ground radiometric traverses indicate the general trend of the mineralized zone (see Plate III).

Although additional work should be conducted on the mode of allanite occurrence, it is postulated at this time that the uranium was introduced into the allanite and other receptor minerals during one or more periods of metasomatism (Ragland, et al., [74] 1967). The allanite, however, appears to be an alteration product of hornblende, as a result of deuteric replacement during the intrusion of one or more of the phonolite dikes that carried uranium, thorium, and rare earth-enriched fluids.

The association of siderite and barite with mineralized allanite also supports a late-stage or multi-stage emplacement of mineralizing fluids. The Death Valley mineralization to the north of the area also shows multi-stage emplacement of fluorine-rich fluids, (discussed later in this paper).

Associated Mineralization: It is possible that one or more types of dikes carried significant quantities of uranium, thorium, rare earth and other elements of interest. The particular avenue of such enriched fluids might be subordinate in importance to the rock type through which such fluids passed. Rock types which should be favorable for uranium precipitation were evaluated in the central area as a principal part of the investigations conducted by URI during the Phase II program. Of particular interest is the migmatitic zone (Unit Mi: [Plate II](#)-Location D2-23: MC: 17-I); see thin-section views (for additional information see [Appendix I](#)). A thin, massive pyrite dike was also reported during the Phase II field program (C2-16: MC: 19-1).



Figures MI-1A and 1B: Unit Mi and Sample C2-29 in Plane Polarized (left) and Cross-Polarized Light (right). 10x magnification. See [Appendix I](#), p. 18 for XRF.

Potential mineralization such as this, combined with potential mineralization associated with intrusive contacts in the vicinity of the carbonate units (unit p ϵ sm: [Plate II](#) - Location D2-46:MC:16-G, etc.) and with the areas of reported geochemical anomalies (see Table 4), should be investigated further but current assessment support the view that the Mi unit (Sample C2-29) represents the remnant of a roof pendant that once covered the intruding plutons.

Implication as Uranium Source Rock

This investigation initiated in the late 1970s and was among the first groups to realize the significance of the uranium anomalies exhibited in the northern area of interest. This is located on the southeast periphery of a closed Tertiary basin of up to 16,000 feet in thickness. The Dry Canyon Creek pluton is, in part at least, anomalous in uranium, and the uranium present is leachable, as indicated previously. The nature of the Tertiary sediments is presently unknown, but they are presumed to be largely fluvial. The potential of classical uranium roll-front and young unconformity-related occurrences in a permafrost environment should be investigated in detail.

As will be discussed later in this paper, a discovery by Houston Oil and minerals (HOM) was made of uranium in a faulted extension of the Death Valley and Darby granites Foley and Barker [27] (1980) in the form of roll-front mineralization among/between active periods of volcanism (See Figure 1 for general location). This has led to subsequent exploration in parts of McCarthy's Marsh.

Low uranium prices brought further uranium exploration in the area to a standstill in the 1980s and the after some improvement, the Japan earthquake caused uranium prices to fall by some 60%. Since then prices have remained stagnant, but recent activities could bring relief with rising prices Campbell [75] (2018). To be clear, any significant rise in the uranium price will certainly bring attention to this region once again and to the eastern McCarthy's Marsh area in particular.

Conclusions on the Kachauik Area Investigations

Preliminary geological, geochemical, and geophysical investigations conducted during the Phase II investigations by URI indicate that mineralized zones of potentially significant extent occur with in and around the three areas of interest discussed above.

The following are the principal conclusions reached during this investigation:

1. Based on samples from the southern area of interest, whole-rock analyses of the allanite-bearing mineralized zones indicate uranium in excess of 0.15 % cU_3O_8 , rare-earth elements in excess of 4% REO, and thorium in excess of 1.0% ThO_2 ,
2. The mineralized zones occur within a composite Cretaceous alkalic and calc-alkaline intrusive complex, which has been dissected by numerous Cretaceous alkaline dikes of various compositions,
3. The mineralized zones occur in monzonitic rocks, adjacent to a prominent “pseudoleucite” phonolite dike. The dike can be traced for approximately one mile over the crest of Hill 2109 before it becomes covered by talus and solifluction lobes of debris. In the areas of lower elevation; outcrops are rare because of the extensive talus; therefore, additional areas similar to the allanite occurrences on Hill 2109 could be difficult to locate. However, detailed ground radiometric and geological traverses would be effective in locating occurrences as that exposed on Hill 2109,
4. The major mineralized zone appears to be at least 20 feet and possibly up to 45 feet in width,
5. The margin of the major mineralized zone can be traced laterally for at least 2,000 feet, although mineralization is not apparent throughout this distance because of poor outcrop and abundant rubble,
6. Petrographic, geochemical, and metallurgical data combined with the results of microprobe and cathodoluminescence investigations indicate that the genesis of the allanite is related to a metasomatic replacement of hornblende and other essential varietal and accessory minerals by allanite with simultaneous entrapment of uranium, rare-earths and thorium as a result of the replacement process. Such a process can occur if microfracturing of the country rock has occurred during the intrusion of the dike,
7. A dike-forming fluid, rich in carbonate, as well as uranium, rare earths, thorium, iron, and other elements, could have migrated away from the main dike conduit into semi-permeable country rock and precipitated during a period of epidotization and related deuteric alteration within the allanite crystalline structure. This structure subsequently became metamict as a result of the damage during any crystallization process created by the abundant radiogenic elements present, creating a mineraloid with petrographic and geochemical characteristics similar to allanite and any other metalloids created during the process,
8. Uranium occurs within the mineralized samples in the following quantities:
 - a. within the allanite mineraloid structure (0.85% total cU_3O_8 and >0.75% leachable cU_3O_8),
 - b. within minerals having a specific gravity less than 3.3 (>0.15% U_3O_8 leachable),
 - c. within such accessory minerals as zircon, apatite, monazite, as well as other high specific gravity minerals, including allanite, siderite and barite: >3.3 (ranges from 0.08% to 1.07% cU_3O_8 , the latter minerals containing soluble uranium incorporating insoluble uranium. This fraction contains approximately 10 to 15% by weight of the total uranium present in the whole rock),
9. Preliminary leachability investigations indicate that, based on whole rock analyses of the mineralized samples, approximately 88% of the total uranium present is leachable. The uranium present in both the greater than and less-than 3.3 specific gravity fractions is therefore leachable,
10. Preliminary cathodoluminescence investigations on one mineralized sample indicate that the allanite mineraloid structure contains abundant spherical inclusions of different catholuminescent colors, indicating a number of separate mineral phases, e.g., uraninite, thorite, cerite, uranothorite, etc. XRD analysis confirmed the metamict condition of the allanite crystalline structure; but the XRD did not confirm allanite.
11. The mean uranium:thorium ratio of 0.24 ($s=0.07$) for six selected samples from widely separated plutonic country and dike rocks include uranium (cU_3O_8) values ranging from 2,650 ppm down to 60 ppm. This indicates that the immediate region is more anomalous with respect to uranium and thorium than indicated by pre-1976 U. S. G. S. field investigations.
12. Preliminary equilibrium analyses indicate that uranium equilibrium is near unity, neither enriched nor depleted with respect to chemical uranium and its radiogenic daughter, i.e., $DNA U_3O_8/Bi^{214}$.
13. Preliminary analyses on the distribution of the specific rare-earth elements present indicate that approximately 96 % by weight of the total REO present are of the cerium (light REO) subgroup, with the yttrium (heavy REO) subgroup constituting approximately 4 % of the total rare-earth elements present,
14. Rare-earth elements occur within the mineralized samples in the following quantities:
 - a. within the allanite mineraloid structures (>12 percent total rare-earth oxides (REO)),
 - b. within minerals having a specific gravity less than 3.3 (approximately 4 % REO),

- c. within such accessory minerals as apatite, monazite, and sphene, as well as other minerals of higher than 3.3 specific gravity, including allanite (estimated at 6 to 8 percent REO).
15. Data available on the Mary Kathleen uranium-rare earth mine (with allanite) in Australia indicate strong similarities to the allanite occurrences within the mineralized zone containing abundant allanite. This type of uranium-rare earth mineralization is a prospective exploration target in other alkali intrusive complexes of the world.
16. Strong geochemical and radiometric anomalies are present in Omega's central and northern claim groups. In the central claim group, six analyses have been completed with a high of 120 ppm cU_3O_8 from allanite amphibole (hornblende) syenite. The highest concentration of uranium from the northern claim group has been reported from an allanite nepheline syenite (150 ppm cU_3O_8) only a total of four chemical analyses have been completed to date on the available samples from this group. Even based on the limited number of samples analyzed, selected rock types, all containing allanite, exhibit strongly anomalous uranium content, and in most of the samples analyzed more than 82% percent of the total uranium present is in leachable form, even when the samples with low uranium content are included.
17. Preliminary ground radiometric investigations indicate that uranium daughter products (Bi^{214}) exceeds thorium (Tl^{208}) in Omega's northern area. This indicates that uranium enrichment could have occurred in the Dry Canyon Creek pluton and surrounding sediments below the local water table.
18. The central group is located, in part, on two aerially extensive aeroradiometric anomalies reported by an earlier DOE regional survey (see [Plate IV](#)).
19. Strong geochemical anomalies appear to exist for other elements in all three of Omega's claim groups. The following elements, presented as groupings for each strongly anomalous sample, are indicated as follows:
 - a. Rubidium
 - b. Bismuth, Lead and Niobium
 - c. Molybdenum, Copper, Nickel, Chromium, Vanadium Scandium, and Lithium
 - d. Silver
 - e. Cesium, Tin, and Rubidium
 - f. Copper, Vanadium and Lithium
 - g. Niobium and Rubidium
 - h. Arsenic, Nickel, Chromium, and Sulfur
 - i. Rubidium
 - j. Bismuth, Molybdenum, Niobium and Lithium
 - k. Silver
20. The various suites of anomalous "pathfinder" elements present show that the region might be a new metallogenic province.
21. The northern claim group contains igneous rocks of anomalous uranium content. Such uranium is considered to be in a leachable form. Acidic near-surface conditions have been present as indicated by investigations conducted by URI on the soil zone. The northern area is located on the southeast periphery of a closed Tertiary sedimentary basin reported to be up to 16,000 feet in depth (State of Alaska, 2005, p. 29). The potential therefore exists for sedimentary uranium occurrences in the vicinity of the northern claim group. The uraniumiferous pluton might have served as a source rock for supplying elevated levels of uranium in solution to the groundwater system of the basin. The nature of the fluvial sediments within the basin is poorly known, but they are known to contain lignite, so conditions are suitable for roll-front uranium formation within Tertiary units.

NURE Report Availability: A comprehensive report was prepared in 1977 as part of the National Uranium Resources Evaluation (NURE) program implemented throughout the U.S. by the U.S. Energy Research and Development Administration in Grand Junction, Colorado, but was not made available to the general public for a number of years later. Earlier, Campbell (1974) had submitted a Rice University proposal to U.S. EDA to fund a U.S.-wide sampling program of groundwater to assess the nation's potential uranium resources and to provide background data for future environmental evaluations (Campbell and Biddle [76] (1977, p.17). This was consistent with the Rice University program of supporting academic-industrial research to benefit the needs of society.

Over the next few years, URI monitored the development of the NURE program and selected areas on the Seward Peninsula for investigations in the subject areas just after the preliminary NURE data were released in 1978, but URI did not have the benefit of the full NURE report at that time. That report became available later and is especially comprehensive and provides additional information on the southern and central areas of interest discussed in this paper Eakins, et al., [29] (1977).

Uranium Source Rocks and the McCarthy Basin

Based on the URI data, the uranium is in balance with the radiogenic daughter products in the Kachauik area of investigations. Whether these rocks experienced appreciable leaching of uranium earlier during plutonic fractionation or oxidation after cooling by leaching of uranium-rich rocks by meteoric water is uncertain but all are considered likely. However, most of the plutonic rocks in the areas sampled (other than those of the mineralized zones) contain uranium in unusually high concentrations. For example, four samples were analyzed for uranium from the northern area of interest, together averaging 44 ppm (Table 5). NURE work also noticed the Dry Canyon Creek pluton, and its proximity to the McCarthy's Marsh, and sampled the area in some detail; see Eakins, et al., [29] 1976-77, especially pp. 2-47 to 2-50, and 2-58.

Combining that potential source with the heavily fractured rocks that exist in the area (as indicated in the thin sections) and below the Tertiary basin that is adjacent to the northern area of interest, then factoring in recharge to the basin's groundwater by uranium-enriched groundwater, combined with the reported lignite among the fluvial sediments of the aquifers in the basin (State of Alaska, 2005, p. 29), these factors meet the conditions necessary to form epigenetic uranium roll-front deposits (Campbell, et al., 2008; Campbell and Biddle [76] (1977); Dickinson and Duval, [78] (1977) and Rackley, (1972). See conceptual model below (Figure CM-1).

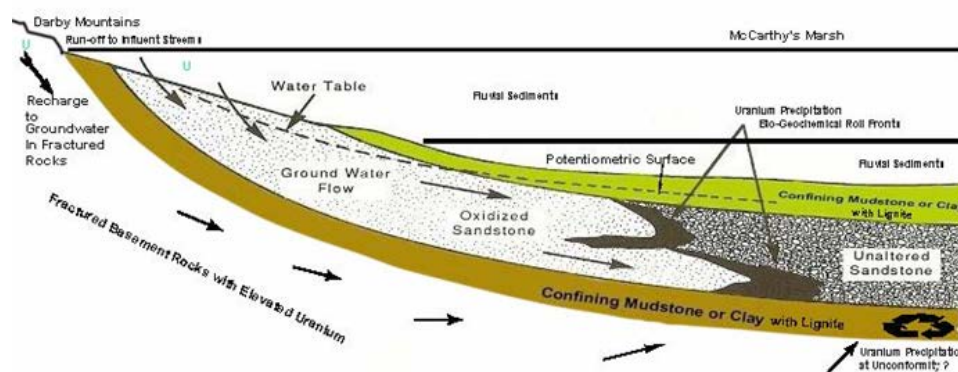


Figure CM-1: Conceptual Model of Two Types of Uranium Mineralization in Subject Area.

(Click on Figure to View Industry Guide to Drilling for Roll-Front Deposits)

The second type of uranium occurrence expected might be located at/near the contact (and above the basin bottom) with the underlying fractured basement rocks is shown in the above model. Many such "unconformity-related" uranium deposits are now known (Jefferson, et al., [79] 2007; and Chi, et al., [80] 2018). We propose that not only have Tertiary uranium roll-fronts likely formed below the eastern areas of the McCarthy's Marsh (termed here as the McCarthy basin below (Barns and Morin [12] (1988)), but given the highly anomalous content of uranium in the basement rocks, in contact with carbonaceous material within either clay or lignite, these conditions could also have formed unconformity-related uranium deposits. These too would be expected to form below the east-central part of the basin where the groundwater flow in the basement fractures from the Darby Mountain plutons turns upward below the basin, through the fluvial sediments and/or faults, to discharge at the surface contributing to the numerous small ponds of melted water present during the summer months in the marsh. At depth, the uraniferous groundwater would interact with the carbonaceous material in the bottom part of the basin to precipitate uranium, especially if the groundwater has been heated by geothermal conditions some 16,000 feet or less at and below the bottom of the basin.

These conditions could exist at favorable sites all along the basin's lower contact with the basement from just east of the plutonic rocks below the northern area of interest at shallow depths, all the way to the center of the basin at various depths. The upper 1,500 feet of the eastern part of the basin would be current exploration targets. Only the Bokan Granite Complex in south eastern Alaska has produced uranium and thorium to date, but there are remarkable similarities of the complex with those of the Darby pluton and especially those of the Kachauik and Dry Creek Canyon plutons and the associated uranium, thorium, and rare-earth mineralization discussed above from the eastern Seward Peninsula (Thompson (1997) [126], especially pp. 475 and 480).

Death Valley Area Investigations

The Death Valley Uranium Deposit: Another feature of interest in the area is that uranium in roll-front masses were discovered in 1977 along the western edge of the southern extension of Death Valley, called Boulder Creek basin Dickinson, et al., [81] (1987). The initial field work was carried by Houston Oil and Minerals in 1978 and drilling occurred during 1979 through 1981. Reserves of at least 1 million pounds U_3O_8 with a grade of 0.27 % U_3O_8 and a thickness of three meters. This deposit was the largest known deposit in Alaska (as of 1987). Based on this discovery and the indicated characteristics of the uranium deposition, the conditions for uranium roll-front and a possible high grade young unconformity-type of uranium deposition are clearly likely within and below the McCarthy's basin.

Drill-logs from the Death Valley uranium exploration program indicate the lithology expected above the basin bottom of the Boulder Creek basin, at the southern extension of Death Valley. Dickinson, et al [81] (1987) report that the uranium of the Death Valley deposit was dissolved from the Darby pluton, migrating eastward in oxidizing groundwater, and precipitated in a chemically reducing environment in Tertiary sediments containing abundant carbonaceous material like lignite (State of Alaska, 2005, p. 30).

Dickinson [82] (1988) later reported on that a sideritic lacustrine mudstone was found in drill core from a uranium deposit in the Death Valley area. The precursor sediments for this rock were apparently deposited in an unusual “iron-meromictic” Eocene lake, herein named Lake Tubutulik, which occupied part of the Boulder Creek basin, a structural graben that is a southern extension of the larger Death Valley basin. The Boulder Creek basin is bounded on the west by granite of the Late Cretaceous Darby Pluton, and on the east by Precambrian to Paleozoic metasedimentary rocks. The small lake basin was formed by basaltic flows that dammed the river valley of the ancestral Tubutulik River running southward through the Death Valley in early Eocene time. Based on carbon isotope analysis of the siderite, the dissolved bicarbonate in the profundal facies was largely inorganic.

Sideritic carbon from the onshore paludal facies has an isotopic signature ($^{13}\text{C} = +16.9$), which is consistent with residual carbon formed during methanogenic fermentation, the generation of which could have accelerated the bio-geochemical cells involved in the otherwise cramped environment on the subsurface of uranium deposition. Deposits in south Texas, for example, are known to be driven by natural gases, CH_4 and/or H_2S , causing re-reduction of ore-zone sediments and “calcretization” of shallow zones that creates issues for production and drilling (ex. Campbell, et al., [83] (2010, pp. 12 and 14)). This is a variation that is not typical in the roll-front deposits of Wyoming, but because of the faulting and involvement of basalt and other volcanics in the above, the shape of the orebody is complex. It might even be classified as an unconformity-type deposit in part because the host rocks lie very near the basement rocks (igneous or metamorphic rocks). This condition is also known in a uranium deposit in South Australia (see Campbell and Campbell, [127](2016, pp. 51-54)).

The cross-section of (Figure BC-1) below presents some of the drilling results for estimating the resources in this deposit. Note that the lignite units are the primary focus of uranium deposition, in places, resting directly on the granite of the basement rocks in this area (State of Alaska, 2005, p. 31).

The minerals identified are either from the reduced zones (e.g., coffinite, pyrite in places) or from the oxidized zone, e.g., autunite with secondary enriched surficial deposits. The deposit exhibits radioactive disequilibrium with the low-grade interval having a surplus of daughter products and the high-grade samples having a deficiency of daughter products, e.g. radium, etc.

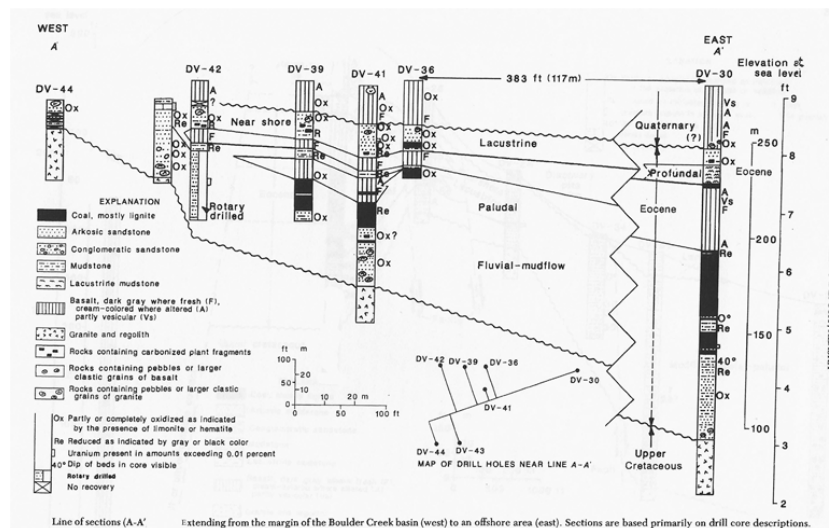


Figure BC-1: Exploration Drilling (Click to Enlarge) (From Dickinson, et al., 1987, p. 1563).

Santos [84] (1975) indicated this condition was related to a continuous redistribution of daughter products, mainly radium²²⁶ was confirmed by the range of ages of the mineralization from early Tertiary to the present. Triex Exploration acquired the HOM properties in the early 2000s and have since conducted follow-up drilling on the Boulder Creek basin properties, and made new discoveries north along strike into Death Valley. A total of 219 State of Alaska claims were held pursuant to two separate option agreements, which included Boulder Creek (39 claims) and a new area in Death Valley (104 claims). Industry reports are summarized in the available information (I2M Web Portal (2018)).

After Canterra acquired both Triex and Full Metal Minerals, Ltd., no further information was made available on the properties. This is likely because the uranium prices have been low since 2011 and the properties are therefore of little economic interest for uranium mining in the U.S. This economic condition was caused by the major earthquake and tsunami that damaged the nuclear power plants in Japan causing all Japanese nuclear plants to shut down creating a major drop in uranium prices and a slowdown in the U.S. uranium exploration industry.

Although there were no serious injuries or deaths during the nuclear power plant tsunami damage, this caused a world-wide oversupply of uranium driving the price to historical lows on the spot market [85] (2015). U.S. and other uranium producers were forced to cut back or cease operations because U.S. could not compete with operations in Kazakhstan, Russia, Canada and other sources of yellowcake (Kat USA, 2018). At this writing, the U.S. Congress is considering a bill to protect U.S. producers, especially as the Russia Duma is considering a ban on all sales of yellowcake to the U.S. (Platts-S&P Global, 2018). When the prices rise, these properties will likely undergo renewed interest and further exploration. In the meantime, the following information is available for the subject properties on the Seward Peninsula.

Boulder Creek Area: The claims subject to the Boulder Creek option agreement originally included a block of 11 federal claims covering the Boulder Creek uranium deposit and a surrounding block of 39 state claims. Beginning in 2005, three successive summer programs were carried out to fully evaluate the Boulder Creek deposit and to explore for additional deposits in the region. This work included some 1,617 line-miles of airborne and ground geophysics, a total of 3,204 soil and biogeochemical samples, both grid-based and reconnaissance and almost 10,000 feet of drilling in 27 drill holes. Full Metal Minerals Ltd. (in JV with Triex) approved C\$1.5 million for their 2007 uranium exploration program for Boulder Creek, Alaska. Cumulative expenditures of more than \$3 million have been spent over the past two years, advancing the Boulder Creek uranium deposit and exploring for additional deposits in the surrounding region.

The Triex [86] 2007 program included about 10,000 feet of core drilling, testing multiple targets on the Boulder Creek properties. This program followed up on the 2006 drilling program, which encountered encouraging grade and thickness at the Boulder Creek uranium deposit (0.317% U_3O_8 over 20 feet in Hole DV06-54, including 0.867% U_3O_8 over 7 feet, and 0.317% U_3O_8 over 7 feet within 16 feet of 0.1647% U_3O_8 in Hole DV06-64. Approximately 5,000 feet of diamond drilling was to complete the delineation of known mineralized zones, and to further evaluate the ten kilometer trend of geochemical anomalies along strike, both to the north and south of the deposit. Two kilometres to the southeast along strike from the Main Zone, a 1,800 feet long multi-element (uranium-arsenic) geochemical anomaly was to be tested; this anomaly is based on anomalously high concentration of geochemical samples from four consecutive grid lines ([more](#)).

Approximately 0.5 mile northwest on trend from the Main Zone, a soil sample at the “990 Hill” area contains 1,540 ppm uranium; about 1,600 feet to the north is a 3,000 feet long multi-element uranium-arsenic-molybdenum anomaly that was tested with several holes. Finally, selected anomalies within an approximate 1,800 feet-long trend, and located at Carbon Creek about 2.5 miles north, and on trend with the Boulder Creek Main Zone, were tested by a fence of drill holes. However, efforts to significantly expand the main Boulder Creek uranium resources were unsuccessful, although isolated uranium mineralization was encountered. Nonetheless, Triex wrote off the approximately \$1,080,000 of mineral property acquisition costs and \$3,438,000 of deferred exploration costs incurred on the properties. A full camp clean up and reclamation program was accomplished in August 2008. During fiscal 2009, the federal claims were returned to the underlying owner.

Death Valley Area: Triex flew approximately 1,155 line-kilometres of airborne radiometrics along the Boulder Creek - Death Valley trend in 2006. Flight line spacing was about 700 feet. Twelve selected radiometric anomalies were followed up on the ground by prospecting and geochemical sampling. Reconnaissance geochemical sampling was also completed along the western side of Death Valley, where the geological setting is similar to that at Boulder Creek. A total of 203 geochemical samples were collected on widely-spaced lines in western Death Valley; eight anomalies were followed up by further sampling and prospecting in 2007. Two or three drill holes were planned for the Death Valley grid area, after ground follow-up and refinement of existing anomaly target areas within a block of 104 contiguous state claims that cover an area of 15,679 acres in the Death Valley, extending some 22 miles to the northwest from the Boulder Creek area. The Fireweed occurrence in Death Valley was discovered in 2008. This is located at the north end of the Boulder Creek state claim block. No further information is available at this date.

McCarthy Marsh Area: Excluding the impact of faulting and associated active volcanism before, during and after the uranium deposition in Boulder Creek basin, it is now reasonable to assume that similar lithology and uranium deposition can be expected in the McCarthy basin located only some 10 miles to the west and in other similar basins in Alaska. As indicated in the earlier section of the Kachauik investigations, source rocks of usually high, leachable uranium is available below the eastern fringe of the McCarthy Marsh where lignite is also known to exist ([State of Alaska, 2005, p. 29](#)).

Triex and joint-venture partners turned to the McCarthy Marsh in 2008 to offset the failure of the Boulder Creek drilling to increase resources. An option agreement was signed for the JV for a block of 76 contiguous state claims that cover an area of 12,160 acres in the McCarthy Marsh area, some 20 miles west of the Boulder Creek deposit. The agreement had a regional area of interest provision which covered about 4,000 square miles centered on the McCarthy Marsh claims. In 2007, they reported on the initial exploration at the McCarthy Marsh with results on soil sampling and surface geophysics, likely evaluating the dipole area mentioned above as well. Approximately 1,841 line-kilometres of airborne radiometrics were completed in three different blocks in this area in 2006. A total of 53 selected anomalies were followed up on the ground. A total of 300 rock samples, soil

samples, and biogeochemical samples were collected. Coincident uranium and molybdenum anomalies were defined in five areas Triex, [87] (2007, pp 19-20).

In the southeastern part of McCarthy Marsh, Triex activities were very near the Omega-URI Northern Area of Interest. Tertiary age sediments occur adjacent to radioactive syenite intrusions on the western flanks of the Darby Mountains (i.e., the Dry Canyon Creek pluton), in a geological setting similar to that found at Boulder Creek. The McCarthy Marsh basin is approximately 30 miles across, and the Boulder Creek basin is only about 2 kilometres across, so the volume of prospective Tertiary sediments at McCarthy Marsh is much greater than at Boulder Creek. The second component of the 2007 program was to drill some 5,000 feet of diamond-tipped drilling/coring on the McCarthy Marsh claims. No other information is currently available.

Death Valley Base and Precious Metals Investigations

Another type of mineralization has been reported on the northern rim of the Death Valley. Field work was carried out by URI personnel in the early 1980s that included outcrop sampling, ground geophysical surveys, and pit excavation to explore a very shallow body exhibiting a major dipole. This anomaly is located only a few thousand feet east of the eastern outcrop of the Windy Creek pluton (an area of significant interest to Placid Oil in the early 1980s). The general area received increased attention from the U.S.G.S. during the latter 1980s and early 1990s (Gamble and Till, [88] (1989) and King, et al., [89](1989), Gamble, [90](1988), Gamble and Till, [91](1993), and Thompson [127] (1997) (1989) and King, et al., (1989), [89] (1988), and [90] (1993).

The U.S.G.S. contributed a surge in field work focused on the Bendeleben and Solomon Quadrangles during the 1980s and 1990s. An area of interest along the northern rim of Death Valley was sampled in some detail over the years of U.S.G.S. activities and reported by Gamble [89] (1988); for particular relevance, see (Table 1) (for cited DV sample locations: see map (here)). It should also be noted that sample #68 reported in that report was obtained before 1976 and was located in the Omega-URI southern area of interest investigated by URI during 1978 and 1979 discussed earlier in this paper.

The Windy Creek Pluton: This intrusive body, located along the western border of Death Valley, is a leucocratic, massive, locally porphyritic to trachytoid, medium-grained monzonite and quartz monzonite, with some nepheline syenite. The intrusive rock is typically fractured and hydrothermally altered (Miller, et al, 1971). A mid-Cretaceous age is based on lithologic similarity to dated rocks in the region Miller, [5] 1972.

As of 1978, Placid Oil Company owned claims (approximately 11,000 acres) covering part of the Windy Creek pluton. Their claims also covered the same previously mentioned quartz-mica schist unit (pεqms), located in fault contact with the pluton, that occurs within the subject properties (see Figure DV-1).

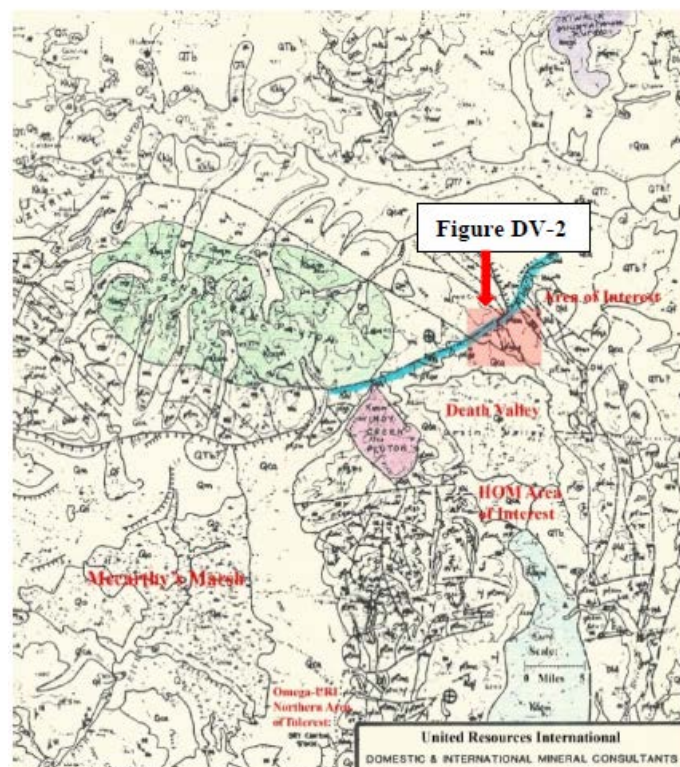


Figure DV-1: Death Valley Area of Interest
(Click to Enlarge).

No other information is presently available on Placid Oil Company’s activities in the area. However, molybdenum, lead, zinc and silver anomalies have been reported in the pluton (Eakind, 1976). The northwest trending fault that forms the western boundary of the pluton has been mineralized with quartz and fluorite over a distance of at least 3,000 feet). It should be noted that the unit (pCqms) is faulted against the pluton in the area containing fluorite mineralization. The Windy Creek pluton is designated Kwcm (purple) in (Figure DV-1).

The Windy Creek pluton exhibits unusual magnetic characteristics that are not apparent in the other plutons in the area. Based on aeromagnetic data presented by the U.S.G.S. Decker and Karl, [51](1977), a highly positive magnetic field (two actually) surrounded on the north by a magnetic trough, extends around into the eastern area of Death Valley. The significance of this feature is unknown but indicates that the Windy Creek pluton likely consists of unusual amounts of magnetic minerals (magnetite, pyrrhotite, etc.), and combined with the reported hydrothermal alteration of the rock in places, mineralizing fluids might have carried significant quantities of metals into the fractured country rock of the shallow subsurface in the area. The large-scale dipole focused over the Windy Creek pluton and the smaller, but still prominent dipole anomaly revealed in the Area of Interest during the URI investigations shown in (Figure DV-1), will be discussed later in this paper.

Precambrian and Devonian Rocks: It is apparent that all of the pre-Cretaceous units in the area examined during the URL investigations of the DV Area of Interest, both sedimentary and volcanic in origin, have been metamorphosed and/or structurally disturbed by the plutons that intruded the overlying country rock, which is generally composed of rocks of Precambrian and Devonian ages (see Figure DV-1). In places, some of the units have been strongly metamorphosed, and major fault complexes have developed allowing avenues for late-stage magmatic fluids to escape the magma chamber into rock units that either overlay or are adjacent to the intrusive. These rock units are therefore potential sites of economic mineralization. Given the appropriate mineralizing fluid and host units, the process of mineralization could have proceeded to potential economic stages, as indicated by the Omilak mine occurrence located a few miles to the southwest, the HOM discovery and other minor occurrences discussed earlier by Berg and Cobb, [91] (1967).

Of particular significance is Kennecott Mining Company’s bornite deposit, located to the north some distance, wherein the copper ore contains: chalcopyrite, bornite, galena, sphalerite, silver, cobalt and pyrite as replacements in a brecciated Devonian limestone or dolomite. This is the same unit (i.e., D1d) that is present in and around the subject DV area and which is one of the units containing geochemical anomalies (see “Laboratory Investigations: Geochemical Analyses and Petrographic Evaluations).

Regional Structural Setting: Thrust faulting within the Seward Peninsula occurred during two different ages of the Cretaceous period and has produced a complex intermix of Precambrian and Paleozoic rocks. Cretaceous age rocks were also involved in thrusting. Following the thrusting, the thrust sheets were fragmented by normal faulting and were intruded by stocks and batholiths ranging in age from 100 to 75 m.y. (Sainsbury, [23] (1972), and [24](1974). Periods of moderate deformation have also occurred during Tertiary time, which is responsible for the volcanism underway during the deposition of uranium in the HOM area of the southern Death Valley.

Local Geologic Setting: The general area of the subject properties is shown on the overlay to (Figure DV-2); the latter illustrates the local geology.

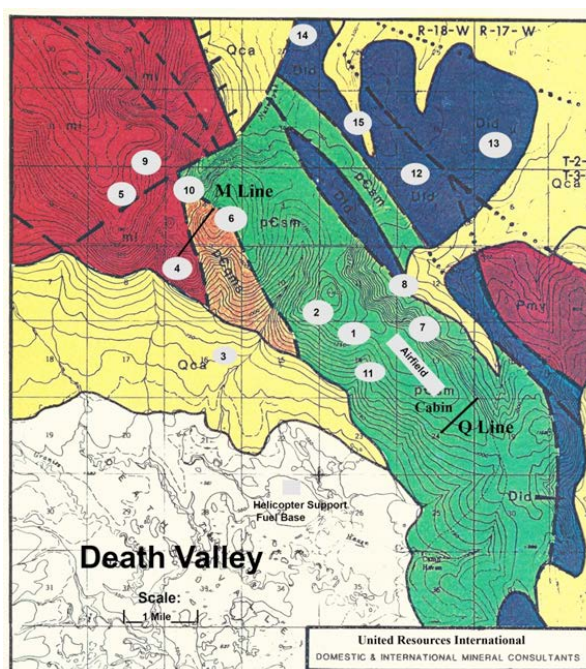


Figure DV-2: Geology, Sampling Sites, and Ground Magnetics Survey Lines in DV Area of Interest
(Click on Figure to Enlarge)

(Click [here](#) for Legend) (Click [here](#) for Ground Magnetics Survey Results)

Figure DV-2 also presents the general location of the samples taken and of the magnetic surveys completed during the URI field reconnaissance program (for specific locations refer to Plate DV-I). The legend presents summary geologic descriptions of the units present in the area of interest (here). In view of previous discussions, special note should be made of the p ϵ qms, p ϵ sm and Dld units and their geologic descriptions.

Local Structural Setting: In the DV Area of Interest, the rocks are heavily faulted. During the three URI visits to the site over three years, the structural contacts are generally apparent across the top of hills and in the deeply eroded creek walls that dissect the hills (see Figure DV-2). When compared to the structures present in nearby areas, the conditions in the subject area are relatively complex (see Figure DV-2). A major fracture zone runs from the east-southeast part of the Bendeleben pluton area, along the north boundary of the Windy Creek pluton (and associated hypabyssal intrusives), through the subject area, north toward the Kiwalik Mountain pluton area (Patton, [117], 1971) and the northeastern margin of Figure DV-1).

In the immediate area, a cluster of faults is present in association with the major fracture zone. These geological conditions might have permitted mineralizing fluids emanating from the Windy Creek intrusive (or the nearby hypabyssal intrusives) to invade fractured (prepared) rocks containing a reduced and/or carbonate environment and to precipitate economically significant ore minerals.

Field Reconnaissance Program: The initial objective of the URI reconnaissance program was to evaluate previous reports of gossanous rocks containing anomalous gold, silver, copper, tantalum, nickel, zinc, arsenic and chromium. URI personnel conducted a preliminary evaluation of available data and a preliminary reconnaissance on the subject properties and vicinity in October, 1981.

Field Operations: Two URI geologists and one field assistant were dispatched to the field via Nome during a forecasted good weather “window”. A helicopter and fixed-wing support base was established on one of large frozen lakes in Death Valley, just a few miles south of the subject area (see Figure DV-2 and DV-3 below). Field accommodations for the field team, including pilot and mechanic, were established at a hunting cabin located ten minutes by helicopter to the south of the fixed-wing, support-base site (Figure DV-4).

Although the forecasted good weather “window” did permit field operations, daily temperatures near zero, snow cover, and high, gusty winds (20-30 mph) hampered progress and limited daily field time.



Figure DV-3: Fixed-Wing and Fuel Dump Support Base. Looking North toward Areas of Interest



Figure DV-4: Cabin Base. Steve Campbell, Field Operations Manager, Reviewing Maps for Reconnaissance by Helicopter (Also See [Figure DV-2](#))

Rock and Geochemical Sampling: An inspection of the claim area was conducted via helicopter and samples were taken of local outcrops. The presence of scattered gossanous rocks was confirmed (e.g. see [Figure DV-5](#)). The northwestern areas of the area of interest were covered by deep snow and neither access nor sampling were possible. The general area, from where the reportedly anomalous sample analyses were previously obtained, is generally rolling country with few outcrops. The rocks present are generally “float” material and are hence not “in place.” (See [Figure DV-6](#)).

Many of the outcrops located, however, consist of gossanous (hematite-limonite -rich) quartz veins or carbonate rocks with abundant quartz veins. Sampling sites are shown in ([Figure DV-7](#)) and [Plate DV-I](#). Samples of surface materials (float) were also taken during the geophysical traverses discussed below. A total of approximately 150 samples were obtained and returned to Houston for subsequent investigation.

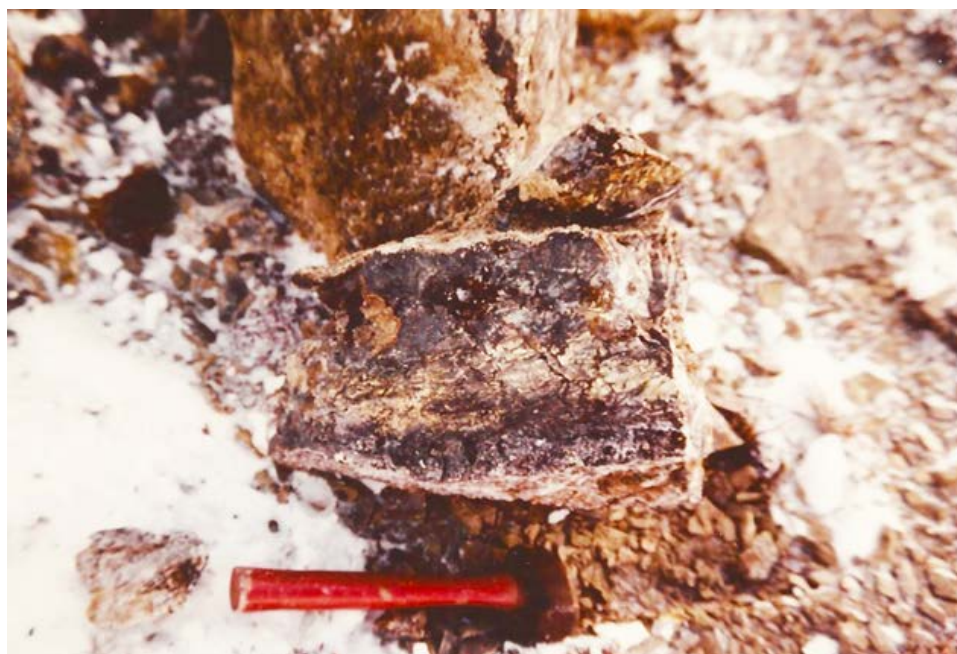


Figure DV-5: Small Outcrop of Gossanous (Iron-Rich) Rock at Sample Site 1: (See [Figure DV-2](#) and [Plate DV-I](#))

Geophysical Traverses: Pre-field estimates of expected field conditions indicated possible snow cover and limited outcrop exposures in tundra and glaciated country. As contingency support equipment, three magnetometers (Geometrics Model G816) and associated geophysical equipment were brought into the field by the field team for purposes of investigating the target units, their fault boundaries and their magnetic characteristics.



Figure DV-6: Float Material with Few “In Place” Outcrops. Near [Sample Site 11](#) Note Claim Corner (Right) of Large Rocks from “Nearby” and Support Base on Frozen Lake in Valley. Looking South.

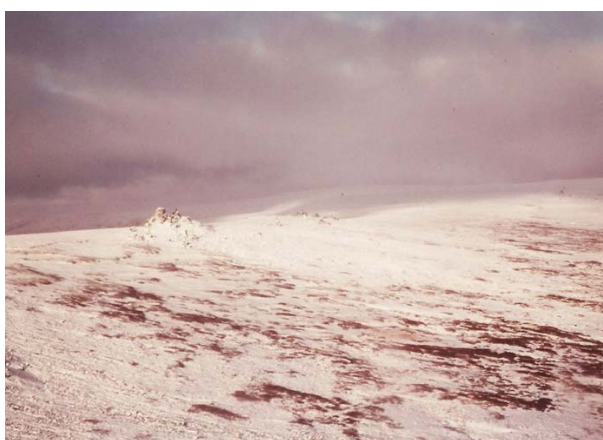


Figure DV-7: Outcrop near Sample Site 6. Field Camp in Center Distance. Notice Closing “Weather Window” of Blowing Snow in Distance. Looking West.

One magnetometer was used for a separate base station. Ambient magnetic readings were recorded at 15-minute intervals during the day to monitor possible magnetic storms and to establish diurnal variations. These data provided the basis for subsequent data reduction in Houston. The second magnetometer was used in the field and the third served as back-up equipment in the event a malfunction occurred in the other two magnetometers, which fortunately did not occur. Approximately 11,500 feet of magnetometer traverses were completed during the field period.

Two areas were investigated. Special emphasis was given to Sections 4 and 9 and units: p ϵ sm - p ϵ qms - Mi because of the confirmed presence of gossanous rocks and because of previously reported geochemical anomalies in the area (M-line) (see Figure DV-8 and [Plate DV-I](#)). The central area of the p ϵ sm unit in Sections 13 and 24 was also surveyed for similar reasons (Q-line). See [Plate DV-I](#).



Figure DV-8: Magnetometer Survey on M-Line. Eric Nelson, Line Lead; Steve Campbell, Probeman; and Senior Author, Recorder.

Note Larger Rock Fragments. Heading Toward Hill 1613. See [Figure DV-2](#) and [Plate DV-I](#).

The surveys were conducted by a three-man field team, i.e., traverse leader and magnetic data recorder, followed at a constant distance by the probe-reader, who, in turn, was followed by the sampling and geological data recorder. Three readings were recorded per station occupied. The last man, also at a constant distance behind the probe-man recorded local geological descriptions of float material at each station occupied and took samples for possible chemical analysis and radiometric and magnetic susceptibility measurements (see Figure DV-8). Approximately 240 stations were occupied during the field program.

Laboratory Investigations: Approximately 150 rock samples were returned to Houston for subsequent laboratory investigations. Thirty-three samples were selected for chemical analysis and 18 elements were sought for each sample. After the chemical analyses were completed 18 samples were selected for petrographic evaluation.

Table DV-2
Geochemical Analyses**

| Rock Type | Sample No. | As(ppm) | Ar(ppm) | Ag(ppm) | Ca(ppm) | Co(ppm) | Cr(ppm) | Cu(ppm) | F(ppm) | Li(ppm) | Mn(ppm) | Ni(ppm) | Pb(ppm) | Sr(ppm) | Ta(ppm) | Tl(ppm) | Zn(ppm) | | |
|--------------------------------|------------|---------|---------|---------|---------|---------|---------|---------|--------|---------|---------|---------|---------|---------|---------|---------|---------|------|--------|
| Quartz-Feldspar Porphyry | M-1* | <.09 | 5 | <.06 | 102 | 9 | 84 | 70 | 240 | 13 | 12.0 | <20 | 37 | 14 | 247 | 5 | 13 | 8.80 | 75.8 |
| Monoclinic Quartz Vein | M-6* | 3,23* | 232 | 23* | <10 | 4 | 30 | 27 | 65 | 3 | 4.7 | 222 | 17 | 60 | 314 | 2 | 13 | 1.79 | 3.6 |
| Amphibolite Schist | M-11* | .12 | 12 | <.06 | 143 | 32 | 119 | 227 | 155 | 21 | 11.8 | <20 | 65 | <2 | 488 | 8 | 19 | .79 | 63.6 |
| Amphibolite Schist | M-11A | .05 | 8 | <.06 | <10 | 35 | 140 | 261 | 155 | 19 | 12.6 | <20 | 86 | <2 | 488 | 7 | 52 | .20 | 59.6 |
| Amphibolite Schist | M-12 | .07 | 10 | <.06 | 53 | 26 | 123 | 121 | 165 | 20 | 9.7 | <20 | 68 | <3 | 399 | 6 | 15 | .51 | 40.6 |
| Vein Quartz & Qtz. Mus. Schist | M-16* | .55 | 1750* | 12* | <10 | 3 | 37 | 29 | 130 | 2 | 4.6 | 262 | 18 | 6 | 213 | 2 | 13 | .26 | 1.3 |
| Calc-Silicate Breccia | M-35* | .82 | 7 | <.06 | <10 | 22 | 117 | 110 | 632 | 23 | 9.3 | <20 | 88 | 18 | 1032 | 5 | <3 | 1.54 | 23.8 |
| Calc-Silicate Breccia | M-35A | <.02 | 4 | <.06 | <10 | 22 | 107 | 98 | 630 | 25 | 9.6 | <20 | 78 | <2 | 426 | 5 | 23 | 1.59 | 24.2 |
| Graphitic Schist | M-42 | .17 | 10 | <.06 | 37 | 11 | 75 | 85 | 230 | 18 | 11.8 | <20 | 72 | 4 | 735 | 4 | 18 | 5.30 | 49.4 |
| Carbonate Breccia | M-53 | .19 | 13 | <.06 | <10 | 18 | 45 | 23 | 652 | 15 | 4.2 | <20 | 54 | 2 | 405 | 2 | 25 | 2.27 | 382.0* |
| Monoclinic Vein Quartz | M-58 | .03 | 1 | <.06 | <10 | 4 | 41 | 44 | 42 | 1 | 7.6 | 75 | 26 | <2 | 344 | 3 | <3 | .03 | 15.0 |
| Graphitic Schist | M-61 | .65 | 1 | <.06 | <10 | 6 | 24 | 24 | 100 | 3 | 4.5 | 50 | 23 | 4 | 117 | 2 | <3 | .28 | 12.0 |
| Calc-Silicate Schist (Marble) | M-62* | .87 | 1 | <.06 | <10 | 22 | 79 | 72 | 370 | 29 | 4.8 | <20 | 66 | 2 | 440 | 2 | 3 | 1.71 | 21.8 |
| Qtz. Mus. Schist Breccia | M-64* | 25.60* | 1780* | <.06 | 81 | 20 | 108 | 380 | 185 | 7 | 12.0 | <20 | 81 | 5300* | 3164* | 13 | 15 | 1.74 | 358.0* |
| Amphibolite Schist | M-66 | .28 | 3 | <.06 | 101 | 25 | 77 | 43 | 240 | 88 | 7.8 | <20 | 75 | 42 | 1105 | 2 | 19 | .26 | 46.0 |
| Quartz Muscovite Schist | M-86* | <.02 | 3 | <.06 | <10 | 20 | 168 | 128 | 240 | 22 | 10.2 | <20 | 91 | <2 | 247 | 7 | 14 | 2.00 | 44.6 |
| Monoclinic Vein Quartz | M-100 | .99 | <1 | <.06 | <10 | 2 | 32 | 29 | 75 | 16 | 3.7 | 173 | 16 | 10 | 344 | 2 | 13 | .19 | 4.2 |
| Granite | R-18 | .06 | 1 | <.06 | 113 | 7 | 88 | 62 | 135 | 11 | 8.0 | <20 | 26 | 2 | 598 | 4 | <3 | 4.29 | 16.2 |
| Monoclinic Vein Quartz | R-24 | .07 | 5 | <.06 | <10 | 4 | 55 | 50 | 120 | 3 | 7.9 | 152 | 23 | 4 | 295 | 3 | 14 | .13 | 5.6 |
| Calc-Silicate Breccia (Marble) | Q-10 | .02 | 5 | <.06 | <10 | 20 | 94 | 93 | 75 | 3 | 8.2 | <20 | 74 | <2 | 131 | 4 | 15 | .34 | 22.6 |
| Quartz Monoclinic Breccia | 1 | .06 | 39 | <.06 | <10 | 18 | 66 | 232 | 38 | 1 | 7.9 | <20 | 69 | 4 | 55 | 3 | 9 | .25 | 10.0 |
| Quartz Monoclinic Breccia | 1A* | .40 | 21 | <.06 | 152 | 88 | 30 | 356 | 65 | 3 | 7.0 | <20 | 138 | <2 | 138 | 3 | 55 | 1.19 | 6.4 |
| Pyritic Vein Quartz | 3 | .99 | 7 | <.06 | <10 | 8 | 113 | 126 | 160 | 23 | 10.1 | <20 | 41 | 4 | 522 | 5 | <3 | 1.20 | 3.6 |
| Granite | 4 + | 25.50* | 2 | <.06 | 81 | 18 | 193 | 145 | 652 | 23 | 7.6 | <20 | 102 | 14 | 2216 | 6 | 31 | 1.16 | 66.8 |
| Granite | 5 | .04 | <1 | <.06 | 140 | 7 | 22 | 19 | 335 | 21 | 2.2 | 20 | 10 | <2 | 158 | 2 | 21 | 1.12 | 51.6 |
| Amphibolite Schist | 6 | .12 | 2 | <.06 | 70 | 30 | 123 | 186 | 80 | 8 | 10.7 | <20 | 73 | <2 | 886 | 5 | 21 | .28 | 16.2 |
| Brown Marble | 7 | <.02 | 49 | <.06 | <10 | 17 | 26 | 29 | 180 | 3 | 3.6 | <20 | 30 | <2 | 387 | 3 | 15 | .23 | 10.6 |
| Carbonate Breccia | 8 + | .08 | 3 | <.06 | <10 | 15 | 39 | 39 | 270 | 3 | 6.0 | <20 | 45 | 8 | 10642* | 3 | 12 | 3.22 | 182.0 |
| Monoclinic Amphibolite | 9 + | .04 | 2 | <.06 | 110 | 18 | 157 | 113 | 550 | 22 | 9.4 | <20 | 65 | <2 | 151 | 5 | 16 | 2.13 | 38.8 |
| Black Quartz Schist | 10 | .04 | 5 | <.06 | 84 | 21 | 227 | 153 | 250 | 22 | 12.1 | <20 | 84 | <2 | 660 | 9 | 27 | 2.84 | 50.0 |
| Black Quartz Schist | 10A | <.02 | 5 | <.06 | 112 | 20 | 261 | 270 | 250 | 21 | 11.2 | <20 | 152 | <2 | 1374 | 11 | 29 | 3.03 | 56.4 |
| Black Vein Quartz | 12 | <.02 | <1 | <.06 | <10 | 14 | 10 | 13 | 183 | 1 | 7.0 | <20 | 21 | <2 | 309 | 2 | 20 | .86 | 4.8 |
| Flux Lam. Breccia | 14* | <.02 | <1 | <.06 | <10 | 14 | 7 | 9 | 140 | 2 | .5 | <20 | 19 | 2 | 289 | 2* | 8 | 1.22 | 6.2 |

* Strong Anomaly Significant Value * See Appendix II for Petrographic Analyses ** See Appendix I for Laboratory Report and Methods

(Click to Enlarge)

Geochemical Analysis: The analytical methods employed on the samples, the detection limits and the anticipated precision of results, as presented by the geochemical laboratory, for (Table DV-2) are in Appendix DV-I. Three sets of duplicate analyses were included in the samples submitted to the laboratory for purposes of independently assessing the analytical error.

Samples designated M-11: M-11A; M-35: M-35A and 10:10A are the duplicate samples: Samples 1 and 1A are not duplicates but are two separate samples taken from sampling site 1. It should be noted that the duplicate samples are not re-runs but two pieces of the same rock, hence some variations in results would be expected and are apparent.

The analyses designated with a letter prefix (M, R, O) in (Table DV-2) were taken during the magnetometer surveys, i.e., M-Line, R-Line, O-Line. The samples designated 1 through 14 were obtained from large boulders or small outcrops in the area. Sample locations are indicated on Plate DV-I. It should be noted that the M, R and Q samples were not “in place” and were probably derived from a nearby near-surface outcrop, now eroded, and covered will talus and scree. Therefore, the samples might or might not represent the immediate subsurface of the area sampled.

In order to evaluate the significance of geochemical data, a definition of anomalous elemental levels must be made on the basis of literature sources and on experience. A number of the samples analyzed clearly show anomalous values of silver, gold, copper, molybdenum, lead, zinc and tin and of pathfinder elements such as arsenic, cerium, cobalt, chromium, fluorine, lithium, niobium, nickel, sulfur, tantalum and uranium. Of special significance is sample M-64 which indicates 26 ppm silver, 1,780 ppm arsenic, 380 ppm copper, 17 ppm molybdenum, 5,300 ppm lead (~ 0. 5%), 3,200 ppm sulfur, high tin and zinc. Other samples of special significance are M-6, M-16, 4 (see Table DV-2 and Plate DV-I).

Of the 33 samples analyzed, 23 are anomalous in at least one element. The anomalies are associated with breccias, altered schists, and quartz veins (see Table DV-3 below) The silver and lead are of particular interest. It is also interesting to note that sample 4 (anomalous in silver, fluorine, lithium, nickel and sulfur) was taken from Hill 1613, the site of a major magnetic anomaly discussed later in this paper.

Petrographic Evaluations: Eighteen samples were thin-sectioned and studied for mineralogical and textural variation in hand sample and under the petrographic microscope. Mineralogy and rock names are summarized in (Table DV-4) below. Two groups of samples are distinguished: one group chosen to characterize the representative lithologies encountered in the area, and one group incorporates the geochemical anomalies.

All of the samples studied, except samples M-1, M-6, M-6i and part of M-16, display deformation fabrics and metamorphic mineral assemblages indicating that they pre-date intrusion of Cretaceous plutonic rocks in the region (see Table DV-3). Samples of hypabyssal porphyry dikes (M-1, M-6i) display no ductile deformation fabrics and are probably associated with the larger Cretaceous intrusions of the Windy Creek pluton to the west of the area discussed in this paper.

Table DV-3
Mineralogy of Samples from the Death Valley Area of interest

| Sample no. | quartz | feldspar | biotite | hornblende | pyroxene | muscovite | chlorite | garnet | epidote | sphene | calcite | opaques | other | Element anomalies | Rock Name | |
|--|--------|----------|---------|------------|----------|-----------|----------|--------|---------|--------|---------|---------|-------|----------------------|----------------------------------|------------------------------------|
| GROUP I: Representation of lithological variation in area. | | | | | | | | | | | | | | | | |
| 8 | x | | | | | x | | | | | | x | P, G | | carbonate breccia | |
| 9 | x | x | x | x | ? | x | | x | x | x | | | Z | | biotite amphibolite | |
| Q14a | x | | | | | x | ? | | | | | | G | | carbonate breccia | |
| M-1 | x | x | x | | | x | | | | | | | H | | quartz-feldspar porphyry | |
| M-6i | x | x | | | | | | | | | | | | | quartz-feldspar porphyry | |
| M-11 | x | x | | x | | | x | x | x | ? | x | | M, H | | amphibolite schist | |
| M-35 | x | x | | x | x | x | x | | ? | x | x | | | | calc-silicate breccia | |
| M-62 | | | | | | x | | x | x | | x | | | Tm | calc-silicate schist | |
| M-88 | x | | | | | x | x | | | | | | M | Tm, Z | quartz muscovite schist | |
| 14a | | | | | | | | | | | | | | x H, M, G | limestone breccia | |
| GROUP II: Samples showing geochemical anomalies. | | | | | | | | | | | | | | | | |
| 1-A | x | | | | | | | | | | | | H | Ce, Co, Cu, Ta(?) Ni | quartz-hematite breccia | |
| 4 | x | x | x | | | x | | x | | | | | M | S, Tm, Z | quartz-biotite schist | |
| 8x | x | | | | | x | | | | | | | G, P | Li, F | quartz-granule limestone breccia | |
| 14 | | | | | | | | | | | | | H | Sn* | hematitic limestone breccia | |
| M-6 | x | | | | | | | | | | | | H, P | Tm | Au*, Nb, Ag* As | vein quartz |
| M-16 | x | | | | | x | | | | | | | H, PT | | As*, Au*, Nb schist breccia | |
| M-51 | x | | | | | x | x | | | | | | H, G | | F, Zn* | carbonate breccia |
| M-64 | x | ? | | | | x | | | | | | | H, L | Galena? | Ag*, As*, Mo* Pb*, Sn, Zn* | brecciated quartz-muscovite schist |
| M-35 | x | x | x | x | x | x | x | ? | x | x | x | | | | F*, Li*, S | calc-silicate breccia |
| M-62 | | | | | | x | | x | x | | x | | | Tm | Li* | calc-silicate schist |
| M-68 | x | x | x | | | x | x | x | ? | x | x | | | Hand Sample | Co, S | amphibolite schist |
| M-100 | x | | | | | | | | | | | | H | Hand Sample | Nb* | hematitic vein quartz |
| R-24 | x | | | | | | | | | | | | H | Hand Sample | Nb* | hematitic vein quartz |
| 10 | x | x | x | | | x | | | | | | | H | Hand Sample | Cr, Ll, Mo S, Ni, Sn | black quartz schist |

(P) Pyrite, (G) Graphite, (H) Hematite, (M) Magnetite, (Z) Zircon, (Tm) Tourmaline, (S) Sphene, (L) Limonite
* Strongly anomalous

(Click to Enlarge)

Ductile deformed and metamorphosed rocks include schistose graphitic marble, calc-silicate schist, and amphibolite schist. Protoliths of these “basement” rocks were limestones and/or impure carbonates, sandstones (graywackes ?) and shales, and basaltic and andesitic igneous rocks. This assemblage characterizes a possible arc-trench paleogeographic setting for these rocks - a setting often associated with exhalative sulfide mineralization in a marine environment [92] (1995).

Subsequent to deposition, this assemblage underwent strong ductile deformation and was metamorphosed to medium grade (grossularite and tremolite in carbonate rocks; almandine garnet and amphibole in pelitic rocks). Penetrative ductile deformation fabrics, which include crystallographic and dimensional preferred orientation, mylonitic ribbon quartz, and flaser structure, and developed mesoscopic foliations, cleavages and lineations in the country rock.

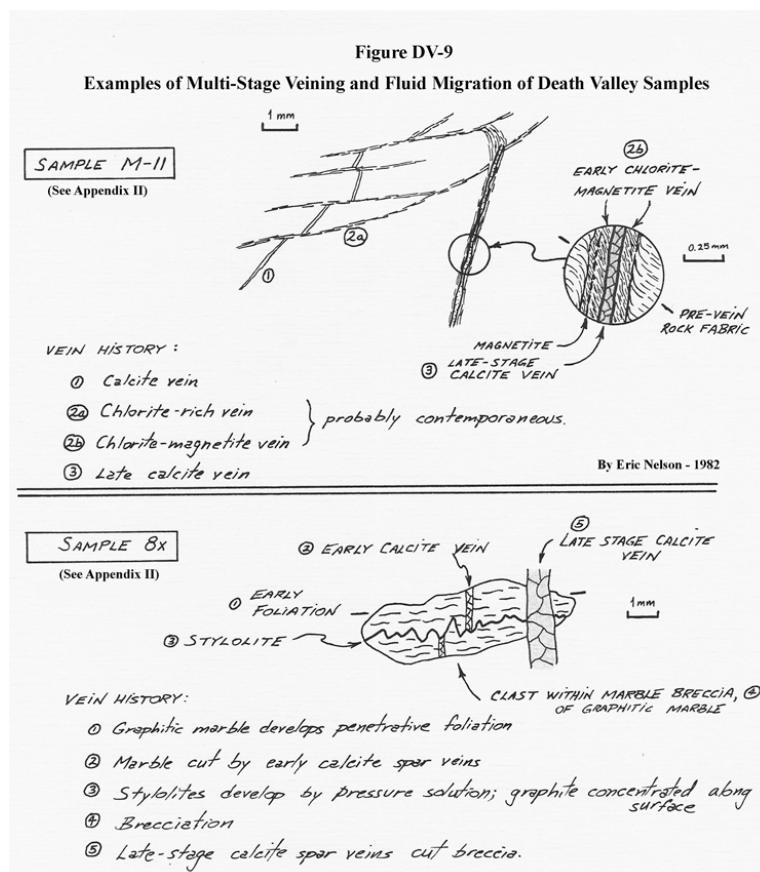
Table DV-4
Distribution of Geochemical Anomalies by Rock Type

| General Rock Type | Total No. of Samples | No. Samples Anomalous | No. Elemental Anomalies | Anomalous Elements |
|-------------------|----------------------|-----------------------|-------------------------|--|
| Breccia | 9 | 8 | 25 | F, Li, S*, Zn, Ag*, As*, Cu, Mo, Pb*, Sn, Co, Ce, Ni, Ta, U, Sn* |
| Schist (Altered) | 13 | 9 | 24 | Cu, Mo, Ta, As*, Au*, Ag*, Nb, Li, Co, Pb, S, F, Ni, Cr, Sn |
| Vein Quartz | 6 | 4 | 8 | Ag, As, Au*, Pb, Nb, Li |
| Porphyry | 1 | 1 | 2 | Mo, U |
| Granite | 2 | 1 | 1 | Li |
| Amphibolite | 1 | 0 | 0 | None detected |
| Marble | 1 | 0 | 0 | None detected |
| Total | 33 | 23 | | |

Note: * indicates strong anomaly

These fabrics are evidence of intracrystalline gliding, syntectonic recrystallization and pressure solution. Retrograde metamorphism is indicated by development of chlorite in pelitic samples. This deformation and metamorphism appears to be a regional event (given its intensity) and could be associated with intrusion of the Cretaceous plutons in the area (probably of the [Windy Creek pluton](#)).

Late-stage brittle deformation in the area is indicated by the extensive development of brecciated rocks, either along faults or associated with regionally developed fracture systems. Late-stage veins of calcite, chlorite + magnetite, and quartz also crosscut earlier foliations. Importantly, the widespread presence of brecciation, multi-stage veining and stylolitization record a long history of fracturing, dissolution and migration of fluids in these rocks. Hydrothermal solutions were most likely present during the extensive magmatic activity in the late Mesozoic or later, and probably account for retrograde metamorphic assemblages observed in veins (see Dr. Nelson's field notations in Figure DV-9). Later calcite veins and stylolitization record the continuation of fluid migration, possibly after the magmatic phase (for additional petrographic analysis, see [Appendix DV-II](#)). Of note is possible parsonite (?) in the DV area Miller and Johnson, [20].



(Click to Enlarge)

Geophysical Data Reduction: The magnetic data obtained in the field have been corrected for diurnal variation (relative to the base station data), replotted and examined. Plate I presents the reduced magnetic data in the form of the traverses made.

A number of significant monopole and dipole magnetic anomalies have been identified on Hill 1613 (see [Plate DV-I:B](#)), the most important is a complex dipole anomaly that appears to represent mineralization at shallow depths. Station 104 to 112 and R-10 to 27 show a complex of reversely magnetized intrusives with associated magnetite mineralization (or other magnetic minerals) and nonmagnetic rocks such as thick quartz veins. Combined with the anomalous character of the geochemical and petrographic data for sample 4 (See Table DV-2), an intrusive with abundant magnetite and associated with high silver, fluorine, nickel, plus many others, appear to be present in mineralization at very shallow depths. The monopole anomalies indicate deeper sources of mineralized rock containing abundant magnetite and, perhaps, minerals of economic interest.

In order to calibrate the field magnetic data, 15 samples were selected for magnetic susceptibility measurements in the laboratory using a Bison 3101 Magnetic Susceptibility System. (Table DV-5) presents the resulting data on the samples. More than one of the samples appears to be layered and heterogeneous, as expected for metamorphic rocks.

Table DV-5
Death Valley Sample Magnetic Susceptibility Measurements

| Sample No. | Rock Type | Volume Ratio | Magnetic Susceptibility (cgs X 10 ⁻⁶) |
|------------|-----------------------|--------------|---|
| ① | Otz. Hem. Breccia | 1.136364 | 1,112.5 |
| ①A | Otz. Hem. Breccia | 1.234568 | 2,530.9 |
| ② | Greenstone | 1.123596 | 390,438.2 |
| ⑤ | Granite | 1.333333 | 1,013.3 |
| ⑦ | Brown Marble | 1.408451 | 912.7 |
| ⑨ | Biotite Amphibolite | 1.219512 | 1,214.6 |
| ⑩ | Black Otz. Schist | 1.136364 | 2,225.0 |
| ⑭ | Pink Lms. Breccia | 1.428571 | 1,115.7 |
| M-11 | Amphibolite Schist | 1.428571 | 515,735.7 |
| M-16 | Otz.&Otz.Mus.Schist | 1.162791 | Below Detection Limit |
| M-61 | Graphitic Schist | 1.315789 | 2,836.8 |
| M-92 | Otz. Mica Schist | 1.136364 | 511,580.7 |
| M-110 | Quartzose Schist | 1.001111 | 3,333.0 |
| R-18 | Granite | 1.298701 | 2,026.0 |
| Q-45 | Calc-Silicate Breccia | 1.204819 | 1,012.1 |

Note: See Plate DV-I Magnetic Traverses Calculations By H. C. Clark, Rice University

But such rocks also can produce problematic data. The values indicated in (Table DV-5) are those expected for background and for source rocks, the latter of which are, in some samples, ferrimagnetic, i.e. 0.39, 0.52 and 0.51 cgs above. For modeling purposes, the susceptibility can be assumed to be in the range of 10⁻³.

In any further exploration, detailed magnetic and other geophysical surveys should be conducted on a grid basis for Hills 1613 and 1920, although no significant magnetic anomalies are apparent for the M-line at station M-1 through M-30 in the vicinity of Hill 1920. Strong geochemical anomalies have, however, been identified in this vicinity (e.g. M-6, M-16, etc.: see Table DV-2 and Plate DV-I).

Excavation over Magnetic Anomaly

During late summer, 1983, the URL field team again traveled to the Death Valley area of interest, this time for the sole purpose of excavating over the top of magnetic dipole discovered earlier (see Plate DV-I) to obtain samples for further evaluation of their geological and geophysical characteristics. The team consisted of: Steve Campbell, URI Field Operations Manager, and M. David Campbell, URI Geologist, and the Senior Author.

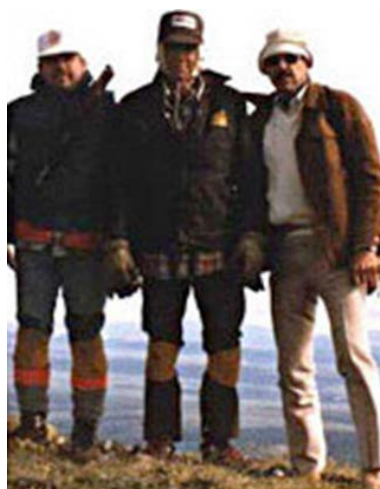


Figure DV-10: Field Team for Pit Excavation and Sampling.
(L to R) Steve Campbell, M. David Campbell, and Michael D. Campbell

The team removed about 5 feet of soil, rock fragments, down to large rounded boulders over an area of 20 feet by 30 feet. A hand-held, gasoline-driven rock drill was used to bore approximately 20 3-inch holes in highly fractured rock. This operation required 10 days. Samples were taken of rocks of interest. All appropriate safety precautions were taken, i.e., hard hats, gloves, and protective eye and ear wear. A professional explosives expert was engaged in Nome to transport, handle, and ignite the dynamite to excavate the pit further.

After excavation, 41 samples were obtained from the pit and transported to Houston for evaluation by URI geologists (the senior author and co-author). Eight (8) were selected and sent to Dr. Eric Nelson, Golden, Colorado for petrographic evaluation and analysis of 21 elements. In addition, H. C. Clark generated data on the magnetic susceptibility of the pit samples (P-series). Table DV-6 contains the analyses of those 8 pit samples.

Table DV-6
Geochemical Analyses for Pit Samples & Magnetic Susceptibility

| Field Description | Sample No. | As (ppm) | As (ppm) | Au (ppm) | Ce (ppm) | Co (ppm) | Cr (ppm) | Cu (ppm) | F (ppm) | Li (ppm) | Mo (ppm) | Nb (ppm) |
|--------------------------------|------------|----------|----------|----------|----------|----------|----------|----------|----------|----------|----------|---|
| Lt. Grey Calc-Silicate | P-1 | <0.01 | <1 | <0.03 | 14 | 27 | 45 | 1.6 | 3150 | 22 | 0.2 | 2 |
| Dark Brown Soil | P-2 | 0.17 | 4.0 | <0.03 | 135 | 29 | 70 | 26.3 | 1950 | 30 | 2.3 | 10 |
| Lt. Brown Calc-Silicate Schist | P-3 | 0.02 | <1 | <0.03 | 106 | 30 | 85 | 12.4 | 2850 | 36 | 1.0 | 17 |
| Lt. Brown Graphitic Schist | P-4 | 0.02 | <1 | <0.03 | 72 | 28 | 80 | 6.4 | 9250 | 63 | 0.6 | 9 |
| Med. Brown Calc-Silicate | P-5 | 0.02 | <1 | <0.03 | 52 | 28 | 40 | 7.6 | 4100 | 40 | 0.3 | 3 |
| Dk. Brown Graphitic Schist | P-6 | 0.60 | 1 | <0.03 | 34 | 28 | 110 | 8.5 | 8000 | 90 | 1.9 | 19 |
| Dk. Brown Calc-Silicate Schist | P-7 | 0.02 | 1 | <0.03 | 32 | 26 | 30 | 9.2 | 3950 | 60 | 0.2 | 6 |
| Dk. Brown Calc-Silicate Schist | P-8 | 0.02 | <1 | <0.03 | 263 | 42 | 120 | 9.9 | 3200 | 53 | 0.6 | 19 |
| Field Description | Sample No. | Ni (ppm) | Pb (ppm) | S (ppm) | Sn (ppm) | Ta (ppm) | U (ppm) | Zn (ppm) | Sb (ppm) | V (ppm) | Be (ppm) | Composite Magnetic Susceptibility CGS X 10 ⁻⁶ |
| Lt. Grey Calc-Silicate | P-1 | 59 | 13 | 3220 | <3 | 3 | 1.75 | 17.0 | <1 | 6 | 4 | <1000 |
| Dark Brown Soil | P-2 | 72 | 18 | 2660 | 4.0 | 6 | 8.07 | 76.2 | <1 | 39 | 6 | <1000 |
| Lt. Brown Calc-Silicate Schist | P-3 | 106 | 5 | 2880 | <3 | 3 | 2.93 | 54.8 | <1 | <2 | 6 | 200,000 |
| Lt. Brown Graphitic Schist | P-4 | 58 | 10 | 1160 | <3 | 3 | 2.51 | 58.9 | <1 | 4 | 5 | 74,600 |
| Med. Brown Calc-Silicate | P-5 | 64 | 9 | 1460 | <3 | 10 | 2.32 | 37.8 | <1 | <2 | 6 | 115,000 |
| Dk. Brown Graphitic Schist | P-6 | 70 | 53 | 1420 | <3 | 3 | 4.03 | 139.0 | <1 | 24 | 6 | 77,700 |
| Dk. Brown Calc-Silicate Schist | P-7 | 57 | 10 | 1380 | <3 | 3 | 2.16 | 27.0 | <1 | <2 | 4 | 73,300 |
| Dk. Brown Calc-Silicate Schist | P-8 | 88 | 5 | 800 | <3 | 8 | 0.70 | 70.7 | <1 | 6 | 7 | 95,200 |

(Click on Table to Enlarge)

Laboratory Analyses: Beryllium was confirmed in all “P” samples and ranged from 4 to 7 ppm. Tantalum is also reported for three of the eight “P” samples and ranged from < 3 to 10 ppm. The low niobium values for the “P” samples indicate a shallow source of metals for the calc-silicate and graphitic schists of the “P” samples and probably for the other samples obtained previously. Niobium values greater than 50 ppm usually indicate a relatively deep source of mineralizing fluids (see Table DV-2).

Samples containing less than 50 ppm show that most of the schists and calc-silicate rocks have been altered by at least one and probably numerous periods of metamorphism (e.g., during Permian, Cretaceous and Quaternary). However, the hematitic quartz veins samples (i.e., M-6, M-16, M-58, M-100 and R-24; see Table DV-2) carry niobium values greater than 50 ppm (as well as anomalous precious metals in some samples) and probably represent the mineralizing fluids that have invaded and further altered fractured metamorphic country rocks. The hematitic quartz veins should be age dated to determine which of the three or more periods of igneous activity is responsible for the veins carrying the precious metals.

The rock unit represented by Sample 4 (see Table DV-2), although not characterized as a hematitic quartz vein, could have been altered by such a vein that intruded nearby supplying anomalous silver concentrations.

Regression analyses were conducted on data of ten selected elemental pairs. Both the 1982 data (see Table DV-2) and 1983 data (Table DV-6) have been combined. The following is a summary of the semi-quantitative results to date:

- F vs. Mo: Inverse: Slope -1.135
- F vs. Nb: Inverse: Slope -3.508 F vs. Li: Direct: Slope +6.430
- F vs. Cu: Inverse: Slope -3.189 (hyperbolic data spread)
- F vs. Magnetic Susceptibility:
 - Direct (for Non-P-series): Slope +1.750
 - Inverse (for P-series): Slope -2.50
- Li vs Mo: Inverse: Slope -0.073
- Li vs. Nb: Inverse: Slope -1.444 (hyperbolic data spread)
- Li vs. Cu: Scattered Plot: Doubtful significance: Slope -0.029
- Mo vs. Cu: Direct: Slope +0.034
- Mo vs. Nb: Direct: Slope +18.26

In summarizing the above, the following conclusions appear to be applicable for the above ten-element pairings:

1. Fluorine apparently occurs in minerals that do not accommodate molybdenum, niobium or copper, whereas fluorine is associated with minerals that accommodate lithium. But molybdenum, copper, and niobium appear to occur together and do not generally occur in minerals that accommodate fluorine and lithium.
2. Magnetite occurs in highly variable amounts. Individual samples (P-series) were broken into three parts and the magnetic susceptibility was measured in the lab for each part (see Table DV-7). Data for magnetic susceptibility analyses were obtained by reconstituting the individual samples via weighted average methods (composites). It is clear that magnetite occurs in layers or veinlets. It is not clear whether fluorine and lithium are present in samples with a high magnetite content or if the latter is associated with the molybdenum-niobium-copper group.
3. Where detailed data are available, there does seem to be an inverse relationship between fluorine-lithium and magnetic susceptibility (in the P-series where fluorine and lithium are anomalously high).

Table DV-7
Magnetic Susceptibility Evaluations

Pit Samples
(Compare with Data in Table DV-5)

| <u>Sample #</u> | <u>Magnetic Susceptibility</u> (cgs X 10 ⁻⁶) |
|-----------------|---|
| P-1 | 1000 |
| P-2 | 1000 |
| P-3A | 333,000 |
| P-3B | 272,300 |
| P-3C | 80,000 |
| P-3(composite) | 200,000 |
| P-4A | 71,100 |
| P-4B | 140,000 |
| P-4C | 62,200 |
| P-4(composite) | 74,600 |
| P-5A | 72,000 |
| P-5B | 110,000 |
| P-5C | 135,500 |
| P-5(composite) | 115,000 |
| P-6A | 51,700 |
| P-6B | 95,000 |
| P-6C | 47,500 |
| P-6(composite) | 115,000 |
| P-7A | 43,300 |
| P-7B | 80,000 |
| P-7C | 126,700 |
| P-7(composite) | 73,300 |
| P-8A | 95,000 |
| P-8B | 120,000 |
| P-8C | 89,400 |
| P-8(composite) | 95,200 |

Of the elemental pairings evaluated by plotting to date, the schists are anomalous in part because of widespread redistribution of metals liberated from pelitic rocks and of preferential concentration during one or more metamorphic events. However, the geochemical character of the granites (high lithium) and quartz-feldspar porphyry (high molybdenum and uranium) sampled are clearly anomalous (see Sample #5, R-18 and M-1; see Table DV-2), and indicate the source for the anomalous metals reported to date, including the silver.

The soil sample (Sample P-2 in Table DV-6 and in Table DV-7) is of particular importance to future exploration programs. This soil sample is anomalous (with respect to the rock samples obtained from the pit) in silver, cerium, fluorine, niobium, sulfur, tin, tantalum, uranium, zinc, tungsten and beryllium (see Table DV-6). The unusually high concentrations of these elements (and the variability indicated for the rock samples) show that soil geochemical surveys are useful for defining target areas.

Integration Death Valley Investigations

Based on the results of URI investigations in the Death Valley area to date, the geochemical analyses (Table DV-2 and Table DV-6) provide evidence for the occurrence of classic silver-lead-zinc, molybdenum-copper and gold silver mineralization.

A review of the geological literature on the Lost River fluorite-tin-tungsten deposit of the western Seward Peninsula by Shawe, [93], 1976, and by Mulligan, [10], 1962, at the Omilak lead-silver mine, combined with later discoveries of lead, zinc, and silver in an altered zone 18 miles long and 2 to 5 miles wide near Quartz Creek west of Granite Mountain, exhibiting anomalies of molybdenum, bismuth, and associated with uranium, copper, lead, and zinc minerals in the upper Peace River drainage northeast of Granite Mountain, all together are indicative of a widespread metallogenic region.

Mineralization associated spatially with felsic plutonic rocks occurring near the western edge of a late Mesozoic province of volcanic and plutonic rocks located by U.S.G.S. reconnaissance projects north of Death Valley near Granite Mountain Miller

and Elliott [17] (1969), indicates that many of the geological requisites for the existence of mineralization are present in the areas of interest investigated on the northern rim of Death Valley and in the Kachauik area northeast of Golovin are present. These deposits would consist of uranium and rare-earths, precious metals and base metals in the areas investigated by URI personnel during the latter 1970s and 1980s. This conclusion is based on the regional and local geological conditions, the geochemical analyses, the petrology of the rock samples, and the magnetic anomalies present within geochemically anomalous areas from the Death Valley in the north to the Kachauik area in the south, just east of the Darby Mountains.

One of the favorable geological conditions in the region is the proximity of the Windy Creek pluton near the north rim of the Death Valley. The inferred edge of the pluton is approximately 5 miles from the area. The pluton is magnetically unique when compared to the other plutons in the region and, based on aeromagnetic data (Decker and Karl, 1977 [84]), it is highly magnetic, indicating a very high magnetite / pyrrhotite content and perhaps the source of previous mineralizing fluids (see general location in [Figure DV-1](#)). The pluton is known to be geochemically anomalous in molybdenum and in fluorite (in breccia pipes along country rock fault-bound zones of the pluton), and in lead, zinc and silver Eakins, [13] 1976 and Forbes, [94] 1976.

As an analog in other areas, the Brooks Mountain pluton, located in the western part of the Seward Peninsula, contains a variety of minerals found near hydrothermally altered contact zones between limestones and quartz and in veins in limestone. Much of the mineralization occurs in disseminated hematitic linings in pegmatitic granite and associated multi-stage quartz-tourmaline veins.

Death Valley Area: The rocks in the area are highly fractured (once highly permeable) and consist of favorable lithologies that are well known hosts elsewhere for ore deposition of both precious metals and other ore minerals, i.e. in carbonates, calc-silicates breccias, graphitic schists, etc. A major fault zone (mineralized in part) extends from the Windy Creek pluton and passes through the Death Valley area of interest. Numerous associated feather faults and fractures are present in the area and would have served as excellent conduits for hydrothermal fluids emanating within the influence of the Windy Creek pluton. Such fluids would have invaded the area, via the main fault zone, and entered the secondary fault zones present within the properties. The presence of “gossanous” zones supports the view that iron-rich hydrothermal fluids have been active in the area and have carried anomalously high concentrations of precious metals, lead and a host of other geochemically anomalous elements. The fluids deposited the materials in highly permeable zones such as breccias and easily dissolved carbonate-rich schists and other hosts. Features of hydrothermal alteration are clearly evident both microscopically and macroscopically in the rock samples. Other petrographic features of interest involves the presence of magnesium-rich tourmaline Burger, [95] 1982, which is an indicator of mineralization in the immediate vicinity, the economic value of which would still need to be determined by drilling, coring, sampling, and a host of additional activities.

The principal feature of the pit samples (at the site of sample 4 and others) is the domination by a fluorine flood of mineralizing fluids during one of more periods of hydrothermal activity in the area, with more than 9,000 ppm fluorine and up to 3,200 ppm sulfur in a highly altered quartz biotite schist containing tourmaline, possibly scapolite and altered garnet with other lesser anomalies such as niobium and lithium, but also beryllium, tungsten, zinc, nickel, uranium, and cerium (see [Table DV-6](#)).

There are other anomalies in the area, such as two samples both showing 25 ppm silver; one sample likely associated with reported galena in a quartz muscovite schist breccia from sample M-64 of the M-Line, and the other associated with fluorine and sulphur (lead is minimal) in quartz biotite schist (see [Table DV-2](#)), located in the vicinity of the major magnetic anomaly at the southern end of the R-Line on Hill 1613 (see [Plate DV-I](#)).

Kachauik Area: The numerous dikes and contacts with the carbonate as well as with the apparent roof pendant of the Mi unit have not been investigated in any detail. The ease of access of these areas being in proximity to Golovin should make follow-up manageable.

Recent reviews of the U.S.G.S activities are showing a well-deserved recent interest in the Kachauik area Karl, et al., [96] (2016); and Karl [97] (2017) and likely soon in the Death Valley area. In the event that the price of uranium begins to rise again, there is little doubt that the eastern sections of the McCarthy Marsh will be the focus of exploration in this new uranium district. Other areas outside the two URI investigations discussed in this paper have been encountered that further support our view that the eastern Seward Peninsula likely exhibits metallogenic prospects of economic interest. For example, in the course of the URI investigations USGS reports exhibit a plethora of geochemical and geophysical data in a range of metals, such as in the watershed of the Omilak mine where cadmium, copper, gallium, indium, lead, antimony, tin, tungsten, and zinc were reported in high concentrations. Also of interest is that the cross-section in the map by Herreid, [4] (1965), shows that the rocks dip into the McCarthy basin. Any follow-up on impact-related matters will be reflected in [Appendix IV](#).

The USGS data generated in the latter 1970s and early 1980s focused on the eastern Seward Peninsula and present extensive data from before, during, and after the NURE funding of widespread sampling in the area (as well as other areas in Alaska and the mainland U.S.), emphasizing uranium and base metals. Those reports reviewed and cited for the URI investigations would be especially useful in any further regional exploration have been marked with asterisks in the References below.

Acknowledgments

Omega Energy Corporation engaged United Resources International (URI) beginning in 1978 to conduct an independent mineral exploration assessment of the geological and geophysical potential in certain areas on the Seward Peninsula, Alaska in response to new geological information released by the government's National Uranium Resources Evaluation (NURE) program.

All funding for two years of field work, claim staking costs, travel, personnel, laboratory and thin section and XRF analyses, and final reports was provided by Omega. Recent laboratory and XRF analyses were provided by I2M Consulting, LLC, Houston, Texas, the authors' current employer.

The authors wish to acknowledge the technical contributions to this paper, after the fact by some 40 years:

The Death Valley investigations were conducted during 1981 through 1983 under the supervision of the senior author, Mr. Michael D. Campbell, who at the time was Chief Geologist, United Resources International, Houston, Texas. The petrographic investigations were performed by Dr. Eric Nelson, Department of Geology, Colorado School of Mines, Golden, Colorado. The geophysical data reduction and interpretations were performed by Dr. H. C. Clark, Department of Geology, Rice University, and Houston.

The field team consisted of Mr. M. Campbell, Dr. Nelson, and Mr. Steven E. Campbell, who served as field operations support supervisor, and Mr. M. David Campbell, Assistant Geologist of URI.

The Kachauik investigations: Phase I and II project activities were supervised by the senior author, with field operations support was managed by Mr. Steven E. Campbell, Vice President-Operations, Omega Energy Corporation. Phase II field and laboratory investigations were conducted by United Resources International on behalf of Omega Energy Corporation. The URI consultants involved in the project at the time were as follows:

Field Investigations:

Kaachuik Area:

Charles C. Wielchowsky, Ph.D., in 1979, Department of Geology, Rice University, Houston,

Kevin T. Biddle, Ph.D., in 1979, Department of Geology, Rice University, Houston,

Charles F. Weisenberg, Ph.D., in 1979, Department of Geology, University of Redlands, Riverside, California

Mr. Herb Nelson, B.A., in 1978 and 1979, Department of Geology, University of Redlands, Redlands, California.

Death Valley and Ridge Area:

Eric Nelson, Ph. D., in 1983, Colorado School of Mines, Colorado (Deceased)

H. C. Clark, Ph. D., in 1983, Department of Geology, Rice University, Houston.

Laboratory Investigations:

Mr. Leroy Jacobs, Ph.D., Manager, in 1978-79, Instrumental Analyses, Division, Commercial Testing and Engineering Co., Denver, Colorado.

Ms. Kathy Balshaw, B. S., in 1979, Department of Geology, Rice University, Houston

J. Krause, Manager, Ph. D., in 1979, Mineralogy Projects, Engineering & Mining Division, Colorado School of Mines Research Institute, Golden, Colorado.

Mr. Glenn Fryer, B. S., in 1979, Department of Geology, Rice University, Houston.

Mr. Ken Wong, Ph.D., in 1979, Bandar-Clegg & Company, Ottawa, Canada.

Recent Thin-Section/XRF Work:

Mr. Graham Eldridge, B.S., in 2017-18, Department of Geology, Rice University, Appendix II, pp. 55-64, Houston

Reviews:

Thomas Sutton, Ph.D., P.G., Loveland, Colorado

The senior author declares no conflict of interest. Further, the original funding client, Omega Energy Corporation, had no role in the design of the URI investigations; in the collection, analyses, or interpretation of data; nor in the initial writing of report to the client and of the manuscript for this paper, or in the decision to publish the results. Permission to publish the results of this investigation is not needed because Omega Energy Corporation was dissolved in the mid-1980s. The authors have received no funds for covering the costs to publish the paper in Open Access. The authors have no beneficial interests in the subject areas at the time of publication.

References

1. Fourier M (1827) Mémoire sur les températures du globe terrestre et des espaces planétaires. Membre de l'Académie Royale des Sciences
2. Mendenhall WC (1901) A Reconnaissance in the Norton Bay Region, Alaska. *US Geol Surv* p.35. [[View Article](#)]
3. Smith PS, HM Eakin (1911) A Geologic Reconnaissance in the Southwestern Seward Peninsula and the Norton Bay-Nulato Region, Alaska, *US Geol Surv.* p.142. [[View Article](#)]
4. Moxham RM, WS West (1953) Radioactivity Investigations in the Serpentine-Kougarok Area, Seward Peninsula, Alaska, 1946. *USGS Circ* p.265 ll. [[View Article](#)]
5. Herreid G (1965) Geology of the Omilak-Otter Creek Area, Bendeleben Quadrangle, Seward Peninsula, Alaska. *Alaska Div. Mines and Minerals* p.12. [[View Article](#)]
6. Miller TP, Grybeck DJ, Elliott RL, Hudson TL (1972) Preliminary geologic map of the southeastern Bendeleben and eastern Solomon quadrangles, eastern Seward Peninsula, Alaska. *U.S. Geological Survey Open-File Report 72-256*, p.11. [[View Article](#)]
7. Miller TP, CM Bunker (1976) A Reconnaissance Study of the Uranium and Thorium Contents of Plutonic Rocks of the Southeastern Seward Peninsula, Alaska. *Journ. Research US Geol Surv.* 4:367-377. [[View Article](#)]
8. Anderson E (1968) Seward Peninsula, Alaska; in Heiner, L.E. and Wolff, E.N., Final Report, Mineral Resources of Northern Alas: Univ. Alaska Mineral Lab. Rept. 16, 305 p. [[View Article](#)]
9. West WS (1953) Reconnaissance for Radioactive Deposits in the Darby Mountain's Seward Peninsula, Alaska, 1948. *U.S. Geol. Surv.* p.7. [[View Article](#)]
10. Miller TP, Elliott RL, Finch WI, Brooks RA (1976a) Preliminary report on uranium-, thorium-, and rare-earth-bearing rocks near Golovin, Alaska: *US Geological Survey* p.12. [[View Article](#)]
11. Mulligan J J (1962) Lead-Silver Deposits in the Omilak Area Seward Peninsula, Alaska. *U. S. Bureau of Mines* p.44. [[View Article](#)]
12. Miller TP, DG Grybeck (1973) Geochemical Survey of the Eastern Solomon and Southeastern Bendeleben Quadrangles, Seward Peninsula, Alaska. *US Geol Surv* p.115. [[View Article](#)]
13. Barnes DF, RL Morin (1988) Results of a Gravity Survey of McCarthy's Marsh, Seward Peninsula, Alaska. *U.S.G.S.* p.13. [[View Article](#)]
14. Eakins GR, BK Jones, RB Forbes (1976) Investigation of Alaska's Uranium Potential. Part 1, *Alaska Depart Natural Resources*, p.331 [[View Article](#)]
15. Drumheller RE (1978) The Petrochemistry of the Allantite-Bearing Granitoids, Red Rock Area, Washoe County, Nevada. *Master's Thesis*, University of Nevada, Reno, p.89, [[View Article](#)]
16. Volborth A (1962) Allantite Pegmatites, Red Rock, Nevada Compared with Allantite Pegmatites in Southern Nevada and California. *Economic Geology*, 57:209-216. [[View Article](#)]
17. Miller TP (1972a) Potassium-Rich Alkaline Intrusive Rocks of Western Alaska. *Geol Soc Am. Bull* 83: 2111-2128. [[View Article](#)]
18. Miller TP, RL Elliott (1969) Metalliferous Deposits Near Granite Mountain Eastern Seward Peninsula Alaska, *U.S. Geological Survey Circular* 614, 26 p. [[View Article](#)]
19. Miller TP (1972b) Preliminary Geologic Map of the Eastern Solomon and Southeastern Bendeleben Quadrangles, Eastern Seward Peninsula, Alaska. *USGS Open-File Report 72-256*, p.11. [[View Article](#)]
20. Miller TP (1976b) Results of Geochemical Sampling Peninsula, Alaska. *U.S. Geol. Survey* p.66. [[View Article](#)]
21. Miller TP, B Johnson (1978) An Occurrence of Parsonite, A Secondary Uranium Mineral, in Alaskite of Wheeler Creek Pluton, Alaska. *U. Geological Survey* p.6. [[View Article](#)]
22. Sainsbury CL, et al (1970a) Geology, Mineral Deposits and Geochemical and Radiometric Anomalies, Serpentine Hot Springs Area, Seward Peninsula, Alaska, *U.S. Geol. Survey Bull.* 1312-H, 19 p. [[View Article](#)]
23. Sainsbury CL, et al (1970b) Structure, Stratigraphy and Isotopic Composition of Rocks of the Seward Peninsula, Alaska, *AAPG Bull.*, Vol. 54, No. 12, pp. 2502-2503. [[View Article](#)]
24. Sainsbury CL, et al (1972) Reconnaissance Geologic Map of the Solomon D-5 and C-5 Quadrangles, U.S. Geol. Survey Open File Rept., 12 p. [[View Article](#)]
25. Sainsbury CL (1974) Geologic Map of the Bendeleben 1:250,000 Quadrangle, Seward Peninsula, Alaska, Pub. By the Map Makers, P. O. Box 145, Anchorage, Alaska. , [[View Article](#)]
26. Winkler HGF (1967) Petrogenesis of Metamorphic Rocks, Springer-Verlag, New New York, 237 p. [[View Article](#)]
27. Till AB, Dumoulin JA, Gambia BM, Kaufman DS, PI (1986) Preliminary Geologic Report and Map and Fossil Data from Solomon, Bendeleben, and Southern Kotzebue Quadrangles, Alaska, U.S.G.S. Open File Report 86-276, 69 p. [[View Article](#)].

27. Foley JY, Barker JC (1980) Uranium Occurrences in the Northern Darby Mountains, Seward Peninsula, AK, U. S. *Geological Survey and Bureau of Mines*, 22 p. [[View Article](#)]
28. Wise HM, Campbell MD (2018) "Wyoming K-T Boundary Thin Sections: A Preliminary Assessment," in AAPG Eclipse Seminary Field Guide, Casper, Wyoming, August 18-22, 2017, Revised in April, 2018, especially pp.128-131. [[View Article](#)]
29. Eakins GR (1977) Reconnaissance Program, West-Central Alaska and Copper River Basin. Part 1 Investigations of Alaska's Uranium Potential, *U.S* p.66. [[View Article](#)]
30. Hawkes HE, Webb JS (1962) *Geochemistry in Mineral Exploration*, Harper & Row, New York, 415p. [[View Article](#)]
31. State of Alaska (2005) Mineral Occurrence and Development Potential Report Leaseable Minerals - Kobuk - Seward Peninsula Resource Management Plan, BLM Alaska State Office Division of Energy and Solid Minerals Branch of Energy, 64 p. [[View Article](#)]
32. Currie KL (1973) The Alkaline Rocks of Canada, *Geological Survey of Canada Bulletin 239*, Department of Energy, Mines and Resources, Canada, 228 p. [[View Article](#)]
33. Young EJ (1989) Felsic-Mafic Ratios and Silica Saturation Ratios – Their Rationale and Use as Petrographic and Petrologic Indicators, U.S.G.S. Open-File Report 89-651, 35 p. [[View Article](#)]
34. Nockolds SR (1954) Average chemical compositions of some igneous rocks: *Geological Society of America Bulletin*, v. 65, p. 1007-1032. [[View Article](#)]
35. Tumiami S, Martin S, Nimis P, Mair V, Godard G(2003) "Dissakisite-(La)" (Mg-Analogue of Allanite) in Peridotite from the Ulten one (Eastern Alps): Evidence for Crustal Metasomatism," *Geophysical Research Abstracts*, Vol. 5, 03875.[[View Article](#)]
36. Alekseev VI, Marin YB (2015) "Accessory Mineralization of Rocks from Late Cretaceous Intrusive Series with Li-F Granites in the Far East," published in Zapiski Rossiiskogo Mineralogicheskogo Obshchestva, 2014, ISSN 10757015, *Geology of Ore Deposits*, 2015, Vol. 57, No. 7, pp. 53 No. 3, pp. 1-22. [[View Article](#)]
37. Alekseev VI, Marin YB, Gembitskaya IM (2013) Allanite(Y) in Areas of Ongonite Magmatism in the Far East: Isomorphism and Petrogenetic Implications National University of Mineral Resources, St. Petersburg, 199106 *Geology of Ore Deposits*, 2013, Vol. 55, No. 7, pp. 503–514 [[View Article](#)]
38. Alekseev VI, Marin YB, Gembitskaya IM (2016) Allanite-(Y) and Allanite-(Ce) Paragenesis in Tourmalinite of the Severnyi Pluton, Chukchi Peninsula, and the Relationship between Yttrium and Lanthanides in Allanite, *Geology of Ore Deposits*, 2016, Vol. 58, No. 8, pp. 674-680. [[View Article](#)]
39. Eby RK, Janeczek J, Ewing RC (1993) Metamict and Chemically Altered Vesuvianite. *Canadian Mineralogist* Vol. 31, pp. 357-369. [[View Article](#)]
40. Smith MP, Henderson P, Jeffries T (2002) The formation and alteration of allanite in skarn from the Beinn an Dubhaich granite aureole, Skye, *Eur J Mineral*, Vol. 14, pp. 471-486. [[View Article](#)]
41. Forster HJ (1998) The chemical composition of REE-Y-Th-U-rich accessory minerals in peraluminous granites of the Erzgebirge-Fichtelgebirge region, Germany Part II: Xenotime. *American Mineralogist* 83: 1302-1315. [[View Article](#)]
42. Himmelberg GR, Miller TP (1980) Uranium- and thorium-rich vesuvianite from the Seward Peninsula, Alaska. *American Mineralogist* 65:1020-1025. [[View Article](#)]
43. Evans JR (1966) California's Mountain Pass Mine, Mineral Information Service. *Calif Div Mines Geology*18: 22-32.[[View Article](#)]
44. Manfred K, Kopf (1967), The petrophysical character of the "granites" of Bornholm: *Geol Fjren Fjrh* 89: 3-14. [[View Article](#)]
45. Saxov S, Abrahamsen N (1964) Some rock densities in Bornholm: *Geol Foren Forh* 86: 83-95. [[View Article](#)]
46. Platou SW (1968) On the petrophysical properties of granitic rocks: *Geol Foren Forh* 90: 427-433. [[View Article](#)]
47. Heinrich EW (1966) *The Geology of Carbonatites. Rand McNally Chicago [book].*
48. Doroshkevich AG, Ripp GS, Moore KR (2010) Genesis of the Khaluta alkaline-basic Ba-Sr carbonatite complex (West Transbaikala, Russia). *Miner Petrol* 98: 245-268. [[View Article](#)]
49. Modreski PJ, Armbrustmacher TJ, Hoover DB (1995) Carbonatite Deposits (Model 10; Singer, 1986a), Summary of Relevant Geologic, Geoenvironmental, and Geophysical Information. [[View Article](#)]
50. Sorensen H (1974) *The Alkaline Rocks*, John Wiley and Sons, London, 622 p. [[View Article](#)]
51. Decker J, S Karl (1977) Preliminary Aeromagnetic Map of Seward Peninsula, Alaska, *U. S. G.S. Open File Report* 77-796E. [[View Article](#)]
52. Berger VI, DA Singer, GJ Orris (2009) Carbonatites of the World, Explored Deposits of Nb and REE: Database and Grade and Tonnage Models. *U.S. Geological Survey Open-File Report 2009-1139* p.17. [[View Article](#)]
53. Gwalani LGK, K Moore, A Simometti (2010) Carbonatites, Alkaline rocks, and the Mantle: A Special Issue to Keith Bell. *Miner Petrol* Vol. 95, pp. 5-10. [[View Article](#)]
54. Sorensen H, (1970b) Internal Structures and Geologic Setting of the Three Agpaitic Intrusions - Khibina and Lovozero of the Kola Peninsula and Ilirnaussaq, 'South Greenland. *Can Mineralogist* Vol. 10 Part 3. [[View Article](#)]

55. White MG, (1953) Reconnaissance for Radioactive Deposits in the Vicinity of Teller and Cape Nome, Seward Peninsula, Alaska, 1946-47. Part 1: Reconnaissance in the Vicinity of Teller, 1947. *US Geol Surv Circ 244* pp.1-4. [[View Article](#)]
56. White MG, GE Tolbert (1954) Reconnaissance for Radioactive Deposits in East-Central Alaska, 1949, Chapter B: Miller House-Circle Hot Springs Area. *US Geol Circ 335* pp. 4-6. [[View Article](#)]
57. Wedow H, GE Tolbert (1954) Reconnaissance for Radioactive Deposits in East-Central Alaska, 1949, Chapter E: Wilson Creek, My Creek, Ben Creek and Chicken Areas, Forty Mile District. *USGS Circ 335* pp. 13-22. [[View Article](#)]
58. West WS, JJ Matzko (1953) Reconnaissance for Radioactive Deposits in the Vicinity of Teller and Cape Nome, Seward Peninsula, Alaska, 1946-47, Part 2: Reconnaissance in the Vicinity of Cape Nome, 1947, *U.S. Geol. Surv. Circ. 244*, pp. 5-8. [[View Article](#)]
59. Smith W L, et al., (1957) Uranium and Thorium in the Accessory Allanite of Igneous Rocks, *American Mineralogist*. Vol. 42, pp. 367-378. [[View Article](#)]
60. Trites A F, EW Tooker, (1953) Uranium and Thorium Deposits in East-Central Idaho, Southwestern Montana. *USGS Bull 988-H* pp. 157-209. [[View Article](#)]
61. Whitfield JM, et al., (1959) The Relationship between the Petrology and the Thorium and Uranium Contents of Some Granitic Rocks. *Geochimica et Cosmochimica* Vol. 17, pp. 249-271. [[View Article](#)]
62. Ford RB, (1955) Mineralogy of a Uraninite-Bearing Pegmatite, Lac La Ronge, Saskatchewan. *Econ Geol* Vol. 50, pp. 196-205 [[View Article](#)]
63. Olson JC, et al., (1954) Rare-Earth Mineral Deposits of the Mountain Pass District, San Bernardino County, California. *USGS Prof. Paper 261*, 75 p. [[View Article](#)]
64. Lang AH, et al., (1960) Never burg, GJ, 1955 Uranium in Igneous Rocks of USA, United Nations International Conf. on Peaceful Uses of Atomic Energy, pp. 201-239. [[View Article](#)]
65. Neverburg (1955) Canadian Deposits of Uranium and Thorium. *Geol. Surv. Canada, Eco. Geology Ser. No. 16*, Department of Mines and Technical Surveys, Ottawa, pp.324. [[View Article](#)]
66. Rose ER, (1979) Rare-Earth Prospects in Canada. *CIM Bull* May, pp.110-116. [paper only]
67. Brooks JH, (1972) Uranium Exploration in Queensland, 1967-71. *Geological Survey of Queensland Report 69 Qld Department of Mines* 26 p. [[View Article](#)]
68. *Engineering and Mining Journal*, (1979) MKU: The Forgotten Link in Australian Exports, 180, No. 2, February, pp. 107, see page 10. [[View Article](#)]
69. Miles KR, (1955) Notes on Rare Earths in the Mary Kathleen Lease-Mt. Isa District. Northwest Queensland, Australasian Oil Exploration Ltd 4 p. [[View Article](#)]
70. Wilde AA Otto, J Jory, C MacRae, M Pownceby, N Wilson, et al., (2013) Geology and Mineralogy of Uranium Deposits from Mount Isa, Australia: Implications for Albitite Uranium Deposit Models. *Minerals*, Vol. pp.258-283, [[View Article](#)]
71. Hughes FE, DL Munro (1967) Uranium Ore Deposit at Mary Kathleen. *Geology of Australia Ore Deposits, Vol. I*, Eighth Commonwealth Mining and Metallurgical Congress, J. McAndrew (ed.), pp. 256-263. [[View Article](#)]
72. Derrick GM, (1977) Metasomatic history and origin of uranium mineralization at Mary Kathleen, Northwest Queensland. *BMR Journal of Australian Geology & Geophysics* Vol. 2, pp. 123-130, [[View Article](#)]
73. Sorensen H, (1970a) Occurrence of Uranium in Alkaline Igneous Rocks, in Proc. Uranium Exploration Geology, International Atomic Energy Agency, Vienna, Austria, IAEA-PL-391122, pp. 161-168. [[View Article](#)]
74. Ragland PC, GK, Billings JAS Adams (1967) Chemical fractionation and its relationship to the distribution of thorium and uranium in a zoned granite batholith, *Geochimica et Cosmochimica Acta*, 31, pp. 17-33, especially pp. 30-32. [[View Article](#)]
75. Campbell MD (2018) Uranium (Nuclear and Rare Earth) Committee of the Energy Minerals Division (AAPG) Releases 2018 Annual Report [[View Article](#)]
76. Campbell MD, KT Biddle (1977) "Frontier Uranium Exploration in the South-Central U.S., Chapter 1, in *Geology {and Environmental Considerations} of Alternate Energy Resources: Uranium, Lignite, and Geothermal Energy in the South Central States*, Houston Geological Society, 364 p., pp. 3-44. [[View Article](#)]
77. Campbell MD (1973) Guest Editorial: "Industrial Progress Through Practical Research," *Ground Water*, Vol. 11, No. 1, pp. 2-4. [[View Article](#)]
78. Dickinson KA, JS Duval (1977) South Texas Uranium: Geologic Controls, Exploration Techniques, and Potential, Chapter 2, in *Geology {and Environmental Considerations} of Alternate Energy Resources: Uranium, Lignite, and Geothermal Energy in the South Central States*, Houston Geological Society, pp. 45-70. [[View Article](#)]
79. Jefferson CW, Thomas DJ, Gandhi SS, Ramaekers P, Delaney G, et al (2007) Unconformity-associated uranium deposits of the Athabasca Basin, Saskatchewan and Alberta, in Goodfellow. WD (ed). *Mineral Deposits of Canada: A Synthesis of Major Deposit-Types, District Metallogeny, the Evolution of Geological Provinces, and Exploration Methods: Geological Association of Canada, Mineral Deposits Division, Special Publication No. 5*, p. 273-305. [[View Article](#)]
80. Chi G, et al., (2018) A Shallow-Burial Mineralization Model for the Unconformity-Related Uranium Deposits in the Athabasca Basin, *Economic Geology*, 113, No. 5, pp. 1209-1217. [[View Article](#)]

81. Dickinson KA, ED Cunningham, TA Ager (1987) Geology and Origin of the Death Valley Uranium Deposit, Seward Peninsula, Alaska, *Economic Geology*, 82:1987, pp. 1558-1574 [[View Article](#)]
82. Dickinson KA (1988) Paleolimnology of Lake Tubutulik, An Iron-Meromictic Eocene Lake, Eastern Seward Peninsula, Alaska, *Sedimentary Geology*, 54, No. 4, pp. 303-320. [[View Article](#)]
83. Campbell MD, HM Wise (2010) Uranium Recovery Realities in the U.S. – A Review, An Invited Lecture to the Houston Geological Society, Environmental and Engineering Dinner Meeting, May 18, 2010, 51 p. [[View Article](#)]
84. Santos ES (1975) A Characteristic Pattern of Disequilibrium in Some Uranium Ore Deposits, *Jour. Research U.S. Geol. Survey* 3, No. 3, May-June 1975, p. 363-368. [[View Article](#)]
85. Seeking Alpha.com (2015) Japan - Uranium Demand Will Recover, [[View Article](#)]
86. Triex (2007) Full Metal, Alaska Uranium Drilling Program, in *Market Wired*. [[View Article](#)]
87. Triex (2007) Mineral Exploration Company, Stock Market Announcement, “Boulder Creek Deposit and Exploration in McCarthy’s Marsh” pp.19-20.[[View Article](#)]
88. Gamble BM, AB Till (1989) Maps Showing Metallic Mineral Resources of the Bendeleben and Solomon Quadrangles, Western Alaska. MF-1838-D Report [[View Article](#)]
89. Gamble BM (1988) Non-placer mineral occurrences in the Solomon, Bendeleben, and southern part of the Kotzebue quadrangles, western Alaska: *U.S. Geological Survey Miscellaneous Field Studies Map 1838-B*, 13 p., 1 sheet, scale 1:250,000. [[View Article](#)]
90. Gamble BM, Till AB (1993) Maps showing metallic mineral resources of the Bendeleben and Solomon quadrangles, western Alaska: *U.S. Geological Survey Miscellaneous Field Studies Map 1838-D*, 22 p., 3 sheets, scale 1:250,000. Report [[View Article](#)]
91. Berg HC, Cobb EH (1967) Metalliferous Lode Deposits of Alaska, *U.S. Geol. Survey Bull.* 1246, 254 p. [[View Article](#)]
92. Kelly KD, et al., (1995) Summary of Relevant Geologic, Geoenvironmental, and Geophysical Information, Sedimentary Exhalative Zinc-Lead-Silver, from Model 31a, Briskey, pp. 225-233. [[View Article](#)]
93. Shawe DR (1976) Geology and Resources of Fluorine in the United States, *U.S. Geological Survey Professional Paper 933*[[View Article](#)]
94. Forbes RB (1976) Investigation of Alaska Uranium Potential, Part 1, Alaska Depart. Natural Resources, Special Report No. 12, *U.S. ERDA Contract at (05-1)- 1627*, p. 1-41. [[View Article](#)]
95. Burger, JR (1982) E&MJ Exploration Roundup: Tourmaline Can Lead to Ore Bodies, *E&MJ Journ.*, October, pp. 29-31 [paper only]
96. Karl SM, JV Jones, TS Hayes (2016) GIS-Based Identification of Areas that have Resource Potential for Critical Minerals in Six Selected Groups of Deposit Types in Alaska, *U.S. Geological Survey Open-File Report 2016-1191*, 107 p. [[View Article](#)]
97. Karl SM (2017) Petrology, Tectonic Setting, and Potential for Concentration of Rare Earth Elements (REE) and High Field Strength Elements (HFSE) in the High-K Darby and Kachauik Plutons, Seward Peninsula, Alaska, *U.S. Geological Survey Current Activities*. [[View Article](#)]
98. Campbell MD (1977) (editor), *Geology [and Environmental Considerations] of Alternate Energy Resources: Uranium, Lignite, and Geothermal Energy in the South Central States*, Houston Geological Society, 364 p. ([here](#)), cited p. 17 of Chapter 1. [[View Article](#)]
99. Alekseev VI, YB Marin, IM Gembitskaya (2013) Allanite(Y) in Areas of Ongonite Magmatism in the Far East: Isomorphism and Petrogenetic Implications *National University of Mineral Resources, St. Petersburg, 199106 Geology of Ore Deposits*, 55, No. 7, pp. 503–514. [[View Article](#)]
100. Berger VI, DA Singer, GJ Orris (2009) Carbonatites of the World, Explored Deposits of Nb and REE: Database and Grade and Tonnage Models, *U.S. Geological Survey Open-File Report 2009-1139*. [[View Article](#)]
101. Bundesanstalt für Geowissenschaften und Rohstoffe (BGR) (Federal Institute for Geosciences and Natural Resources) and Mineral Resources Authority of Mongolia (MRAM) (2015) Rare Earths of Mongolia: Evaluation of Market Opportunities for the Principal Deposits of Mongolia, 68 p.[[View Article](#)]
102. Churkin M (1973) Paleozoic and Precambrian Rocks of Alaska and Their Role in Its Structural Evolution, *U.S. Geological Survey Prof. Paper 740*, 64 p.[[View Article](#)]
103. Cobb EH (1967) Metallic mineral resources map of the Solomon Quadrangle, Alaska: *U.S. Geological Survey Open-File Report 67-60*, 10 p., 1 sheet, scale 1:250,000.[[View Article](#)]
104. Cobb EH (1972) Metallic mineral resources map of the Solomon quadrangle, Alaska: *U.S. Geological Survey Miscellaneous Field Studies Map MF-445*, 1 sheet, scale 1:250,000. [[View Article](#)]
105. Cobb EH (1978) Summary of references to mineral occurrences (other than mineral fuels and construction materials) in the Solomon quadrangle, Alaska: *U.S. Geological Survey Open-File Report 78-181*, 185 p. [[View Article](#)]
106. Dayton S (1979) Alaska: A Land and People in Search of a Future, Federally Owned Lands in Alaska - 1979, *Engineering and Mining Journal*, May, pp.72-87. [paper only]
107. Dostal J (2017) Rare Earth Element Deposits of Alkaline Igneous Rocks, *Resources*, 6, No. 34, 12 p. [[View Article](#)]

108. Hudson T (1977) Geologic Map of Seward Peninsula, Alaska, *U.S. Geol. Survey Open File Rept. 77-769A*. [[View Article](#)]
109. Hudson H, Miller ML, Pickthorn W J (1977) Map Showing Metalliferous and Selected Non Metalliferous Mineral Deposits, Seward Peninsula, Alaska, *U.S. Geol. Survey Open File Rept. 77-796b*. 45 p. [[View Article](#)]
110. Hummel CL (1977) Review of Exploration Geochemical Surveys, on Seward Peninsula, Western Alaska, *U.S. Geol. Survey Open File Rept. 77-796D*, 27 p. [[View Article](#)]
111. Johnson BR, Miller TP, Karl, Susan, (1979) Uranium-thorium investigations of the Darby pluton, Seward Peninsula, Alaska: *U.S. Geological Survey Circular 804-B*, p. B68-B70. [[View Article](#)]
112. Lu, FC. J, LE Heiner, DP Harris (1968) Known and Potential Mineral Resources; Seward Peninsula, Alaska; *Alaska Univ. Min. Indust. Res. Lab. Rept. 18*, 107 p. [[View Article](#)]
113. Miller TP, CM Bunker (1975) Uranium, Thorium and Potassium Analyses of Selected Plutonic Rocks from West-Central Alaska, *U. S. Geol. Surv. Open-File Report 75-216*, 6 p. [[View Article](#)]
114. National Uranium Resources Evaluation Program (NURE),(1974) History of the National Uranium Resource Evaluation Hydrogeochemical and Stream Sediment Reconnaissance Program, *U. S. Geological Survey* [[View Article](#)]
115. Nockolds SR (1947) The relation between chemical composition and paragenesis in the biotite micas of igneous rocks: *American Journal of Science*, 245:401-402p. [[View Article](#)]
116. Pan KL, Overstreet WC, Robinson K, Hubert AE, Crenshaw GL (1980) Equivalent uranium and selected minor elements in magnetic concentrates from the Candle Quadrangle, Solomon Quadrangle, and elsewhere in Alaska: *U.S. Geological Survey Professional Paper 1135*, 115 p., 1 sheet, scale 1:500,000., [[View Article](#)]
117. Patton WW (1971) Regional Geologic Map of the Candle Quadrangle, Alaska, *U.S. Geol. Survey Misc. Geol. Inc. Map I-492*., [[View Article](#)]
118. Parker RL, Adams JW (1973) Niobium (Columbium) and Tantalum, in *U.S. Geol. Survey Prof. Paper 820*, pp. 443-454. [[View Article](#)]
119. Rosenblum S, EL Mosier(1983) Mineralogy and Occurrence of Europium-Rich Dark Monazite, *U.S. Geological Survey Professional Paper 1181* [[View Article](#)]
120. Sharp RR, Hill DE (1978) Uranium Concentrations in Stream Waters and Sediments from Selected Sites in the Eastern Seward Peninsula, Koyukuk, and Charley River Areas, and across South-Central Alaska, *U.S. Dept. Energy, Los Alamos Scientific Laboratory Report LA-6649-MS*, April, 39 p. [[View Article](#)]
121. Smith PS, Eakin HM (1910) Mineral Resources of the Nulato Council Region, in Mineral Resources of Alaska, Report of Progress of Investigation in 1909, *U.S. Geol. Survey Bull*, 442, pp. 316-352. [[View Article](#)]
122. Triex (2007) Minerals and Full Metal Minerals: Alaska Program Completed-New Uranium Mineralization Discovered at Fireweed, [[View Article](#)]
123. U. S. Bureau of Mines, (1978) Mining Claims in the Bendeleben Quadrangle, *U.S. Bureau of Mines Open File Rept. 20-73* (Revised). [[View Article](#)]
124. Campbell, MD (2017) Publishing Buried Geological Data for the Benefit of Professional Geologists, *Journ Geol and Geosci*, Vol.1 [[View Article](#)]
125. Haxel, GB (2005) Ultrapotassic Mafic Dikes and Rare Earth Element- and Barium-Rich Carbonatite at Mountain Pass, Mojave Desert, USGS OF Report 2005-1219, 56 p. [[View Article](#)]
126. Thompson TB (1997) Uranium, Thorium, and Rare Metal Deposits of Alaska, *Economic Geology Monograph 9*, pp. 466-482. [[View Article](#)]
127. Campbell, MD, and MD Campbell, II, (2016), Independent Assessments of Gold, Phosphate, Potash, Uranium, and Rare-Earth Deposits, An Invited Presentation to the Houston Geological Society at the Dinner Meeting of the Environmental and Engineering Group, March 9, 62 p.; of special interest pp. 51-54 [[View Article](#)].
128. Rubin, B, (1970), Uranium Roll-Front Zonation in the Southern Powder River Basin, Wyoming; *Wyoming Geological Society Earth Science Bull.*, Vol. 3, No. 4, December, pp. 5-12 ([View Article](#)).

Appendices

APPENDIX I

Primary Petrographic Figures

APPENDIX II

Cited Petrographic Analyses and Data

APPENDIX III

- A. Preliminary XRD Report: Rice University, Houston, Texas
- B. Chemical Analyses: CT & E, Denver and Float-Sink Analyses: CT&E, Denver
- C. Duplicate Chemical Analyses: Bandar-Clegg, Ottawa
- D. Miscellaneous DOE, Alaska Geological Survey, and U. S. Geological Survey Data for Areas of Interest.

APPENDIX DV-I

Analytical Results and Methods (Line Samples)

Analyses from Pit (P Samples)

APPENDIX DV-II

Petrographic Analyses

Citation: Characterization of the Occurrence of Uranium, Thorium, Rare Earths and Other Metals in Basement Rocks as a Source for New Uranium Roll-Front District in the Tertiary Sediments in the McCarthy Marsh and Death Valley and Associated Metallogenic Areas in the Eastern Seward Peninsula, Alaska, by Campbell, MD, RI Rackley, RW Lee, M David Campbell, HM Wise, JD King, and SE Campbell, *Journal Geology and Geosciences*, Vol. 2(1), 2018, 65 p.

Copyright: © 2018 Michael D. Campbell. This is an open-access article distributed under the terms of the Creative Commons Attribution License, which permits unrestricted use, distribution, and reproduction in any medium, provided the original author and source are credited. [Final Manuscript](#) and any PDF [UPDATE](#)